TECHNISCHE UNIVERSITÄT MÜNCHEN

Fakultät für Medizin

Institut für Allgemeine Pathologie
und Pathologische Anatomie

(Direktor: Prof. Dr. Wilko Weichert)

Claudin-18 in Pancreatic Carcinogenesis

Ralph-Tobias Daraban

Vollständiger Abdruck der von der Fakultät für Medizin der Technischen Universität München zur Erlangung des akademischen Grades eines Doktors der Medizin genehmigten Dissertation.

Vorsitzender: Prof. Dr. Ernst J. Rummeny
Prüfer der Dissertation:
1. Prof. Dr. Irene Esposito
2. Prof. Dr. Roland M. Schmid

Die Dissertation wurde am 25.03.2019 bei der Technischen Universität München eingereicht und durch die Fakultät für Medizin am 06.11.2019 angenommen.

Index

Abbreviations

5-FU	5-Fluorouracil
Ab	Antibody
ADCC	Antibody-dependent cellular cytotoxicity
AP-1	Activator protein 1
BCA	Bicinchoninic acid
Bp	Base pair
BSA	Bovine albumin serum
CDC	Complement-dependent cytotoxicity
cDNA	Complementary desoxyribunucleic acid
CEA	Carcinoembryonic antigen
CFTR	Cystic fibrosis transmembrane conductance regulator
CPE	Clostridium perfringens enterotoxin
CSF-I	Colony stimulating factor subclass I
CT	Computed tomography
DAB	Diaminobenzidine
DAG	Diacylglycerol
DMEM	Dulbecco's modified eagle medium
DMSO	Dimethyl sulfoxide
DNA	Desoxyribunucleic acid
ECL	Enhanced chemiluminescence
ECL	Extracellular loop
EDTA	Ethylenediaminetetraacetic acid
EGFR	Epidermal growth factor receptor
EGTA	Ethylene glycol tetraacetic acid
EMT	Epithelial mesenchymal transition
ERCP	Endoscopic retrograde cholangiopancreatography
FBS	Fetal bovine serum
fwd	Forward
GAPDH	Glyceraldehyde 3-phosphate dehydrogenase
Gas	Gastric type IPMN
H	Hour/hours
HCG	Human chorionic gonadotropin
HE	Hematoxylin and eosin stain
HRP	Horseradish peroxidase
ICC	Immunocytochemistry

IEM	Immunogold electron microscopy
IF	Immunofluorescence
Ig	Immunoglobulin
IHC	Immunohistochemistry
Int	Intestinal type IPMN
IPMN	Intraductal papillary mucinous neoplasm
ITPN	Intraductal tubulopapillary neoplasm
kb	Kilobase
kDa	Kilodalton
LOH	Loss of heterogeneity
M	Molar
mM	Millimolar
mAb	Monoclonal antibody
MAPK	Mitogen-activated protein kinase
MCN	Mucinous cystic neoplasm
Min	Minutes
MR	Magnet resonance
MRCP	Magnet resonance cholangiopancreatography
MRI	Magnet resonance imaging
mRNA	Messenger RNA
MUC	Mucin
NCBI	National center for biotechnology information
NP-40	Nonyl phenoxypolyethoxylethanol
Onc	Oncocytic type IPMN
pAb	Polyclonal antibody
PanIN	Pancreatic intraepithelial neoplasia
Pb	Pancreatobiliary type IPMN
PBS	Phosphate buffered saline
PCR	Polymerase chain reaction
PDAC	Pancreatic ductal adenocarcinoma
PDZ	Post synaptic density protein, Drosophila disc large tumor suppressor, Zonula occludens-1 protein
PI3K	Phosphatidylinositol-4,5-bisphosphate 3-kinase
PKC	Protein kinase C
PMA	Phorbol 12-myristate 13-acetate
rev	Reverse
RIPA	Radioimmunoprecipitation assay

RNA	Ribonucleic acid
RNAi	RNA inhibition
Rpm	Rounds per minute
RT	Room temperature
SDS	Sodium dodecyl sulfate
Sec	Second
SiRNA	Small interfering RNA
TBE	Tris/borate/EDTA
TBS	Tris buffered saline
TBST	Tris-buffered saline + Tween 20
TER	Transepithelial resistance
TF	Transcription factor
TJ	Tight junction
UICC	Union internationale contre le cancer
UV	Ultraviolet
WB	Western blot
WHO	World health organization
WT	Wildtype
Y	Years

Abstract

Gene activation and down-regulation are common processes during carcinogenesis affecting biological properties of cancer cells. Claudin-18 has only recently been shown to be activated in the process of neoplastic transformation in the pancreas by transcriptional analysis. Claudins are membrane-bound epithelial proteins and harbor more than simple structural functions. Up-regulation or silencing of claudins affects intricate cellular pathways thereby influencing cell-cycle mechanisms and the proliferative potential of cells, which are in turn closely related to tumor formation.

The present study aims at assessing the expression of claudin-18 in PDAC and in its most common precursor lesions, thereby giving us a better understanding of its role in the process of pancreatic carcinogenesis.

Immunohistochemistry was used to analyze expression patterns of claudin-18 in pancreatic ductal adenocarcinomas (PDAC) of various degrees of differentiation as well as in a number of precursor lesions, such as pancreatic intraepithelial neoplasia (PanIN), intraductal papillary mucinous neoplasm (IPMN), mucinous cystic neoplasm (MCN) and intraductal tubulopapillary neoplasm (ITPN). The tissue analysis was complemented by cell line experiments of pancreatic and gastric cancer cells treated with the protein kinase C (PKC) enhancer Phorbol 12-myristate 13-acetate (PMA) to gain further insight into the mechanisms and possible functional properties of claudin-18 up-regulation.

Being completely absent in normal pancreatic tissue, claudin-18 expression was detected in PDAC precursors PanIN, MCN and IPMN in a predominantly membranous pattern. In all lesions, expression was correlated with low grade dysplasia, suggesting a down-regulation of this molecule during pancreatic carcinogenesis. In PDAC, expression of claudin-18 was lower than in precancerous lesions; in addition, well-differentiated tumors displayed higher expression levels. Correlation of staining results of PDAC samples with clinicopathological parameters revealed no significant differences between claudin-18-positive and negative tumors. *In vitro* experiments showed PKC-dependent regulation of claudin-18 expression.

In conclusion, claudin-18 is robustly expressed in the early phases of PDAC progression and in well-differentiated PDAC, rendering it a potential biomarker.

Zusammenfassung

Aktivierung und Inaktivierung von Genen bestimmt den Prozess der Tumorentstehung und beeinflusst maßgeblich das biologische Verhalten von Tumorzellen. Erst vor kurzem wurde durch Transkriptionsanalysen aufgezeigt, dass Claudin-18 im Rahmen der Pankreaskarzinogenese hochreguliert wird. Claudine sind epitheliale Membranproteine, deren Bedeutung allerdings über reine Strukturfunktionen hinausgeht. Veränderungen in der Expression von Claudinen haben Auswirkungen auf komplexe zelluläre Signalwege, die ihrerseits den Zellzyklus und das Wachstumsverhalten von Zellen beeinflussen, was wiederum in enger Beziehung zur Tumorentstehung steht.

Mittels immunhistochemischer Verfahren wurde das Expressionsmuster von Claudin-18 in Pankreaskarzinomen unterschiedlicher Differenzierungsgrade sowie in einigen Vorläuferläsionen wie PanIN, IPMN, MCN und ITPN untersucht. Die histologischen Untersuchungen wurden durch Zelllinienexperimente verschiedener Pankreas- und Magenkarzinomzellen ergänzt. Durch Vergleich der Expression mit und ohne Exposition gegenüber Phorbol-12-myristat-13-acetat (PMA) erhoffte man sich weitere Erkenntnisse über die Mechanismen sowie die funktionelle Bedeutung der Expression von Claudin-18.

Während Claudin-18 in der gesunden Bauchspeicheldrüse nicht vorkommt, verzeichnete man eine Expression in den Vorläuferläsionen PanIN, IPMN und MCN, wobei hier v.a. ein membranöses Expressionsmuster festgestellt werden konnte. In allen Läsionen ist eine Korrelation der Expression mit einem niedrigen Dysplasiegrad aufgefallen, was zu der Annahme verleitet, dass Claudin-18 im Verlauf der Tumorentstehung wieder herunterreguliert wird. Die Expression in PDAC war deutlich geringer als in den entsprechenden Vorläufern, doch auch hier war eine deutliche Assoziation mit einem höheren Differenzierungsgrad zu verzeichnen.

Ein Vergleich der Färbeergebnisse mit klinisch-pathologischen Parametern ergab keinen Überlebensunterschied. In den Zelllinienexperimenten konnte eine Beteiligung des PKC-Signalwegs in der Expressionsregulation von Claudin-18 ermittelt werden.

Zusammenfassend konnte gezeigt werden, dass Claudin-18 v.a. in den Frühphasen der Tumorentstehung des Pankreaskarzinoms sowie in gut differenzierten Karzinomen in relevantem Ausmaß exprimiert wird, sodass Claudin-18 als Biomarker der frühen Phasen der Pankreaskarzinogenese Pankreaskarzinoms verstanden werden kann.

I. INTRODUCTION

1. Pancreatic Ductal Adenocarcinoma (PDAC) and Its Precursor Lesions

1.1 Pancreatic Ductal Adenocarcinoma – A Clinical Overview

1.1.1 Epidemiological Features and Risk Factors

Despite being a rather rare cancer entity, pancreatic ductal adenocarcinoma (PDAC), is most feared due to its dismal prognosis with an overall 5-year survival of only 6% (Ilic and Ilic 2016). Age-adjusted incidence rates are 14.3/100000 for men and 11.1/100000 for women in the US, thus PDAC ranks 10th for men and 11th for women among all cancer sites. Death rates are only slightly lower than incidence rates (12.6/10000 for men and 9.5/10000 for women) underlining its lethality and therefore ranking PDAC 4th among cancer related deaths for each sex (Jemal, Ward et al. 2017). PDAC affects men slightly more often than women with a ratio of about 1.3 to 1.0. Furthermore, PDAC is more common among the Afro-American than the Caucasian subpopulation of the US, indicating ethnicity as a risk factor (Jemal, Simard et al. 2013). Almost 90% of patients are older than 55 years at the time of diagnosis (Ilic and Ilic 2016). Although the exact mechanisms of pathogenesis are still unclear, PDAC is related to certain life style factors. Among those, cigarette smoking seems to play the most important role, associated with a doubled risk of disease (Bosetti, Lucenteforte et al. 2012). Furthermore, obesity (BMI > 30 kg/m^2) is also, if only slightly, associated with PDAC (Berrington de Gonzalez, Sweetland et al. 2003). Other factors like a Western diet characterized by a higher intake of red and processed meat and a lower consumption of fruit and vegetables as well as physical inactivity, seem to contribute to an increased risk, too (Michaud, Giovannucci et al. 2001, Lu, Shu et al. 2017). PDAC has also been observed to be more frequent in patients with a long history of diabetes mellitus, suggesting an involvement of insulin-dependent pathways in tumorigenesis (Everhart and Wright 1995). Finally, some studies investigated the risk of PDAC in patients suffering from chronic pancreatitis, especially hereditary chronic pancreatitis (Raimondi, Lowenfels et al. 2010). On the other hand, both pancreatitis in its chronic-obstructive form and diabetes mellitus can be secondary complications of PDAC, which might lead to misinterpretation of possible risk factors in retrospective analyses (Hruban, Pitman et al. 2007).

Although the vast majority of cases are sporadic, patients with one or more first-degree relatives with a history of PDAC clearly have an increased risk (Klein, Brune et al. 2004). About 10% of PDAC are familial, and only a fraction of those are associated with certain syndromes caused by germline mutations of known genes, e.g. *BRCA1 and 2, CDKN2, STK11/LKB1* and *PRSS1* (Shi, Hruban et al. 2009).

1.1.2 Clinical Presentation

PDAC is usually not revealed by early, or by any means specific symptoms, which is a reason why many cases are only detected at an advanced stage. Most carcinomas develop in the head of the gland, causing obstruction of the main bile duct with retention of both pancreatic juice and bile. Consequently, patients might present with jaundice, which is often painless. Bile retention further leads to discoloring of the stool, as well as to hepatomegaly and pruritus. Other symptoms frequently reported are abdominal pain, as well as back pain, nausea and unexplained loss of weight due to wasting and maldigestion. Moreover, tumor related thrombosis is observed in some patients (Keane, Horsfall et al. 2014). Diabetes mellitus and pancreatitis, as stated above, are not only risk factors for PDAC, but also two of its possible complications. Infiltrating and destructive tumor growth as well as duct obstruction leads to a loss of parenchyma and endocrine islets and to inflammatory responses within the gland. Especially late onset hyperglycemia in old patients might be related to PDAC (Hruban, Pitman et al. 2007). Tumors in an advanced stage can infiltrate the duodenum, evoking upper intestinal obstruction or bleeding; ascites due to peritoneal and hepatic metastasis is a common finding (Hidalgo 2010). Interestingly, depression in patients with PDAC must not be taken as a mere psychooncologic phenomenon, but has to be considered as an independent symptom, which might be related to other, possibly inflammatory, responses (Breitbart, Rosenfeld et al. 2014).

1.1.3 Treatment Approaches and Prognosis

Surgical resection is the only option for a curative approach for patients with PDAC. Sadly, only a fraction of cases, i.e. 10 to 20%, are deemed resectable by preoperative radiologic staging (Sperti, Pasquali et al. 1997). Pancreatoduodenectomy or Whipple procedure is performed for tumors of the head of the gland and therefore is the most exercised surgical procedure to treat early disease (Shaib, Davila et al. 2007). However, only a small proportion of resected patients show long term survival. Adjuvant chemotherapy with gemcitabine has been shown to be beneficial in terms of overall survival for patients undergoing surgery for PDAC (Oettle, Post et al. 2007).

Unfortunately, the majority of patients with PDAC are diagnosed with an advanced regional or even metastatic disease. For those patients all approaches of treatment must be considered as solely palliative. For a long time, a gemcitabine-based cytotoxic therapy has been the treatment of choice for advanced/metastatic PDAC with the addition of a second agent such as a platinum-based drug, the EGFR (epidermal growth factor receptor) inhibitor erlotinib or a fluoropyrimidine, e.g. 5-fluorouracil (5-FU) (Hidalgo 2010). In recent years, promising clinical phase III studies have offered new therapeutic options. The combination of 5-FU/folinic acid, irinotecan and oxaliplatin, called FOLFIRINOX, was showed to be superior to monotherapy with gemcitabine, resulting in a benefit for median overall survival (11.1 vs. 6.8 months) (Conroy, Desseigne et al. 2011). Other approaches were

the administration of nanoparticle albumin-bound (nab-) paclitaxel (Abraxane; Celgene, Summit, NJ) or MM-398 (Merrimack Pharmaceuticals, Cambridge, MA), a nanoliposomal derivate of irinotecan in patients pretreated with gemcitabine. Other, partly experimental, trials for future treatment contain immunotherapy and intervention in stroma formation as well as in cell signaling (Ko 2015).

With resectability being one of the most important prognostic factors, patients that are diagnosed at an advanced stage are considered incurable, with a median survival of only 5 months (Sener, Fremgen et al. 1999). However, patients that undergo pancreatoduodenectomy show a median survival of 15 months and a five-year survival of 15 to 20% (Hruban, Pitman et al. 2007).

1.2 PDAC and Its Precursors – Pathological Differential Diagnosis

1.2.1 PDAC – Characteristics of Cancer and Microenvironment

PDAC is the most common malignancy of the pancreas. The cellular origin is the topic of controversial discussion. Although PDAC and most of its precursor lesions display a ductal phenotype, studies performed in transgenic mouse models have suggested that acinar cells might represent the cell of origin of PDAC (Aichler, Seiler et al. 2012, Esposito, Konukiewitz et al. 2012). Most frequently, PDAC affects the head of the gland (60-70%), but some tumors are localized in the body (5-15%) or tail (10-15%) of the pancreas or even infiltrate the organ diffusely (Bosman, Carneiro et al. 2010). The tumor usually appears as a solid, poorly defined mass of white-yellowish coloring (Bosman, Carneiro et al. 2010). The size is variable, but carcinomas of the head are usually about 3 cm in diameter, whereas those of the body or tail are larger when detected and resected (Sohn, Yeo et al. 2000). The pancreatic parenchyma adjacent to the tumor shows signs of atrophy and fibrosis, which can be difficult to distinguish from the tumor itself (Hruban, Pitman et al. 2007). Apart from growing within the gland, the tumor infiltrates adjacent tissues and organs. The extensive growth within the head of the pancreas often causes obstruction of the bile duct, which is then dilated and thickened. Furthermore, most tumors infiltrate retroperitoneal structures including nerve plexus. Invasion of blood vessels is also quite common, which induces vascular stenosis and thrombosis (Nakao, Harada et al. 1995). Tumors of the head frequently show infiltration of the duodenal wall and of the ampulla (Bosman, Carneiro et al. 2010). Angiolymphatic invasion is associated with lymph node metastasis and can be detected in the vast majority of resected cancers. Apart from locoregional spread and metastasis, PDAC is often detected in stage IV with evidence of distant metastases, commonly found in the liver, the lungs, the adrenal glands, the skin and the peritoneum (Hruban, Pitman et al. 2007). Both undetected locoregional and distant tumor residuals mostly represent the source of cancer recurrence after surgical resection.

Microscopic features of PDAC are an invasive gland-forming growth, the production of mucin and an extensive desmoplastic stroma formation. Carcinoma cells show interaction with myofibroblasts,

called pancreatic stellate cells, which are responsible for the secretion of matrix components, thereby contributing to the formation of desmoplastic stroma (Erkan, Adler et al. 2012). Desmoplasia is not just a morphologic feature of PDAC, but it markedly contributes to tumor formation, progression and spread (Mahadevan and Von Hoff 2007).

Architectural and cellular composition of neoplastic glands largely depends on the grade of differentiation. Whereas well differentiated (G1) tumors exhibit well defined glands composed of cuboidal to columnar cells with basally oriented uniform nuclei, poorly differentiated (G3) tumors show small heterogeneous and poorly formed glands. The stroma contains single invasive cells or solid sheets. Nuclei are typically large and pleomorphic, sometimes bizarrely shaped, and contain large, numerous nucleoli (Hruban, Pitman et al. 2007). Various histologic variants of PDAC are described such as adenosquamous, colloid, undifferentiated and signet ring cell carcinoma, some of them bearing distinct molecular characteristics (Esposito, Segler et al. 2015).

PDAC is considered a genetic disease with each carcinoma harboring over 60 genetic aberrations. Despite an extremely heterogeneous genetic profile, some key defects could be identified (Jones, Zhang et al. 2008). Over 90% of carcinomas show activating mutations of the *KRAS* oncogene, causing constant enhancement of pathways promoting proliferation and survival. Other oncogenes that are affected are *BRAF*, *c-MYC* and *ERBB2*. Biallelic inactivation affects tumor suppressor genes like *CDKN2A/*p16, *TP53* and *SMAD4/DPC4* (Ottenhof, de Wilde et al. 2011). Other genetic alterations promoting carcinogenesis are mitochondrial mutations, overexpression of telomerase and, rarely, microsatellite instability (Hezel, Kimmelman et al. 2006).

1.2.2   Pancreatic Intraepithelial Neoplasia (PanIN) – A Sequence Model for Pancreatic Tumorigenesis

On microscopic investigation of resected PDAC, non-invasive ductal lesions have been identified which exhibited various degrees of cellular and architectural atypia. They share morphological and molecular characteristics with PDAC suggesting the progression of these non-invasive lesions to invasive cancer of ductal differentiation. They have been called pancreatic intraepithelial neoplasia (PanIN) and are thought to be the most common precursor of PDAC.

According to the degree of atypia, three forms of PanIN are distinguished. PanIN 1 are characterized by flat (PanIN 1A) or papillary/micropapillary (PanIN 1B) epithelium consisting of uniform columnar cells with basal round nuclei and supranuclear mucin. PanIN 2 usually show a papillary growth pattern, but may also be flat. The nuclei of epithelial cells show some signs of atypia. PanIN 3 constitute carcinoma in situ and thus exhibit features of high grade dysplasia. Pancreatic intraepithelial neoplasms are per definition smaller than 0.5 cm and therefore not grossly visible (Hruban, Adsay et al. 2001).

PanIN are strongly associated with PDAC, but whereas low grade PanIN (PanIN 1 and 2) were also observed in healthy pancreata of adults, high-grade PanIN (PanIN 3) are almost exclusively found in patients with PDAC and there often in close vicinity to the invasive carcinoma (Hruban, Takaori et al. 2004). This finding might indicate that it is only a small step from non-invasive PanIN 3 to actual PDAC, making them high risk lesions with a different clinical significance than low-grade lesions (PanIN 1 and 2). All in all, the prevalence of PanIN increases with age and PanIN are reported to be more frequently located in the head of the pancreas, both features they have in common with PDAC. Additionally, low-grade PanIN have also been identified in cases of pancreatitis, even though less frequently than in cases of ductal adenocarcinoma (Andea, Sarkar et al. 2003).

Genetic profiling of PanIN of various grades of dysplasia revealed numerous genetic alterations that could also be observed in PDAC. Although there is no defined sequence model, some changes seem to take place earlier in the course of transformation than others, making them triggers for changes in morphology and cellular behavior (figure 1).
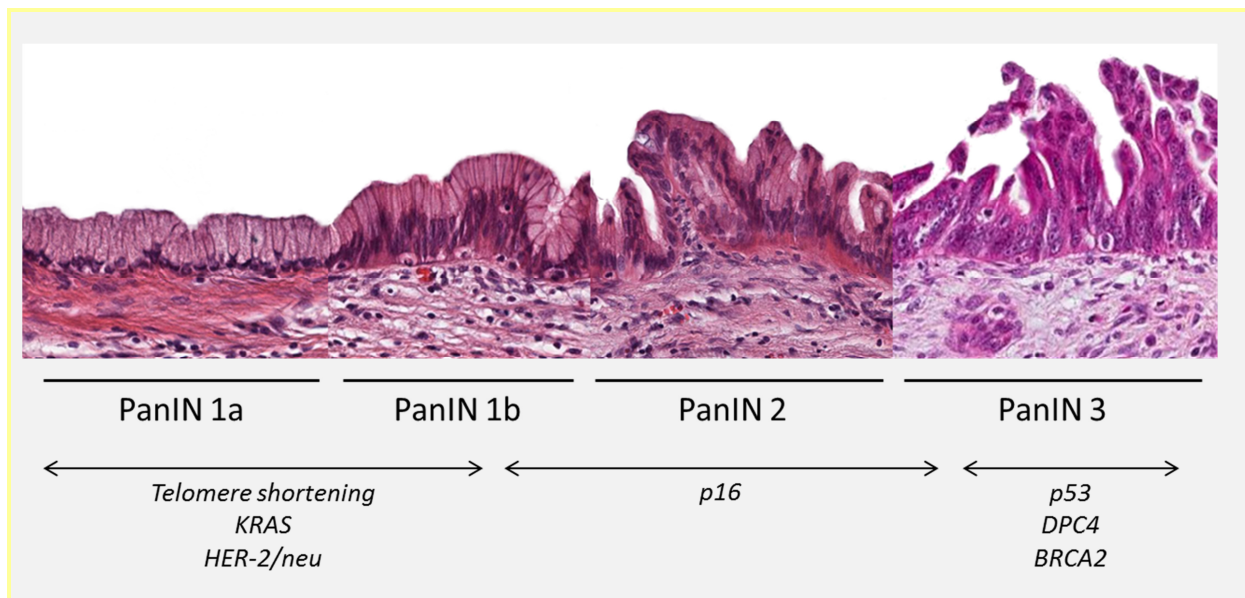
Figure 1 Progression Model of Pancreatic Carcinogenesis from PanIN

PDAC is thought to evolve mostly from ductal lesions called PanIN. Initiation and progression of carcinogenesis is triggered by various genetic alterations that cause both morphological changes and determine the classification in PanIN 1, 2 and 3 as well as behavioral changes like invasive potential. Whereas telomere shortening and mutations affecting *KRAS* are early events, changes in *TP53*, *CDKN2A* and *SMAD4* are predominantly detectable in lesions of higher grading.

1.2.3   Intraductal Papillary Mucinous Neoplasm (IPMN) – Morphological Subtypes and Clinical
         Significance

Intraductal papillary mucinous neoplasms (IPMN) are macroscopically visible epithelial neoplasms of the pancreas characterized by papillary growth on the gross and microscopical level and by the production of vast quantities of mucin. IPMN can harbor an invasive component and therefore

progress to PDAC. IPMN constitute 3-5% of all pancreatic neoplasms and 20% of pancreatic cystic tumors (Kosmahl, Pauser et al. 2004). They appear slightly more often in men than in women (3:2) and the mean age of patients presenting with IPMN is 63 years (de Wilde, Hruban et al. 2012).

IPMN cause obstruction of the pancreatic ductal system with ductal dilatation and retention of pancreatic secretion, evoking non-specific symptoms such as abdominal pain, back pain, loss of weight and recurrent episodes of pancreatitis. Later symptoms are associated with insufficiency of both the exocrine and endocrine gland, resulting in symptoms of maldigestion, e.g. steatorrhea, and diabetes mellitus (Castillo and Adsay 2010). Due to their size, IPMN can be detected by imaging such as CT-scan, endoscopic ultrasonography (Yamao, Ohashi et al. 2001) and ERCP/MRCP (Koito, Namieno et al. 1998), which reveals a dilated pancreatic duct and numerous cyst-like formations. However, histologic examination of the resected specimen still represents the gold standard for diagnosis.

70% of IPMN are localized in the head of the gland, 20% are found in the body/tail section and 5-10% affect the entire gland (Schnelldorfer, Sarr et al. 2008). The neoplasm is mostly larger than 1 cm and shows a papillary and villous growth pattern, but a relatively flat appearance is possible as well. Depending on the involvement of different parts of the duct system, IPMN can be subclassified as main duct type and branch duct type IPMN, although there is a combination of both types in some cases (Hruban, Takaori et al. 2004). In contrast to IPMN involving the main duct, branch duct IPMN are more often localized in the head of the pancreas and less frequently found to harbor an invasive carcinoma (Bernard, Scoazec et al. 2002).

IPMN show various grades of dysplasia which determines the classification of the neoplasm as low grade and high grade IPMN along with architectural changes (Basturk, Hong et al. 2015). Various morphological manifestations of IPMN have been described (table1), depending on architectural and cellular differentiation (gastric, intestinal, pancreatobiliary and oncocytic IPMN), some in correlation with degrees of dysplasia. Moreover, the respective subtype is characterized by its own expression profile of apomucins MUC1, MUC2 and MUC5AC (Furukawa, Kloppel et al. 2005).

Table 1 Classification and Features of IPMN

Subtype	Histological features	Grading	MUC1	MUC2	MUC5AC
Gastric	Columnar cells with basal nuclei and apical mucin, often flat or forming low thick papillae	Low grade	-	-	+
intestinal	Columnar cells with oval nuclei, pseudostratification, forming elongated villous papillae	intermediate to high grade	-	+	+
pancreatobiliary	Cuboidal cells with rounded nuceli, featuring thin complex papillae with bridging and cribrifom growth patterns	High grade	+	-	+
Oncocytic	Eosinophilic cells forming thick branching papillae with cribriform patterns (intraepithelial lumina)	High grade	+	-	-/+

One third of IPMN are associated with an invasive carcinoma (Matthaei, Schulick et al. 2011). The invasive component can either show the characteristic features of PDAC or it can emerge as a so called colloid carcinoma with huge quantities of extracellular mucin, forming pools that contain free floating neoplastic cells. This form of cancer is associated with intestinal IPMN and bears a better prognosis than PDAC (Nakata, Ohuchida et al. 2011).

Molecular investigation has revealed several genetic alterations that arise during transformation in IPMN. Similar to PanIN, *KRAS* mutations seem to be an early event with an increasing frequency in higher grade of dysplasia (Schonleben, Qiu et al. 2008) with the exception of oncocytic IPMN which exhibit wild type *KRAS* (Patel, Adams et al. 2002). Whole-exome sequencing of IPMN tissue samples has further revealed *GNAS* mutations and consecutive activation of G-protein signaling to be a hallmark of some IPMN subtypes (Furukawa, Kuboki et al. 2011). Other genes, like *TP53* are later inactivated by loss of heterogeneity (LOH) (Wada 2002). In contrast to PDAC, both non-invasive and invasive IPMN almost never show alterations affecting *SMAD4/DPC4*, which might be diagnostically valuable (Iacobuzio-Donahue, Klimstra et al. 2000). Hypermethylation can be found in the majority of IPMN which affect various genes, e.g. *CDKN4*/p16 (Sato, Ueki et al. 2002). A smaller proportion of IPMN, exclusively intestinal type, has been reported to show missense mutation in *PIK3CA* (Schonleben, Qiu et al. 2006).

1.2.4 Mucinous Cystic Neoplasm (MCN)

Mucinous cystic neoplasms (MCN) are cyst-forming neoplasms featuring a mucin-producing epithelium and a characteristic ovarian-like stroma. MCN have a significant malignant potential and can progress to PDAC and thus must be considered as another precursor disease thereof. With 6% of all pancreatic cystic tumors, MCN range among the rare pancreatic neoplasms (Kloppel and Kosmahl 2001). They are far more common in women than in men with a female/male ratio of about 20/1 and most patients are between 40 and 50 years of age at the time of diagnosis (de Wilde, Hruban et al. 2012).

Patients diagnosed with MCN usually present with rather non-specific abdominal symptoms such as epigastric pain, a sense of abdominal fullness, but also, even though less commonly, with nausea, vomiting, diarrhea and loss of weight. Due to the size of the cystic lesions, MCN are accessible to imaging techniques like (endoscopic) ultrasound, MRI-Scan or CT-Scan (Brugge 2015). Notably, peripheral calcifications of a mucinous cystic lesion revealed by imaging are considered as a relevant feature of malignancy (Procacci, Carbognin et al. 2001).

Macroscopically, MCN usually consist of a solitary, large cyst that is confined by a thick fibrotic pseudocapsule. In contrast to other pancreatic neoplasms, MCN are typically localized in the body or the tail of the pancreas (Matthaei, Schulick et al. 2011). The cysts are mostly multilocular with a smooth inner surface. Papillary masses as well as solid mural nodules are a feature of high grade dysplasia or even invasive cancer (Distler, Aust et al. 2014). Another important characteristic is that MCN do not communicate with the ductal system of the pancreas (Bosman, Carneiro et al. 2010).

Histologic examination reveals a mucin-producing epithelium that lines the cystic walls in flat sheets or papillae. Similar to IPMN, MCN are classified as low or high grade lesions determined by the extent of cellular and architectural atypia (Basturk, Hong et al. 2015). An impressive feature of MCN that is quite unique among pancreatic neoplasms, is their ovarian like stroma which consists of densely packed spindle cells with sparse cytoplasm and uniform elongated wavy nuclei (Hruban, Pitman et al. 2007).

One third of MCN are associated with an invasive carcinoma (Crippa, Fernandez-Del Castillo et al. 2010) that can exhibit the growth patterns of PDAC with a tubular arrangement of tumor cells and the characteristic desmoplastic reaction (Luttges, Feyerabend et al. 2002).

Concerning molecular alterations, sequential genomic changes have been observed similarly to those in PanIN. Activating point mutations of *KRAS* seem to be an early event of tumor progression, whereas affection of *TP53* and *SMAD4/DPC4* occur later (Yonezawa, Higashi et al. 2008). Moreover, a marked proportion of MCN feature inactivating mutations of tumor suppressor gene *RNF43*, a characteristic shared with other mucinous lesions like IPMN (Wu, Jiao et al. 2011). Alternated methylation of *CDKN2A* is observed in only a small proportion of cases (Kim, Wu et al. 2003).

1.2.5 Intraductal Tubulopapillary Neoplasms (ITPN) – A New and Evolving Entity

Intraductal tubulopapillary neoplasms (ITPN) of the pancreas have been recognized as a new entity of pancreatic neoplasms in the last WHO Classification of Tumours of the Digestive System (Bosman, Carneiro et al. 2010). Apart from morphological descriptions, only little is known about the biology of ITPN and their pathogenesis. Accounting for less than 1% of pancreatic exocrine neoplasms, ITPN are rare, grossly visible intraductal epithelial neoplasms characterized by ductal differentiation, a tubular growth pattern and both cellular and architectural high grade dysplasia (Yamaguchi, Shimizu et al. 2009).

ITPN seem to afflict both sexes equally and the mean age is 58 years with a relatively wide range (Yamaguchi, Shimizu et al. 2009). Clinical signs of ITPN are unspecific and similar to those in patients with IPMN. As macroscopic lesions, ITPN are detectable by imaging techniques and are often discovered incidentally (Basturk, Adsay et al. 2017).

On gross examination, ITPN consist of a solid nodular mass growing in association with the ductal system and dilating the affected sections. In contrast to IPMN, the formation of cysts and the production of mucin are uncommon for ITPN. The lesion is usually large (with an average diameter of 6 cm) and is mostly located in the head (~50%) or involves the gland diffusely in about one third of cases (Bosman, Carneiro et al. 2010).

Microscopically, ITPN are characterized by a homogeneous tubular and occasionally tubulopapillary growth pattern of back-to-back glands which create cribriform structures within dilated pancreatic ducts. The glands consist of cuboidal cells displaying frequent mitoses and significant nuclear atypia (Bosman, Carneiro et al. 2010).

ITPN display cellular and architectural features of high grade dysplasia and 40% are associated with an invasive carcinoma (Klimstra DS 2007). In some cases, the invasive component is not readily identifiable as it only consists of thin strands of neoplastic cells embedded within the stroma in the circumference of the lesion (Bosman, Carneiro et al. 2010).

Genetic profiling has shown that *KRAS* and *BRAF* mutations are rare among ITPN, as are mutations of *SMAD4/DPC4*. Aberrant expression of p53 and p16 could be observed more frequently, in 20% and 54%, respectively (Yamaguchi, Shimizu et al. 2009). A more recent analysis on genetic changes affecting *PIK3CA* revealed somatic mutations in 3 of 14 cases of ITPN and none in a control group of gastric type IPMN (Yamaguchi, Kuboki et al. 2013).

2. Claudins in Cancer

2.1 Claudins and the Physiology of the Tight Junction

Epithelial and endothelial cell layers form boundaries that separate tissues from environment, body cavities and luminal compartments. A hallmark of epithelial function is the control of exchange of

molecules and other solutes across that border. Cell-cell contacts and interactions are essential to control transepithelial transport. Tight junctions (TJ) set up the most apical of junctional complexes between epithelial cells responsible for the control of paracellular transport and maintaining cell polarity. Claudins, whose name is derived from the Latin verb "claudere" ("to close"), have been identified as the critical component of TJ (Furuse, Fujita et al. 1998, Crippa, Salvia et al. 2008). They are part of a genetic superfamily that involves more than 24 members. From a phylogenetic point of view, they are assumed to be a rather old family of proteins, since similar genes have been identified not only in vertebrates but also in lower chordates and even invertebrates (Wu, Schulte et al. 2004).

The expression products of claudin genes vary in size between 20 and 27 kDa and share some structural as well as functional features (figure 2). Claudins are tetraspan membrane proteins with 4 helical transmembrane domains. Both termini are oriented towards the cytoplasm: the short, more conserved N-terminus of ~7 residues and the C-terminus, which is more variable in length and sequence. Whereas the functions of the N-term remain unknown, the C-term is better characterized. Among others, it contains a PDZ-binding domain that enables claudins to interact with cytoskeleton components which is vital for the structural and functional integrity of TJs (Itoh, Furuse et al. 1999). Other motifs and their binding partners suggest the involvement of claudins in the regulation of other cell functions and signaling pathways. Furthermore, the carboxy-terminal sequence exhibits various sites and residues that are eligible for posttranslational modification (see below). Two loops make up the extracellular unit of the molecule, whereas the first loop is significantly larger than the second and contains a highly conserved sequence that defines all claudins. While the big loop is responsible for paracellular charge selectivity, transepithelial resistance (TER) and intramolecular stabilization (Angelow, Ahlstrom et al. 2008), the second loop seems to be involved in trans-interaction with claudins of adjacent cells via hydrophobic interactions of aromatic amino acid residues (Piontek, Winkler et al. 2008).
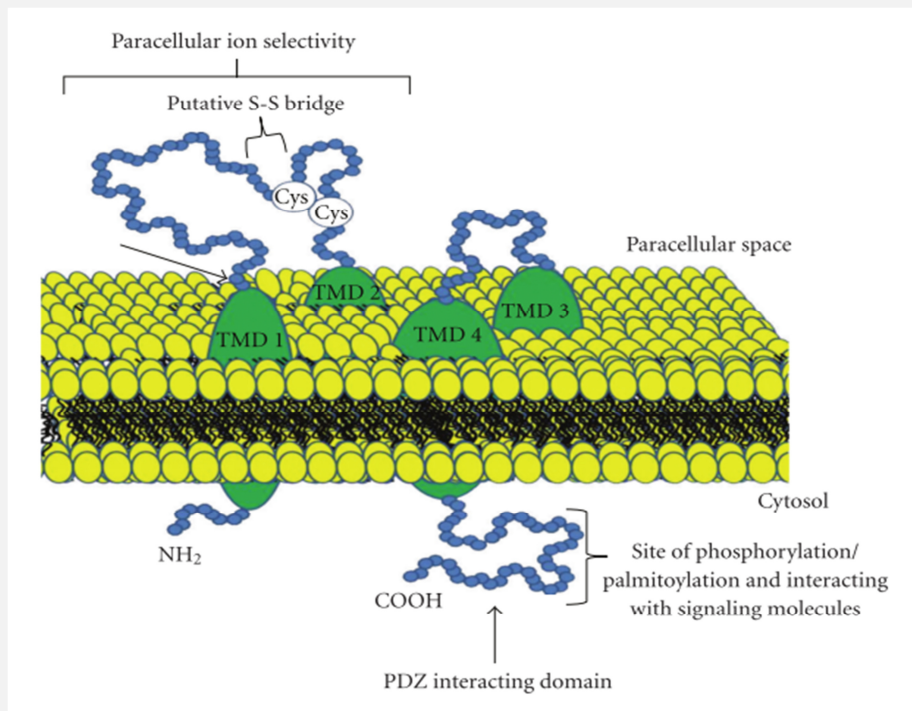
Figure 2 Structure and Functional Elements of Claudins (Singh, Sharma et al. 2010)

Claudins are tetraspan integral membrane proteins with two extracellular loops (ECL) and both termini oriented towards the cytoplasm. The first ECL contains a recognition sequence that characterizes claudin family members; amino acid residues at certain positions are crucial for functional properties of claudins as TJ components, e.g. charge selectivity for paracellular transport of solutes. The second ECL is supposed to play a role in heterotypic oligomerization of claudins forming TJ strands. The carboxy-terminal sequence contains sites for posttranslational modification as well as binding motifs for various molecules involving claudins in signaling pathways and linking them to cytoskeleton elements.

Among the functions of TJs, the maintenance of cell polarity must be highlighted. By forming a highly selective barrier, TJs contribute to compartmentation by restricting diffusion of solutes across the barrier and by inhibiting membrane components, e.g. receptors, from migrating between luminal and basolateral membrane sections. Compartmentation is vital for complex cellular mechanisms like signaling and transport (Singh, Sharma et al. 2010).

Although claudins are expressed in a tissue specific pattern, some of those patterns were shown to change during tumorigenesis, but the effect of these alterations is not altogether understood and is therefore in the focus of cancer research (Singh, Sharma et al. 2010).

2.2 Expression and Regulation of Claudin-18 in Normal and Neoplastic Tissue

2.2.1 Orthotopic Expression of Claudin-18

In contrast to a variety of other claudins that are more widely expressed, the expression of the tight junction protein claudin-18 has been shown to be restricted to lung and gastric mucosal epithelia (figure 3) (Hewitt, Agarwal et al. 2006). Interestingly, the molecule appears in at least two tissue

specific isoforms, lung-specific claudin-18a1 and stomach-specific claudin-18a2, differing in the amino acid sequence of the first ECL, which, as described above, is crucial for functional properties of claudins. On the genetic level, *CLDN18* contains two different sequences for exon 1 with their own independent promoter sequences, resulting in different transcripts by alternate splicing. Both human alternate transcripts encode a protein sequence of 261 residues with a calculated mass of 27,589 kDa (stomach-specific claudin-18a2, NCBI Reference Sequence: NP_001002026.1) and 25,562 kDa (lung-specific claudin-18a1, NCBI Reference Sequence: NP_057453.1), respectively. To this point, little is known about the regulation of claudin-18 expression on transcriptional as well as on post-transcriptional level, though there seem to be differences in the expression of the two isoforms. Investigation of gastric cancer cells demonstrated that the expression of claudin-18a2 is susceptible to stimulation by phorbol esters, which indicates the involvement of PKC/MAPK/AP-1 dependent pathways in the regulation of claudin-18a2 expression (Yano, Imaeda et al. 2008). Phorbol esters, like Phorbol 12-myristate 13-acetate (PMA), are herbal molecules that function as exogenous activators of protein kinase C (PKC) by mimicking diacylglycerol (DAG), the natural activator of PKC. They have been shown to influence cell signaling and metabolism promoting inflammatory responses and tumorigenic cellular changes (Goel, Makkar et al. 2007).

Immunogold electron microscopy (IEM) was performed to determine the subcellular localization of claudin-18. IEM revealed that the molecule is exclusively expressed as membrane bound complexes and is absent from other organelles or compartments which is consistent with its function as a tight junction component (Niimi, Nagashima et al. 2001). In the lung, claudin-18a1 is expressed in pneumocytes I and II, but seems to be absent in the bronchial epithelium. The expression is often maintained in lung derived tumors, notably in adenocarcinomas (Merikallio, Paakko et al. 2011). Gastric expression of claudin-18a2 is limited to exocrine and endocrine glandular cells of the gastric mucosa. It is noteworthy that highly proliferating cells of the neck region of the gastric glands seem to lack claudin-18a2 expression, whereas cells of the pit region and base of the glands showed robust expression. Those findings suggest that claudin-18a2 is absent in proliferating cells and stem cells of the upper isthmus and is a marker of gastric differentiation of an advanced level (Sahin, Koslowski et al. 2008). Claudin-18 expression is maintained during the process of carcinogenesis, thus the majority of primary gastric carcinomas also show significant expression of claudin-18a2 as a sign of gastric lineage (figure 3). However, expression is more frequently observed in diffuse type gastric cancer than in adenocarcinomas exhibiting intestinal features of differentiation (Sahin, Koslowski et al. 2008).

2.2.2   Ectopic Expression of Claudin-18 in Pancreatic Neoplasms

According to the results of expression profiling, claudin-18 expression is not limited to lung and stomach tissue, but it could also be detected in a set of other primary tumors, like esophageal cancer, non-small cell lung cancer, ovarian cancer and pancreatobiliary neoplasms. Another interesting

finding was the association of claudin-18 expression with certain phenotypical features of tumors, as for example being limited to ductal adenocarcinomas and not observed in neuroendocrine or acinar cell neoplasms of the pancreas. With the exception of lung cancer, all other malignancies expressed the stomach-specific isoform claudin-18a2. Hence, it was postulated that claudin-18, as a cell surface antigen, could be useful in targeted therapeutic strategies for the treatment of various forms of cancer (Sahin, Koslowski et al. 2008).

Claudin-18 expression in PDAC is particularly interesting since it might strike a new path in terms of early detection and treatment. We still have little understanding about the ectopic activation of claudin expression in tumors, but similar regulatory mechanisms seem to be at work as in the normal tissue. Induction of claudin-18 expression was observed in PDAC cells when treated with PMA, a potent PKC-activator, and this expression could be modified by DNA methylation in these cells (Ito, Kojima et al. 2011).

Immunohistolabeling of pancreatic tissue has revealed that claudin-18 is absent in normal pancreatic parenchyma and also in reactive glands in samples of chronic pancreatitis (Karanjawala, Illei et al. 2008). Furthermore, claudin-18 expression in PDAC is associated with certain features of differentiation. Whereas samples of well-differentiated adenocarcinomas often showed strong labeling for claudin-18, expression decreased over moderately to poorly differentiated tumors. Those findings suggest that loss of claudin-18 as an epithelial marker is part of the changes that take place during epithelial-mesenchymal transition (EMT), which coincides with loss of differentiation of tumor cells (Soini, Takasawa et al. 2012).

Another noteworthy aspect is the expression of claudin-18, not only in invasive cancer, but already in premalignant lesions. Claudin-18 has been found to be solidly expressed in low grade and high grade PanIN (Karanjawala, Illei et al. 2008). Concerning IPMN, claudin-18 expression is notably strong in cases that exhibit a gastric phenotype in contrast to intestinal type IPMN (Tanaka, Shibahara et al. 2011). Finally, claudin-18 was also detected in the majority of cases of MCN (Lee, Kim et al. 2011). These findings indicate that activation of claudin-18 expression is an early event in the process of carcinogenesis in pancreatic neoplasms, rendering it attractive for approaches of early detection (Tanaka, Shibahara et al. 2011). Additionally, similarly to what was described for gastric cancer (Singh, Toom et al. 2017), the expression of claudin-18 has been tested in a panel of pancreatic cancer tissues using the specific antibody IMAB362 which can be employed for individualized cancer therapy (Woll, Schlitter et al. 2014).

3. Aim of the Study

The present study was conducted to contribute to the characterization of claudin-18 as a possible biomarker and therapeutic target in pancreatic neoplasms and to gain further understanding about its functional properties in the course of tumorigenesis. A large collective of well-characterized PDAC

and its precursors was analyzed for claudin-18 expression. Results were then correlated with clinicopathological data including overall patient survival.

II. MATERIAL AND METHODS

1. Material

1.1 Reagents

Product	Company
3,3'-Diaminobenzidine (DAB)	Medac GmbH, Wedel (D)
Acetic acid	Merck KGaA, Darmstadt (D)
Acrylamide/Bis Solution 40%, 37.5:1	Bio-Rad Laboratories GmbH , Munich (D)
Adefofix fixing concentrate	Adefo-Chemie, Dietzenbach (D)
Adefofur developing concentrate	Adefo-Chemie, Dietzenbach (D)
Agarose LE for gel electrophoresis	Biozym Scientific GmbH, Hessisch Oldendorf (D)
Alexa Fluor 546 goat anti rabbit IgG	Life Technologies GmbH, Darmstadt (D)
Ammonium persulfate	Sigma-Aldrich Chemie GmbH, Steinheim (D)
Antibody diluent Dako REAL™	Dako Deutschland GmbH, Hamburg (D)
Biozym LE Agarose	Biozym Scientific GmbH, Hessisch Oldendorf (D)
Bovine Serum Albumin (BSA)	Sigma-Aldrich Chemie GmbH, Steinheim (D)
Bromophenol blue	Sigma-Aldrich Chemie GmbH, Steinheim (D)
Citric acid	Merck KGaA, Darmstadt (D)
Complete mini Protease Inhibitor Cocktail Tablets	Roche Diagnostics, Mannheim, (D)
Deoxycholic acid	Sigma-Aldrich Chemie GmbH, Steinheim (D)
Dimethylsulfoxid	Sigma-Aldrich Chemie GmbH, Steinheim (D)
DNA-Loading dye 6X	Thermo Fisher Scientific, Schwerte (D)
dNTP Set, 100 mM Solutions	Invitrogen™, Darmstadt (D)
Dulbecco's Modified Eagle Medium (D-MEM) (1X), liquid (high glucose) 4.5 g/L	Gibco®, Darmstadt (D)
ECL mouse IgG, HRP-linked whole Ab (from sheep)	GE Healthcare, Munich (D)
ECL rabbit IgG, HRP-linked whole Ab (from sheep)	GE Healthcare, Munich (D)
Eosin	Sigma-Aldrich Chemie GmbH, Steinheim (D)

Ethanol	Merck KGaA, Darmstadt (D)
Ethidium bromide	Amresco, Solon (USA)
Ethylene glycol tetraacetic acid	Sigma-Aldrich Chemie GmbH, Steinheim (D)
Ethylenediaminetetraacetic acid	Sigma-Aldrich Chemie GmbH, Steinheim (D)
Fetal Bovine Serum (FBS)	Gibco®, Darmstadt (D)
Formalin	Staub & Co. GmbH, Munich (D)
GeneRuler™ 1 kb DNA Ladder	Thermo Fisher Scientific, Schwerte (D)
GeneRuler™ 100 bp DNA Ladder	Thermo Fisher Scientific, Schwerte (D)
Glycerin	Merck KGaA, Darmstadt (D)
Glycine	Sigma-Aldrich Chemie GmbH, Steinheim (D)
Goat serum	Abcam plc, Cambridge, (UK)
Hemalm	AppliChem GmbH, Darmstadt (D)
HistoMark Biotin-Streptavidin Peroxidase Kit	KPL Inc., Gaithersburg (USA)
Hoechst 33342	Sigma-Aldrich Chemie GmbH, Steinheim (D)
Hydrogen chloride	neoLab, Heidelberg (D)
Hydrogen peroxide 30%	Merck KGaA, Darmstadt (D)
Isopropanol	Merck KGaA, Darmstadt (D)
Methanol	Merck KgaA, Darmstadt (D)
Nonfat dry milk	Carl-Roth GmbH & Co.KG, Karlsruhe (D)
Nonidet-P40	Sigma-Aldrich Chemie GmbH, Steinheim (D)
Opti-MEM®, reduced serum media	Gibco®, Darmstadt (D)
Penicillin-Streptomycin, liquid	Gibco®, Darmstadt (D)
Pertex mounting medium	Medite GmbH, Burgdorf, (D)
Phorbol 12-myristate 13-acetate	Sigma-Aldrich Chemie GmbH, Steinheim (D)
Phosphate buffered saline (PBS)	GE Healthcare, Munich (D)
PhosSTOP Phosphatase Inhibitor Cocktail Tablets	Roche Diagnostics, Mannheim (D)
Ponceau S dye	Sigma-Aldrich Chemie GmbH, Steinheim (D)
Potassium chloride	Sigma-Aldrich Chemie GmbH, Steinheim (D)
Prestained Protein ladder Plus, PageRuler™	Thermo Fisher Scientific, Schwerte (D)
Prestained Protein ladder, PageRuler™	Thermo Fisher Scientific, Schwerte (D)
Propidiumiodid	AppliChem GmbH, Darmstadt (D)

Proteinase K	Roche Diagnostics, Mannheim (D)
RNase inhibitor RNaseOUT™	Life Technologies GmbH, Darmstadt (D)
Sodium chloride	Merck KgaA, Darmstadt (D)
Sodium dodecyl sulfate 20% (w/v) solution	AppliChem GmbH, Darmstadt (D)
Sucrose	Sigma-Aldrich Chemie GmbH, Steinheim (D)
Super Signal West Femto Chemiluminescent Substrate	Thermo Fisher Scientific, Schwerte (D)
Super Signal West Pico Chemiluminescent Substrate	Thermo Fisher Scientific, Schwerte (D)
Taq DNA Polymerase BioTherm™	Ares Bioscience GmbH, Köln (D)
Taq DNA Polymerase 10X reaction buffer	Ares Bioscience GmbH, Köln (D)
Tetramethylethylenediamine (TEMED)	Bio-Rad Laboratories GmbH , Munich (D)
Triton X-100	Merck KGaA, Darmstadt (D)
Trizma® base	Sigma-Aldrich Chemie GmbH, Steinheim (D)
Trypan blue solution 0.4%	Sigma-Aldrich Chemie GmbH, Steinheim (D)
Trypsin, 0.05% with EDTA	PAA Laboratories GmbH, Cölbe (D)
Tween 20	Merck KGaA, Darmstadt (D)
Vectashield mounting medium for fluorescence	Vectashield, Loerrach (D)
Water, Aqua ad iniectabilia	AlleMan Pharma GmbH, Rimbach (D)
Xylol	Merck KGaA, Darmstadt (D)
β-Mercaptoethanol	Sigma-Aldrich Chemie GmbH, Steinheim (D)

1.2 Consumables

Product	*Company*
Amersham Hybond™ ECL™ Nitrocellulose Membrane	GE Healthcare Lifescience, Freiburg (D)
Amersham Hyperfilm ECL	GE Healthcare Lifescience, Freiburg (D)
Cell Scraper	SARSTEDT AG & Co., Nümbrecht (D)
Combitips® for Multipette® 5 ml	Eppendorf AG, Hamburg (D)
Corning®DeckWorks® Pipette tips, 10 μl	Sigma-Aldrich Chemie GmbH, Steinheim (D)
Corning®DeckWorks® Pipette tips, 20 μl	Sigma-Aldrich Chemie GmbH, Steinheim (D)

Corning®DeckWorks® Pipette tips, 200 µl	Sigma-Aldrich Chemie GmbH, Steinheim (D)
Corning®DeckWorks® Pipette tips, 1000 µl	Sigma-Aldrich Chemie GmbH, Steinheim (D)
Coverslips	Carl Roth GmbH & Co.KG, Karlsruhe (D)
Cryotubes	A. Hartenstein, Würzburg (D)
Cyto Chamber 2 ml	Andreas Hettich GmbH & Co.KG, Tuttlingen (D)
Embedding cassettes	A. Hartenstein, Würzburg (D)
Microscope Slide	Thermo Fisher Scientific, Schwerte (D)
Mini-PROTEAN Tetra Electrophoresis System	Bio-Rad Laboratories GmbH , Munich (D)
PCR tube strips 0.2 ml	Eppendorf AG, Hamburg (D)
Pipettes, Pasteur glass 3.2 ml	Carl-Roth GmbH & Co.KG, Karlsruhe (D)
Pipettes, serological CELLSTAR® 2 ml	Greiner Bio-One, Frickenhausen (D)
Pipettes, serological CELLSTAR® 5 ml	Greiner Bio-One, Frickenhausen (D)
Pipettes, serological CELLSTAR® 10 ml	Greiner Bio-One, Frickenhausen (D)
Pipettes, serological CELLSTAR® 25 ml	Greiner Bio-One, Frickenhausen (D)
Pipettes, serological CELLSTAR® 50 ml	Greiner Bio-One, Frickenhausen (D)
PowerPac Basic Power Supply	Bio-Rad Laboratories GmbH , Munich (D)
Reaction tubes 1.5 ml	Eppendorf AG, Hamburg (D)
Reaction tubes 2 ml	Eppendorf AG, Hamburg (D)
Reaction tubes Falcon^{TM} Blue Max 15 ml	BD Bioscience, Heidelberg, (D)
Reaction tubes Falcon^{TM} Blue Max 50 ml	BD Bioscience, Heidelberg, (D)
Richard-Allan Scientific™ HistoGel™	Thermo Fisher Scientific, Schwerte (D)
Safe seal microtubes	Eppendorf AG, Hamburg (D)
Syringe, single-use 20 ml	B. Braun Melsungen AG, Melsungen (D)
Tissue culture dish (60,1 cm^2)	TPP, Trasadingen (CH)
Tissue culture flasks (25 cm^2, 75 cm^2)	TPP, Trasadingen (CH)
Tissue Culture Test Plates (96-well, 24-well, 6-well)	TPP, Trasadingen (CH)
Whatman filter paper	Neolab, Heidelberg (D)
Wide mini Sub Set GT electrophoresis system	Bio-Rad Laboratories GmbH , Munich (D)

1.3 Equipment

Product	Company
Accu-jet® pro	Brand GmbH + CO KG, Wertheim (D)
Aperio ScanScope® CS2	Leica Biosystems Nussloch GmbH, Nussloch (D)
ASYS Expert Plus Microphotometer 8 Kanal	Biochrom AG, Berlin (D)
Axio Observer Z1	Carl Zeiss AG, Jena (D)
Axiocam ICm1	Carl Zeiss AG, Jena (D)
Axiovert 135	Carl Zeiss AG, Jena (D)
Axiovert 25	Carl Zeiss AG, Jena (D)
Branson Digital Sonifier® 250-D	G. Heinemann Ultraschall- und Labortechnik, Schwäbisch Gmünd (D)
Cat SRX 101 A development machine	Konica minolta, Langenhagen (D)
Dako Autostainer Universal Staining System	Dako Deutschland GmbH, Hamburg (D)
Dispenser Multipette® plus	Eppendorf AG, Hamburg (D)
Ebox VX2 gel documentation system	Peqlab Biotechnology GmbH, Erlangen (D)
Electrophoresis Transfer Cell mini Trans-Blot®	Bio-Rad Laboratories GmbH , Munich (D)
Eppendorf Mastercycler gradient	Eppendorf AG, Hamburg (D)
Filter set 38 Endow GFP shift free	Carl Zeiss AG, Jena (D)
Filter set 43 Cy3, d=25 shift free	Carl Zeiss AG, Jena (D)
Filter set DAPI	Carl Zeiss AG, Jena (D)
Filterset 38 Endow GFP	Carl Zeiss AG, Jena (D)
Filterset 43 Cy3	Carl Zeiss AG, Jena (D)
Gel documentation system	Vilber Lourmat, Eberhardzell (D)
GFL incubation waterbath	GFL GmbH, Burgwedel (D)
Glass coverslipper Promounter RCM2000	Medite GmbH , Burgdorf (D)
Haereus Hera Safe CO2 incubator	Thermo Fisher Scientific, Schwerte (D)
Heating block Thermomixer® comfort 1.5 ml	Eppendorf AG, Hamburg (D)
Heating block ThermoStat plus 1.5 ml	Eppendorf AG, Hamburg (D)
Heating oven type BE400	Memmert, Schwabach (D)
Heating plate HP 30 digital IKATHERM	IKA®-Werke GmbH & CO. KG, Staufen (D)

Heracell 150i CO2 incubator	Thermo Fisher Scientific, Schwerte (D)
Hood Uniflow UVUB 1800	UniEquip, Planegg (D)
Hotplate stirrer IKAMAG® RCT	IKA® Werke GmbH und Co.KG, Staufen (D)
IKA® MS1 minishaker	IKA® Werke GmbH und Co.KG, Staufen (D)
Ikamage® RCT magnetic stirrer	IKA® Werke GmbH und Co.KG, Staufen (D)
Incubator innova CO-170	New Brunswick Sci., Edison (NJ, USA)
Incubator shaker Model G25	New Brunswick Sci., Edison (NJ, USA)
Laboratory balance BP 310 S	Sartorius AG, Göttingen (D)
Leitz Labovert FS	Leica Microsystems GmbH, Wetzlar (D)
Liquid Nitrogen tank MVE TEC 3000 (1500 series)	Chart MVE BioMedical GmbH, Wuppertal (D)
Magnetic stir bars, various sizes	NeoLab, Heidelberg (D)
Magnetic stirrer MR2000	Heidolph Instruments, Schwabach (D)
Manual Tissue Arrayer	Beecher Instruments Inc., Sun Prairie (USA)
Microm HM 335 E	Thermo Fisher Scientific, Schwerte (D)
Microplate Reader Model 680	Bio-Rad Laboratories GmbH , Munich (D)
Microscope EVOS xl	Life Technologies GmbH, Darmstadt (D)
Microtome blade	Pfm medical AG, Köln (D)
Microwave Privileg 1034HGD	Otto, Hamburg (D)
Miniprotean system 3 cell	Bio-Rad Laboratories GmbH , Munich (D)
Mini-PROTEAN Tetra Electrophoresis System	Bio-Rad Laboratories GmbH , Munich (D)
Nanodrop ND 2000c	Peqlab Biotechnology GmbH, Erlangen (D)
Neubauer counting chamber	Carl-Roth GmbH & Co.KG, Karlsruhe (D)
Olympus CX31 Binocular Microscope	Olympus Deutschland GmbH, Hamburg (D)
Paraffin Embedding System Medite TBS 88	Medite GmbH, Burgdorf, (D)
pH-Meter (pH 211)	HANNA Instruments GmbH, Kehl am Rhein (D)
Pressure cooker	WMF, Geislingen/Steige (D)
Rocker table Rocky®	Fröbel Labortechnik, Lindau (D)
Scales Sartorius universal	Sartorius AG, Göttingen (D)
Shandon Excelsior ES	Thermo Fisher Scientific, Schwerte (D)
Spectrophotometer NanoDrop® ND-1000	Thermo Fisher Scientific, Schwerte (D)

Spectrophotometer UV/VIS Novaspec II	Pharmacia LKB, Uppsala (S)
Stuart Scientific SD Rocking Platform STR	Keison products, Chelmsford (GB)
Thermomixer compact	Eppendorf AG, Hamburg (D)
Tissue Cool Plate COP 20	Medite GmbH, Burgdorf, (D)
Tissue Floatation Baths TFB 35	Medite GmbH, Burgdorf, (D)
Water bath shaker #1083	GFL GmbH, Burgwedel (D)
Wide mini Subset GT electrophoresis system	Bio-Rad Laboratories GmbH , Munich (D)

1.4   Kits

Product	*Company*
BCA Protein Assay Kit	Thermo Fisher Scientific, Schwerte (D)
High capacity cDNA Reverse Transcription Kit	Invitrogen™, Darmstadt (D)
Pierce® BCA Protein Assay Kit	Perbio Science Deutschland GmbH, Bonn (D)
QIAprep Spin Maxiprep Kit	Qiagen GmbH, Hilden (D)
QIAprep Spin miniprep Kit	Qiagen GmbH, Hilden (D)
RNeasy Mini Kit	Qiagen GmbH, Hilden (D)

1.5   Buffers

Blotting buffer

TRIS base	48 mM
Glycine	39 mM
SDS	0.025%
Methanol	20%

Citrate buffer

Citric acid	10 mM
pH 6	

Lämmli 5X

TRIS	312.5 mM
Glycerol	40%
SDS	10%
Bromophenol blue	0.005%

| β-Mercaptoethanol | 20% |

Ponceau S

| Ponceau S | 1 g |
| Acetic acid | 1% |

RIPA buffer

TRIS pH 7.4	20 mM
NaCl	150 mM
EDTA	1 mM
EGTA	1 mM
NP-40	1%
Deoxycholic Acid	0.5%

RLN

TRIS-HCl	50 mM
NaCl	140 mM
$MgCl_2$	1.5 mM
Nonidet P-40	0.5% (v/v)
pH 8.0	

Running buffer (SDS Page)

TRIS base	12.5 mM
Glycine	9.6 mM
SDS	0.05%

Running gel buffer 4X

| TRIS-HCl | 1.5 M |
| pH 8.8 | |

Stacking gel buffer 4X

| TRIS-HCl | 0.5 M |
| pH 6.8 | |

Stripping buffer

| MetOH | 10% |
| Acetic acid | 10% |

TBS 10X for immunofluorescence and immunocytochemistry

| TRIS base | 500 mM |
| NaCl | 1380 mM |

| KCl | 27 mM |
| pH 7.6 | |

TBS 10X for Western Blot
TRIS base	200 mM
NaCl	1360 mM
pH 7.6	

1.6 Tissues and Cell Lines

1.6.1 Tissue Samples

Tissue samples of PDAC, PanIN, IPMN, ITPN and MCN were obtained from the archive of the Institute of Pathology of the Technische Universität München, Germany. Additional samples of IPMN and ITPN were obtained from the archive of the Institute of Pathology of the University of Heidelberg. Tissue samples were used in fully anonymized form. IPMN had been previously characterized according to their mucin profile. Both tissue arrays and whole tissue sections were assessed for the expression of claudin-18 in pancreatic neoplasms. Cases of PDAC were staged according to the 7th edition of the UICC TNM classification of malignant tumors from 2009 (Sobin, Gospodarowicz et al. 2009). In line with the revised classification of premalignant lesions of the pancreas, a two-step grading system was applied for PanIN, IPMN and MCN (Basturk, Hong et al. 2015). Table 2 gives an overview of the investigated tissue samples.

Table 2 Sample Types and Numbers of Investigated Pancreatic Lesions

Sample	n [%]	in TMA	as whole tissue sections
PDAC	142[100]	142	-
Grading			
G1	9 [6,3]	9	-
G2	60 [42,3]	60	-
G3	73 [51,4]	73	-
T-stage			
T1/2	8 [6,4]	8	-
T3/4	117 [93,6]	117	-
Not applicable	17	17	-
N-stage			
N0	37 [29,6]	37	-
N1	88 [70,4]	88	-
Not applicable	17	17	-
PanIN	104 [100]	104	-
Low grade	83 [79,8]	83	-
High grade	21 [20,2]	21	-
IPMN	75 [100]	61	14
Subtype			
Gastric	30 [40,0]	30	-
Intestinal	21 [28,0]	21	-
Pancreatobiliary	14 [18,7]	8	6
Oncocytic	8 [10,7]	-	8
Null	2 [2,7]	2	-
Grading			
Low grade	42 [56,0]	42	-
High grade	33 [44,0]	19	14
MCN	44 [100]	-	44
Low grade	30 [68,2]	-	30
High grade	14 [31,8]	-	14
ITPN	6 [100]	-	6

1.6.2   Cell Lines

1.6.2.1 PDAC Cell Lines

All PDAC cell lines are derived from human malignant neoplasms of the pancreas; their origin, culture properties, characteristics and more are listed hereafter. Most PDAC cell lines were obtained from ATCC, The Global Bioresource Center with the exception of the cell lines BxPC-3, Colo-357 and T3M4, which were kindly provided by the AG Kleeff, Department of Surgery, Technische Universität München.

AsPC-1

Organism	Female, 62y, Caucasian
Tissue	Adenocarcinoma, ascites metastasis
Grade	G2 (moderately differentiated)
Culture properties	Adherent
Cellular products	carcinoembryonic antigen (CEA), human pancreas associated antigen, human pancreas specific antigen and mucin
Mutations	*TP53* -/- *KRAS* activating mutation *CDKN2A* frameshift mutation

BxPC-3

Organism	Female, 61y, Caucasian
Tissue	Adenocarcinoma, primary tumor
Grade	G2 (moderately differentiated)
Culture properties	Adherent
Cellular products	Mucin; pancreas cancer specific antigen (pancreas cancer associated antigen); CEA
Mutations	*TP53* inactivating mutation *KRAS* WT *CDKN2A* homozygous deletion

Capan-1

Organism	Male, 40y, Caucasian
Tissue	Adenocarcinoma, liver metastasis
Grade	G1 (well differentiated)
Culture properties	Adherent
Cellular products	Cystic fibrosis transmembrane conductance regulator (CFTR), mucin
Mutations	*TP53* inactivating mutation *KRAS* activation mutation *CDKN2A* homozygous deletion

Colo-357

Organism	Female, 77y, Caucasian
Tissue	Adenocarcinoma, lymph node metastasis
Grade	G2 (moderately differentiated)
Culture properties	Adherent
Cellular products	Pancreatic enzymes (trypsin, elastase and chymotrypsin), CEA, human chorionic gonadotropin (HCG)
Mutations	*TP53* WT *KRAS* WT *CDKN2A* WT

MIA Paca-2

Organism	Male, 65y, Caucasian
Tissue	Carcinoma, primary tumor
Grade	G3 (poorly differentiated)
Culture properties	Adherent, single cells and loosely attached clusters
Cellular products	human colony stimulating factor subclass I (CSF-I), plasminogen activator
Mutations	*TP53* inactivating mutation *KRAS* activating mutation *CDKN2A* homozygous deletion

PANC-1

Organism	Male, 56y, Caucasian
Tissue	Epitheloid carcinoma, ductal origin
Grade	G3 (poorly differentiated)
Culture properties	Adherent
Cellular products	-
Mutations	*TP53* inactivating mutation *KRAS* activating mutation *CDKN2A* homozygous deletion

SU.86.86

Organism	Female, 57y, Caucasian
Tissue	Ductal carcinoma, liver metastasis
Grade	G2-3 (moderately to poorly differentiated)
Culture properties	Adherent
Cellular products	CEA
Mutations	*TP53* inactivating mutation *KRAS* activating mutation *CDKN2A* homozygous deletion

T3M4

Organism	Male, 65y, Asian
Tissue	Adenocarcinoma, lymph node metastasis
Grade	G2 (moderately differentiated)
Culture properties	Adherent
Cellular products	CEA
Mutations	*TP53* inactivating mutation *KRAS* WT *CDKN2A* transcriptional inactivation (methylation)

1.6.2.2 Gastric Cancer Cell Lines

The following gastric cancer cell lines are derived from human malignant neoplasms of the stomach and were kindly provided by the AG Luber, Department of Pathology, Technische Universität München.

KATO III

Organism	Male, 55y, Asian
Tissue	Gastric carcinoma (signet ring cell adenocarcinoma), metastatic pleural effusion, lymph node metastasis and Douglas cul-de-sac
Grade	G3 (poorly differentiated)
Culture properties	Mixed, adherent and suspension
Cellular products	-

| Mutations | E-cadherin inactivating mutation |
| | *TP53* -/- |

MKN28

Organism	Female, 70y, Asian
Tissue	Gastric tubular adenocarcinoma, metastatic origin
Grade	G1 (well differentiated)
Culture properties	Adherent
Cellular products	-
Mutations	E-cadherin WT
	TP53 inactivating mutation

MKN45

Organism	Female, 62y, Asian
Tissue	Gastric adenocarcinoma, liver metastasis
Grade	G3 (poorly differentiated)
Culture properties	Adherent
Cellular products	CEA
Mutations	E-cadherin inactivating mutation
	TP53 WT

1.7   Antibodies and Primer Pairs

1.7.1   Antibodies

Primary antibodies

Antibody	*Dilution/Application*	*Provider*
Claudin-18 ABfinity™ Recombinant Rabbit Monoclonal Antibody	IHC: 1:1000 WB: 1:500 IF: 1:200	Invitrogen Corp., Carmillo (CA)
Claudin-18 (C-Term) Rabbit Polyclonal Antibody	IHC: 1:1000 WB: 1:500 ICC: 1:2000	Invitrogen Corp., Carmillo (CA)
Anti-α-Tubulin	WB: 1:10000	Santa Cruz Biotechnology, Inc., Heidelberg (D)

Secondary antibodies

Antibody	Dilution/Application	Provider
Alexa Fluor® 546 Goat Anti-Rabbit IgG (H+L) Antibody	IF: 1:200	Life Technologies GmbH, Darmstadt (D)
Biotin-labeled Rabbit IgG (H+L) Antibody	IHC: ready to use	KPL, Inc., Gaithersburg (USA)
ECL Mouse IgG, HRP-linked whole Antibody (from sheep)	WB: 1:2000	GE Healthcare, Munich (D)
ECL Rabbit IgG, HRP-linked whole Antibody (from sheep)	WB: 1:2000	GE Healthcare, Munich (D)

1.7.2   Primer Pairs

Primers for Mycoplasma nested PCR:

Primer Supermix 1

Myco-Fwd 1	5'-ACA CCA TGG GAG TTG GTA AT-3'	5 µM
Myco-Fwd 1t	5'-ACA CCA TGG GAG CTG GTA AT-3'	5 µM
Myco-Rev 1tt	5'-CTT CTT CGA CTT TCA GAC CCA AGG CAT-3'	2.5 µM
Myco-Rev 1	5'-CTT CAT CGA CTT TCA GAC CCA AGG CAT-3'	2.5 µM
Myco-Rev 1cat	5'-CCT CAT CGA CTT TCA GAC CCA AGG CAT-3'	2.5 µM
Myco-Rev 1ac	5'-CTT CAT CGA CTT CCA GAC CCA AGG CAT-3'	2.5 µM

Primer Supermix 2

Myco-Fwd 2a	5'-ATT CTT TGA AAA CTG AAT-3'	2.5 µM
Myco-Fwd 2	5'-GTT CTT TGA AAA CTG AAT-3'	2.5 µM
Myco-Fwd 2cc	5'-GCT CTT TCA AAA CTG AAT-3'	2.5 µM
Myco-Rev 2ca	5'-GCA TCC ACC ACA AAC TCT-3'	2.5 µM
Myco-Rev 2	5'-GCA TCC ACC AAA AAC TCT-3'	2.5 µM
Myco-Rev 2at	5'-GCA TCC ACC AAA TAC TCT-3'	2.5 µM

Primer pair for reverse transcription PCR/cDNA amplification (Tanaka, Shibahara et al. 2011) provided by Eurofins Genomics GmbH, Ebersberg (D):

cDNA fwd	5′-TGT GCG CCA CCA TGG CCG TG-3′	5.0 µM
cDNA rev	5′-ACT CGG TGA AGC CAG AGC TC-3′	5.0 µM

2. Methods

2.1 Histopathological Investigation

2.1.1 Hematoxylin and Eosin Stain

Formalin-fixed, paraffin-embedded tissue sections were dewaxed in xylene and rehydrated in a graded alcohol series. After that, sections were rinsed in distilled water and stained with hematoxylin for 5 min for nuclear staining. Differentiation was obtained by rinsing the slides with tap water for 5 min. Eosinophilic structures were stained with eosin for 5 min. Then the slides were rinsed once more in water and dehydrated in alcohol and xylol before applying coverslips with mounting medium to protect the tissue.

2.1.2 Immunohistochemistry

Slides were dried for 15 min at 65 °C. The samples were then dewaxed in xylene and rehydrated in a graded alcohol series. Subsequently, antigen retrieval was performed by cooking the slides in citrate buffer (10 mM, pH 6.0) for 20 min at 120 °C. After cooling down, they were rinsed 3 times in buffer solution before being subjected to the staining process. Staining was performed automatically by an autostainer (Dako) at RT following the subsequent protocol. To block endogenous peroxidase activity, slides were treated with methanol containing 3% hydrogen peroxide for 10 min. In the next step, buffer containing 3% (mAb) or 10% (pAb) normal goat serum, respectively, was added for 30 min to reduce non-specific staining/background staining. Then, tissues were incubated with the primary antibodies with a dilution of 1:1000 in a diluent solution for 60 min. After washing off the primary antibody, slides were coated with a solution of secondary biotinylated antibody for 30 min. To allow an enzymatic color reaction, a peroxidase binding streptavidin-biotin-complex was added for 30 min. Finally, sections were covered with 3,3′-diaminobenzidine (DAB) as a chromogen for 5 min. Between all incubation intervals, stages were rinsed in buffer solution. After the color reaction, the tissue slides were removed from the machine and the sections were counterstained with hematoxylin for 10 min. Rinsing the slides under running warm tap water turns the color of the counterstain solution blue for better contrast. Finally, sections were dehydrated in a graded alcohol series and xylene before coverslips were applied with a drop of mounting medium to protect the sensible tissue.

2.1.3 Scoring of IHC Staining

Tissue samples were investigated for the percentage of stained cancer cells in relation to all visible tumor cells as well as their staining intensity. For semi-quantitative evaluation, only tissue stained with a polyclonal primary antibody was examined. Membranous as well as cytosolic staining was taken into account and staining intensity levels were scored as negative (0), weak (1+), moderate (2+) and strong (3+). Positive controls for 3+ staining were PanIN 1, whereas non-dysplastic pancreatic duct epithelium was used as reference for a negative result. A case was considered positive if at least 40% of cells displayed moderate (2+) and/or strong (3+) immunostaining. This scoring scheme is suggested for the evaluation of cancer tissue of patients, who are potentially eligible for therapy with IMAB362, an anti-claudin-18.2 antibody, which was tested for treatment of advanced gastric cancer with promising results (Singh, Toom et al. 2017). For this purpose, Claudetect^{TM}18.2 (Ganymed Pharmaceuticals, Mainz (D), a semi-quantitative immunohistochemical assay, was established to determine expression levels of claudin-18.2 in tissue samples. Additionally, a sample or lesion was assigned an overall intensity depending on the predominant staining intensity displayed by labeled cells ranging from 0 to 3+. For intensity scoring, a case was only rated as 0, if at least 80% of tumor cells did not show any immunostaining (0), otherwise it was classified as 1+.

2.2 Cell Culture

2.2.1 General Cell Culture

2.2.1.1 Propagation of Mammalian Cancer Cells

Mammalian cancer cells were cultivated in high glucose DMEM GlutaMAX^{TM} medium that was supplemented with 10% FBS. Before adding FBS to the culture medium, it underwent heat denaturation at 56 °C for 30 min. The medium contained 1% penicillin/streptomycin for protection against microbiological contamination. Cells were maintained in 75 cm^2 culture flasks at 37 °C in a humidified atmosphere of 5% CO_2. To rule out mycoplasma contamination, a mycoplasma specific nested PCR was performed shortly after thawing (see 2.2.1.5).

2.2.1.2 Cell Splitting and Counting

Having reached 80% confluence, cells were rinsed once with sterile PBS. Trypsin was added to detach cells from the underground. Both PBS and trypsin were preheated to 37 °C before use. After satisfying detachment of cells, the reaction was stopped by adding standard culture medium. For quantification of cells, a cell suspension of 15 µl was collected and mixed with trypan blue 1:1 to distinguish dead from living cells, and afterwards added to a hemocytometer (improved Neubauer hemocytometer).

Eventually, cells were transferred into a new flask at the appropriate concentration or seeded into wells for further experiments.

2.2.1.3 Freezing of Culture Cells

80% confluent cells were rinsed and detached as described above. After the addition of standard medium to stop trypsinization, the cell suspension was collected in a 15 ml centrifugation tube and spun at 800 x g for 5 min to form a pellet. The pellet was then resuspended in 2 ml complete medium containing 20% DMSO. 1 ml aliquots were transferred into cryovials and frozen slowly at -80 °C in a freezing container before being conveyed into liquid nitrogen for long term storage.

2.2.1.4 Thawing of Culture Cells

Frozen cell suspensions were slowly thawed in a 37 °C water bath. After that, the cell suspension was collected and added to a 15 ml centrifugation tube containing 10 ml preheated culture medium. To remove toxic DMSO, cells were spun at 800 x g for 5 min. The supernatant was discarded and the cells were resuspended in 1 ml of culture medium and transferred into a culture flask.

2.2.1.5 Mycoplasma PCR

Freshly thawed and seeded cells were kept in a separate incubator to prevent a possible contamination with Mycoplasma species from spreading. To show evidence that the cultures were not contaminated, a nested primer PCR was used. For sample preparation, 1 ml of medium was taken from a culture flask, which contained at least 80% of confluent cells. The sample was diluted 1:10 and heated for 5 min at 95 °C. After short centrifugation, the upper fraction was collected and used as a template. For the first PCR a 25 µl reaction was set as follows:

dH$_2$O	15 µl
10x buffer (15mM Mg^{2+})	2.5 µl
dNTPs (10mM each)	0.5 µl
Primer supermix 1	1.0 µl
Taq Polymerase	1.0 µl
Template sample	5.0 µl

Thermocycling conditions were set as follows:

Step	Temperature	Time
Initial denaturation	94 °C	4 min
35 cycles of		
Denaturation	95 °C	30 sec
Annealing	55 °C	2 min
Elongation	72 °C	1 min
Final extension	72 °C	7 min
Hold	4 °C	∞

For the second PCR another 25 µl reaction was set as follows:

dH$_2$O	19 µl
10x buffer (15mM Mg^{2+})	2.5 µl
dNTPs (10mM each)	0.5 µl
Primer supermix 1	1.0 µl
Taq Polymerase	1.0 µl
Template sample (product of 1st PCR)	1.0 µl

The amplification parameters of the second PCR were set as follows:

Step	Temperature	Time
Initial denaturation	95 °C	4 min
30 cycles of		
Denaturation	95 °C	30 sec
Annealing	55 °C	2 min
Elongation	72 °C	1 min
Final extension	72 °C	7 min
Hold	4 °C	∞

10 µl of the PCR product were analyzed by 1% agarose (in TBE) gel electrophoresis containing 0.5 µg/ml ethidium bromide and standardized using a GeneRuler 100 bp DNA ladder. A UV gel documentation system was used to take gel images.

2.2.2 PMA Stimulation of Culture Cells

PMA, a synthetic Phorbol ester, is supposed to enhance PKC signaling due to its stereo analogy to the physiological PKC activator DAG. It is suspected that claudin-18 expression is regulated via a PKC-dependent pathway. Thus, claudin-18 expression was investigated by exposing cells to PMA. Therefore, cells were seeded in 6-well plates for protein collection (for immunoblotting), in 24-well plates for immunofluorescence and immunocytochemistry and in culture dishes for mRNA retrieval and subsequent transcriptional analysis. After a monolayer was formed, the medium was discarded and the cells were rinsed with PBS once. DMEM culture medium containing 200 μmol PMA was added and the cells were incubated for 24 h under routine circumstances before harvest.

2.3 Immunolabeling of Culture Cells

Immunostaining of both stimulated and unstimulated cancer cells was performed using fluorescence as well as peroxidase dependent chromogens. For the latter, cells were either fixed in paraffin or in methanol. Whereas for immunofluorescence and immunocytostaining of formalin-fixed cells both antibodies were used, immunocytochemistry of methanol-fixed cells was exclusively performed with a polyclonal anti-claudin-18 antibody.

2.3.1 Immunofluorescence

Cells were seeded onto coverslips in 24-well plates and cultivated overnight under standard conditions to allow adherence to the glass pad. Stimulated cells were exposed to the PKC activator PMA for 24 h. If not otherwise mentioned, the following steps were performed at RT. The medium was discarded and the wells were briefly rinsed with PBS. Fixation was performed with pre-chilled methanol (-15 °C) for 5 min. After being rinsed 3 times with Tris-buffered saline (TBS), cells were permeabilized with TBS containing 0.25% Triton X-100 for 5 min. The samples were rinsed again 3 times with TBS, afterwards, blocking solution (1% normal goat serum and 0.1% Triton X-100 in TBS) was added for 30 min to reduce non-specific antibody reactions. The cells were then incubated overnight with a 1:200 dilution of primary antibody in blocking solution at 4 °C in a humidified chamber. The following day, cells were rinsed 3 times with TBS. From now on working in the dark, a fluorescent-labeled anti-rabbit secondary antibody, diluted 1:200 in blocking solution, was applied for 60 min. The coverslips were rinsed 3 times with washing solution (TBS containing 0.1% Triton X-100), subsequently, the nuclei were counterstained for 5 min with the use of Hoechst33342 (0.5 μg/ml in dH$_2$O). The samples were finally rinsed twice with washing solution and once with dH$_2$O. The coverslips were then carefully transferred onto microscope slides with a drop of mounting medium. The edges were sealed with transparent nail polish. The staining result was investigated using a

fluorescence microscope (Carl Zeiss AG, Jena, Germany). Images were taken with the Zeiss AxioVision software. The slides were stored at -15 °C in the dark for future inspection.

2.3.2   Immunocytostaining of Methanol-fixed Cells

Cells were fixed, permeabilized and blocked as described above in 2.3.1. Again, all steps took place at RT if not otherwise specified. The primary antibody was diluted 1:2000 in blocking solution and applied overnight at 4 °C in a humidified chamber. After 3 rinsing steps with TBS, the samples were incubated with a biotinylated secondary goat-anti-rabbit antibody for 30 min. The coverslips were again rinsed 3 times with washing solution before incubation with streptavidin-peroxidase for 30 min. After another triple rinsing with washing solution, the cells were exposed to DAB for 5 min. The wells were finally rinsed with dH$_2$O and counterstaining was done using hematoxylin, before coverslips were mounted onto microscope slides as described above. The staining result was examined under a light microscope.

2.3.3   Immunocytostaining of Formalin-fixed Cells

Cells were trypsinized as described above and collected in a 50 ml tube. After spinning at 400g for 10 min, the supernatant was discarded and cells were fixed by resuspending in 5ml of 4% formalin and spun again for sedimentation. Formalin was removed save for 0.5 ml. Cells were mixed with the remaining fluid and then transferred to a 2 ml Hettich© cyto chamber mounted onto a microscope slide. The chamber was spun once more and the remaining supernatant was removed. Both the cyto chamber and a pipette were incubated at 60 °C for 5 min. Meanwhile, Richard-Allan Scientific™ HistoGel™ specimen processing gel was heated in a microwave at 600 W until it was just about to cook. The chamber was removed from the incubator and the warmed pipette was used to add 2-3 drops of fluid processing gel into the cyto chamber. The mixture was briefly vortexed and the chamber was transferred into a centrifuge and spun at 1000g for 10 sec. After cooling for 15 min at 4 °C, the cyto chamber was removed leaving the cell block mounted on the slide. The block was subsequently embedded in paraffin and immunolabeling was performed as described for paraffin embedded tissue using a Dako autostainer.

2.4   Semi-quantitative Protein Analysis

For the assessment of claudin-18 expression of PDAC cell lines on protein level, Western Blotting of protein extracts was performed using both a polyclonal and a monoclonal anti-claudin-18 antibody. Gastric cancer cell lines were intended as a positive control. Since claudin-18 is orthotopically expressed in lung and stomach tissue of vertebrates, protein extracts from murine stomach and lung

tissue were chosen as further control samples. Housekeeping gene product α-tubulin was used as loading control.

2.4.1 Cell Lysis and Protein Extraction

To produce lysis buffer, cold (4 °C) RIPA-buffer was mixed with commercial phosphatase and protease inhibitor and put on ice. Stimulated cells and controls were cultivated in 6-well plates until processing. The medium was discarded and the cellular layers were rinsed once with cold PBS. Lysis buffer was added to the wells and the cells were scraped thoroughly from the underground and collected in 1.5 ml centrifuge tubes to be put on ice for 15 min. To separate the protein extract from cellular debris, the samples were centrifuged at 4 °C for 15 min at 13000 rpm. The supernatant, which is considered as the protein homogenate, was carefully transferred to another tube. Before quantification, each lysate was sonicated once for 30 min at low intensity using an ultrasonic processor.

For protein concentration analysis of the lysates a BCA Protein Assay Kit was used. In accordance with the manufacturer's instructions, lysates were mixed with the required reagents and absorption was measured at 550 nm in a microplate reader after 20 min of incubation at 37 °C. Alongside the samples, a serial albumin dilution was measured to create a standard curve that permitted the calculation of protein concentrations of the investigated samples. Lysates were stored at -15 °C until further processing.

2.4.2 SDS-Page and Immunoblotting

Before being loaded on a gel, the required amount of protein extract was mixed with 5 μl of 5 X Laemmli buffer and boiled for 5 min at 95 °C in a heat block shaking the samples at 700 rpm. The samples were then put on ice to cool down and centrifuged shortly. Samples as well as protein ladders were loaded into the slots of a gel containing 12% polyacrylamide due to the size of the protein investigated. Electrophoretic separation was performed in running buffer at 25 mA in a Biorad mini-PROTEAN Electrophoresis 3 cell System. Proteins were then transferred onto nitrocellulose membranes (Amersham Hybond ECL) applying 100 V for around 2.5-3 h in a medium of blotting buffer. After careful separation of the membrane from the gel, the transfer result was checked by a non-specific protein stain (Ponceau S). The stain was rinsed off with TBST containing 1% Tween20. Nonspecific binding sites were blocked by incubation in 5% nonfat dry milk in TBST for 1 h at RT. Membranes were rinsed 3 times with TBST before primary antibodies were applied in the proper dilution (1:500 for rabbit anti-Claudin-18 and 1:10000 for mouse anti-αTubulin in TBST containing 3% BSA) and the membranes were incubated at 4 °C overnight on a shifting table. The following day, primary antibody dilutions were removed and the membranes were rinsed 3 times with TBST. After

that, the membranes were exposed to peroxidase-conjugated secondary antibody (diluted 1:2000 in TBST with 5% nonfat dry milk) for 1 h at RT. The membranes were rinsed again three times with TBST before results were visualized with a chemiluminescence substrate kit and developed with the help of a light-sensitive imaging film. All the steps were performed with gentle agitation on a rotary shaker. Membrane stripping was performed using a stripping buffer (10% methanol and 10% acetic acid) for 30 min at RT.

2.5   Reverse Transcription PCR

2.5.1   Extraction of mRNA and Reverse Transcription PCR

Stimulated cells and controls were cultivated in 61 cm^2 dishes until procession. Cells were trypsinized and collected in centrifuge tubes. The cell suspension was centrifuged for 3 min at 4 °C and 1000 rpm. The supernatant was discarded and the pellet was rinsed with cold PBS carefully so as not to destroy the pellet. The pellet was eventually resuspended in cold PBS and transferred to a new tube. After another centrifugation for 1 min at 4 °C and 13000 rpm, the supernatant was discarded once more. The pellet was resuspended in 175 μl of cold RLN buffer and put on ice for 5 min. To isolate RNA, a RNAeasy Mini Kit was used, gaining a watery solution of RNA following the manufacturer's instructions. RNA samples were stored at -80 °C.

Total concentration of RNA was measured using a spectrophotometer and the appropriate software.

For reverse transcription reagents were mixed as follows:

RNA extract	Amount containing 5 μg of total RNA
Ribolock	0.5 μl
OligodTs (10 μM)	2.0 μl
dH$_2$O	Up to 12.5 μl in total

The mixed sample was incubated for 5 min at 65 °C and afterwards put on ice for another 5 min. Subsequently, the reverse transcription reaction was complemented with the following reagents to a 20 μl sample:

Ribolock	0.5 μl
5X buffer	4.0 μl
dNTP 10 mM	2.0 μl
Reverse Transcriptase	1.0 μl

Samples were incubated for 60 min at 42 °C and then heated up to 70 °C for 5 min. Total concentration of cDNA was measured using a spectrophotometer and the appropriate software. Aliquots containing 100 ng/μl of cDNA were stored at -15 °C.

2.5.2 cDNA Amplification and Analysis

Having produced transcript complementary cDNA of claudin-18, splice variant 2, PCR was used to amplify the reverse transcription product. Thus a 25 μl PCR reaction was set as follows:

dH$_2$O	15,375 μl
10x buffer (15 mM Mg^{2+})	2.5 μl
dNTPs (10 mM each)	0.625 μl
Taq Polymerase	0.5 μl
Forward primer (5 μM)	2.5 μl
Reverse primer (5 μM)	2.5 μl
Template sample	1.0 μl

The amplification parameters were set as follows:

Step	Temperature	Time
Initial denaturation	94 °C	3 min
35 cycles of		
Denaturation	95 °C	30 sec
Annealing	57 °C	2 min
Elongation	72 °C	1 min
Final extension	72 °C	7 min
Hold	4 °C	∞

10 μl of the PCR product were taken to be analyzed by 1% agarose (in TBE) gel electrophoresis containing 0.5 μg/ml ethidium bromide and standardized using a GeneRuler 100 bp DNA ladder. Gel images were taken with the help of an UV gel documentation system. Amplificates of cDNA from stimulated cells were run next to controls to allow comparative evaluation of stimulation effects.

3. Statistical Analysis

Correlation of lesion grading as well as subtypes in case of IPMN with both staining positivity and intensity was determined using Chi^2-test, whereas statistical significance of differences in patient survival was tested with log rank test (Mantel-Cox test). A significance level of 0.05 was assumed for the present evaluation. IBM SPSS statistics 22.0 software was applied for statistical assessment as well as for illustration of patient survival (Kaplan-Meier curve). Graphs were created using Microsoft Excel 2010 software.

III. Results

1. Establishment of IHC Staining Protocols

Before immunostaining of pancreatic tissue samples, both primary antibodies were tested in various concentrations on murine stomach and human gastric cancer tissue, serving as potential controls, to establish the respective staining protocols. As expected, the investigated specimens showed clear membranous but also cytoplasmic staining patterns for claudin-18 (figure3).
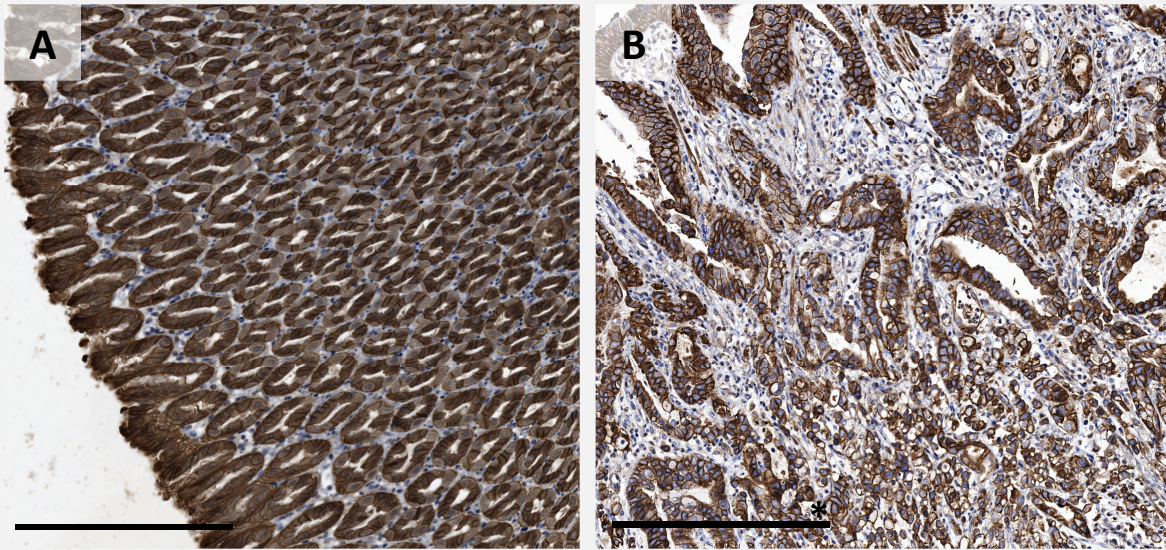
Figure 3 Claudin-18 Expression in Control Samples

Immunolabeling of murine gastric mucosa (A) targeting claudin-18 reveals strong and frequent immunopositivity in epithelial components. IHC for claudin-18 of mixed type gastric adenocarcinoma (B) shows robust claudin-18 immunoreactivity in both neoplastic glands and loose tumor cells. Claudin-18 expression is maintained in the course of carcinogenesis marking tumor cells as being of gastric lineage.
Bar = 200 μm/300μm*

2. Expression of Claudin-18 in Precursor Lesions of PDAC

2.1 Claudin-18 Expression in Pancreatic Intraepithelial Neoplasia

One-hundred-four PanIN lesions, identified in resection specimens of PDAC patients, were examined for claudin-18 expression.

Expression of claudin-18 was detected in the vast majority of cases with only 8 (7.7%) lesions displaying no labeling (0). Of the negative samples, only one was a low-grade lesion. Consequently, claudin-18 was more frequently detected in low-grade than in high-grade PanIN (p<0.001); nevertheless, claudin-18 expression could be observed in two thirds of high-grade lesions. Whereas 86.7% of low-grade PanIN could be classified as positive according to the defined criteria, this

fraction was significantly lower among high-grade PanIN (23.8%). Also, low-grade lesions mostly (83.1%) displayed moderate to strong staining intensity, whereas a strong immunoreactivity was observed only in a few (14.3%) high-grade lesions (p<0.001).The staining pattern was predominantly membranous, in some cases accompanied by cytoplasmic positivity, mostly in high-grade lesions. Membranous staining in general was more pronounced in cells containing large amounts of apical mucin, which is a feature of low-grade PanIN, in particular of PanIN 1. Here, the expression could be assessed in even further detail. Whereas the apical membrane was mostly not or only weakly stained, the immunoreaction was strongest on the lateral membrane of adjacent cells especially in areas close to the apical section of the lateral membrane consistent with the localization of tight junctions (figure 5E). Detailed immunohistochemical evaluation is shown in table 3, representative samples are illustrated in figures 4 & 5.

Table 3 Claudin-18 Expression in PanIN

	Positivity [%]	Intensity [%]			
		3+	2+	1+	0
all (*n*=104)	77 [74,0]	54 [51,9]	18 [17,3]	24 [23,1]	8 [7,7]
low grade (*n*=83)	72 [86,7]	54 [65,1]	15 [18,1]	13 [15,7]	1 [1,2]
high grade (*n*=21)	5 [23,8]	0 [0,0]	3 [14,3]	11 [52,4]	7 [33,3]
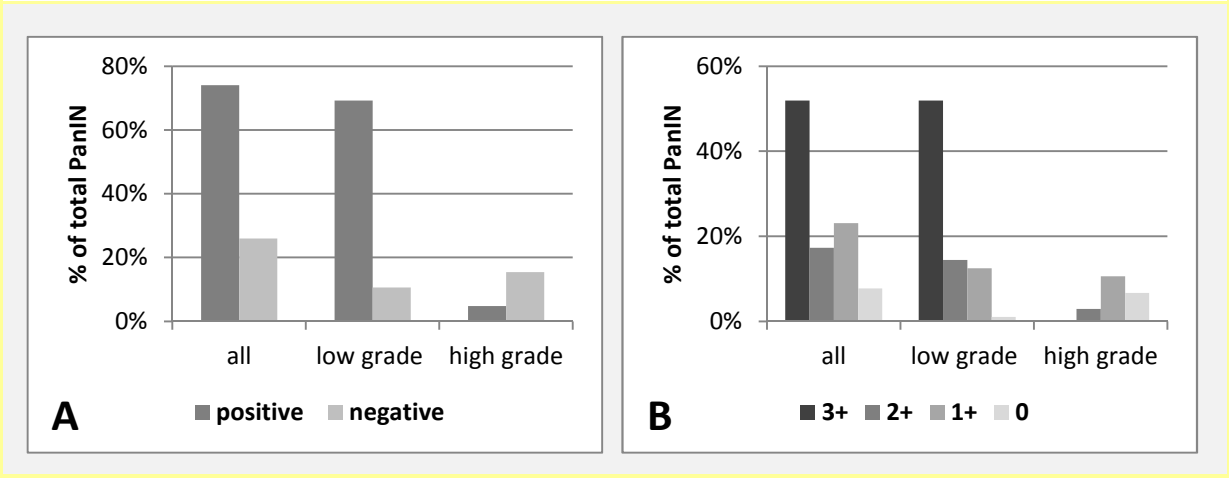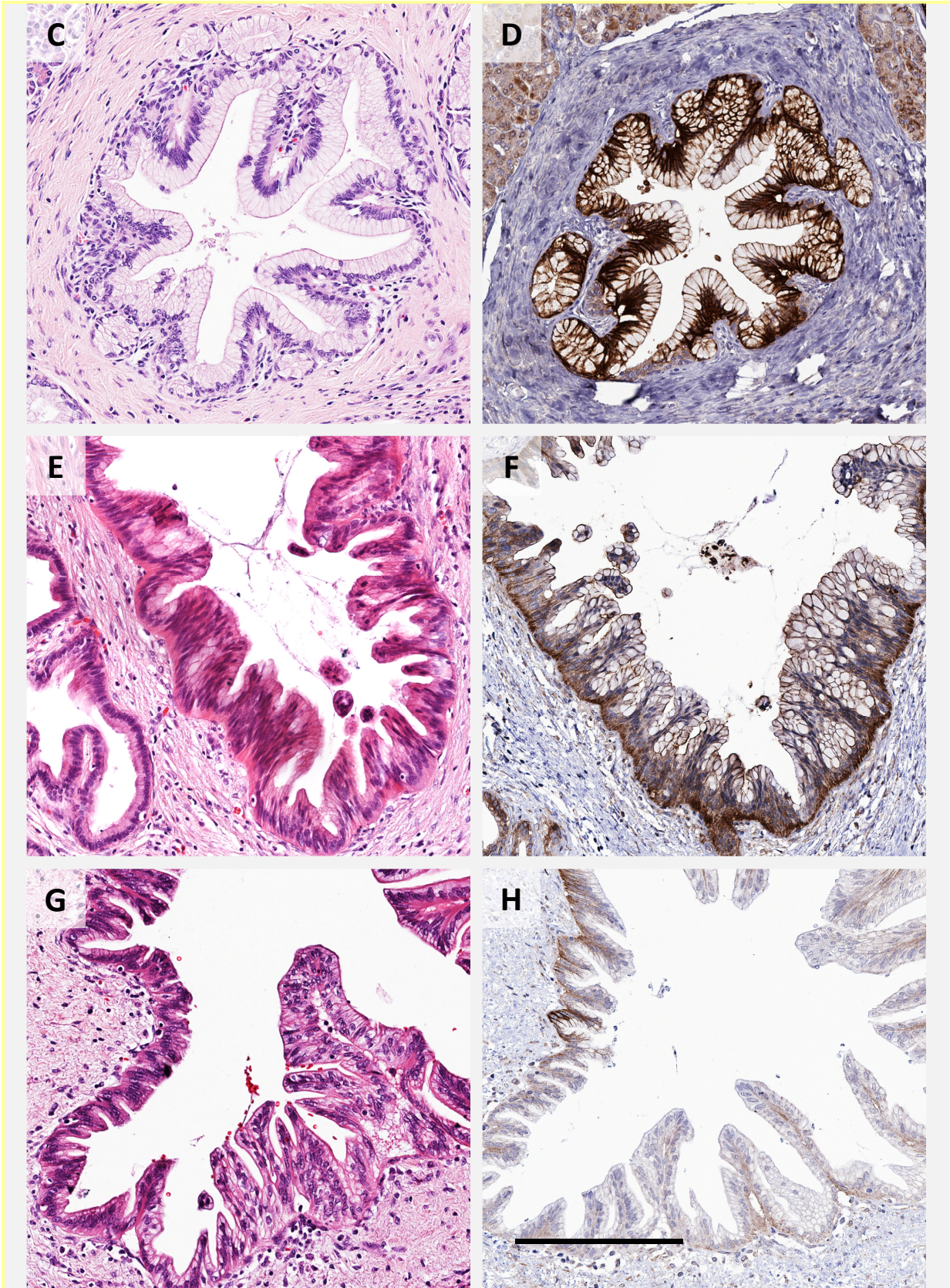
Figure 4 Expression of Claudin-18 in PanIN

IHC for claudin-18 in PanIN showed that the TJ protein is regularly expressed in these premalignant lesions. Whereas positivity (A, p<0.001) and intensity (B, p<0.001) of claudin-18 expression was high and strong, respectively in low grade PanIN (C-F), including PanIN 1 (C,D) and PanIN 2 (E,F), expression levels were significantly lower in high grade lesions (PanIN 3, G,H). Bar = 200 μm

Of note, PanIN were found often in the vicinity of normal ductal structures and pancreatic parenchyma, which always remained negative (figure 5). This clear difference in expression could be readily seen by observing ductal structures with partial PanIN (figure 5D).
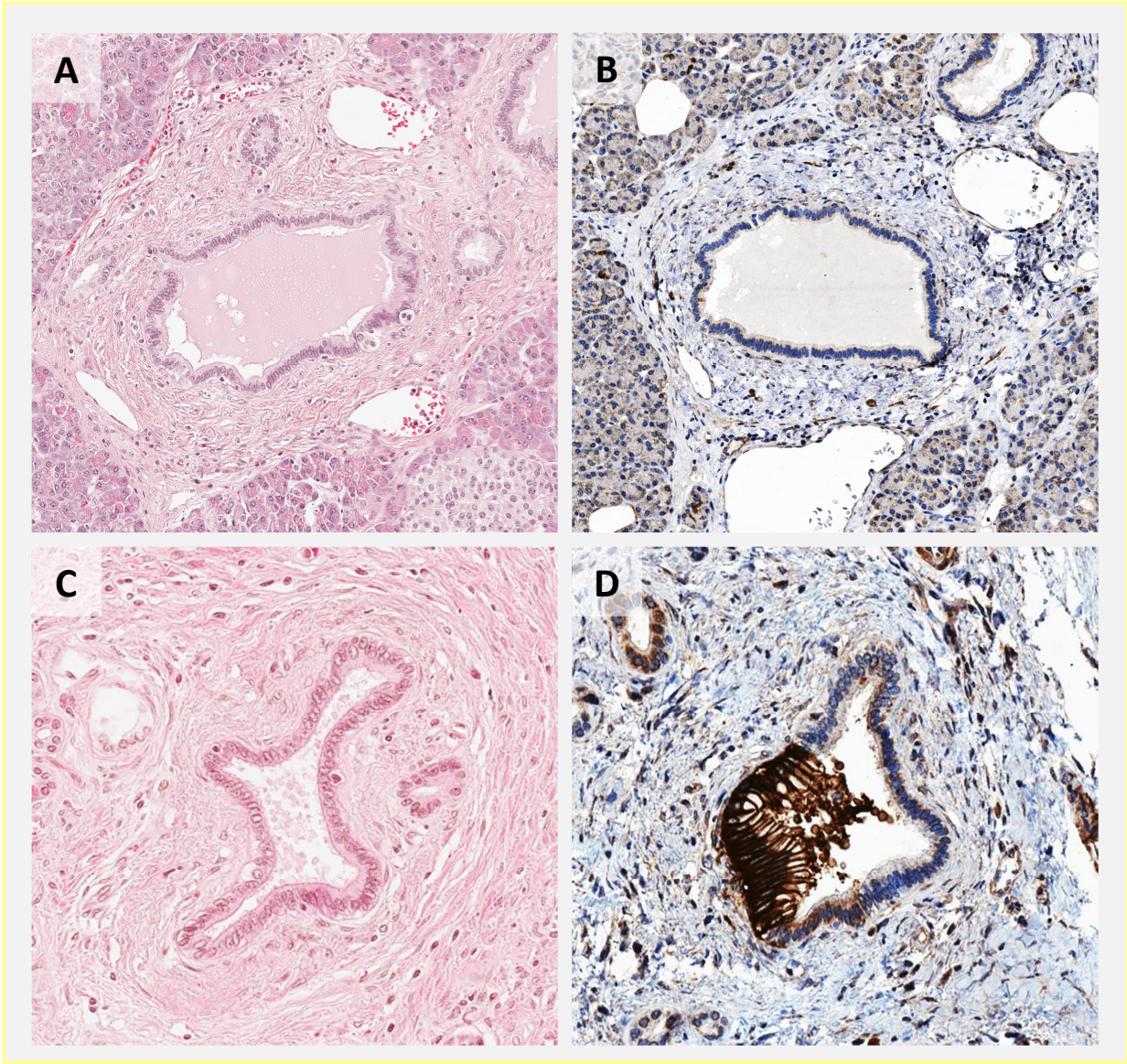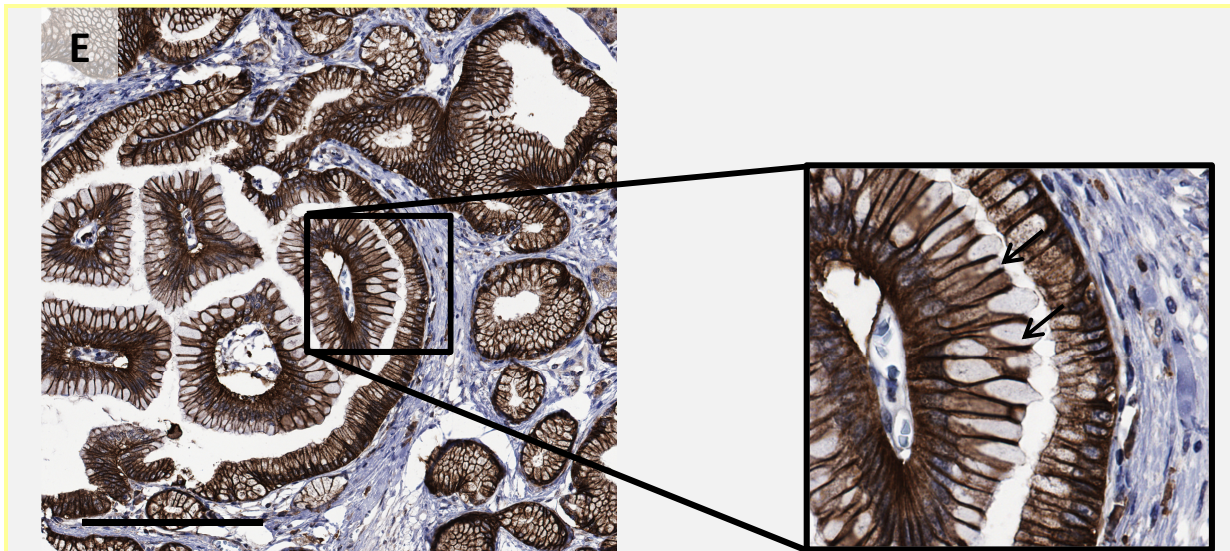
Figure 5 Peculiarities of Claudin-18 Expression in Pancreatic Ductal Structures

HE and IHC of PanIN lesions with special focus on expression patterns for claudin-18. Immunolabeling revealed that the TJ protein was not detectable in normal pancreatic ducts (B) in contrast to low grade PanIN lesions that exhibited strong immunoreactivity. This contrast was most prominent in sections with partial PanIN (D). Higher magnification showed that immunopositivity was concentrated on the basolateral membrane close to the ductal lumen (G) and was absent from the apical membrane (arrows). This observation indicates that claudin-18 is expressed in its biological pattern as a part of TJ complexes. Bar = 200 μm

2.2 Claudin-18 Expression in Intraductal Papillary Mucinous Neoplasm

In this set of 75 IPMN, expression patterns were rather homogeneous irrespective of histological grading or subtype. Again, claudin-18 expression could be detected in the vast majority of cases with only 5 specimens (6.7%) displaying no labeling in immunohistochemistry. Although claudin-18 was expressed on a significant level in both low-grade and high-grade IPMN, with a positivity rate of 76.2% and 45.5% (p=0.006), respectively, low-grade IPMN labeled with a stronger intensity (p=0.002). With respect to immunoreactivity in IPMN subtypes, expression patterns in gastric IPMN mimicked those in early PanIN. Being mostly low-grade lesions, gastric type IPMN displayed a strong membranous staining pattern. Among pancreatobiliary and oncocytic type IPMN, 42.6% and 75.0%, respectively were scored positive and were mostly represented by high-grade lesions sometimes with an associated invasive carcinoma. Furthermore, in pancreatobiliary and intestinal IPMN significant levels of cytoplasmic staining could be observed in some cases. Both frequency as well as intensity of claudin-18 staining was lowest in intestinal type IPMN with only a fraction of 28.6% classified as positive, mostly with a cytoplasmic pattern (positivity: p<0.001, intensity: p<0.001). Table 4 shows the staining results in detail; diagrammatic representations of results as well as illustrative cases are shown in figure 6.

Table 4 Claudin-18 Expression in IPMN

	Positivity [%]	Intensity [%]			
		3+	2+	1+	0
All (*n*=75)	47 [62,7]	20 [26,7]	24 [32,0]	26 [34,7]	5 [6,7]
Grading					
low grade (*n*=42)	32 [76,2]	18 [42,9]	12 [28,6]	11 [26,2]	1 [2,4]
high grade (*n*=33)	15 [45,5]	2 [6,1]	12 [36,4]	15 [45,5]	4 [12,1]
Phenotype					
gastric (*n*=30)	29 [96,7]	18 [60,0]	10 [33,3]	2 [6,7]	0 [0,0]
Intestinal (*n*=21)	6 [28,6]	0 [0,0]	5 [23,8]	15 [71,4]	1 [4,8]
oncocytic (*n*=8)	6 [75,0]	0 [0,0]	5 [62,5]	2 [25,0]	1 [12,5]
pancreatobiliary (*n*=14)	6 [42,9]	2 [14,3]	4 [28,6]	6 [42,9]	2 [14,3]
null (*n*=2)	0 [0,0]	0 [0,0]	0 [0,0]	1 [50,0]	1 [50,0]

45
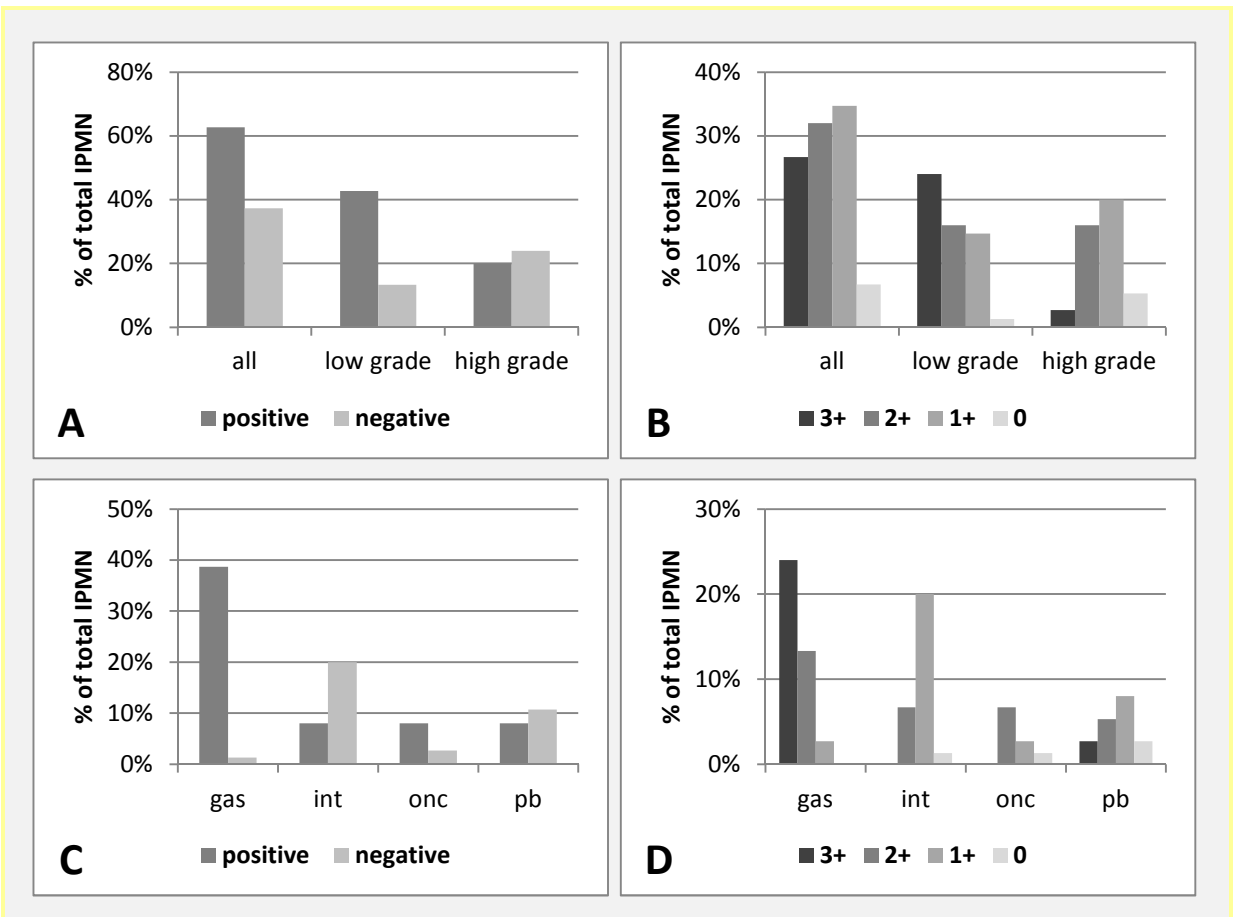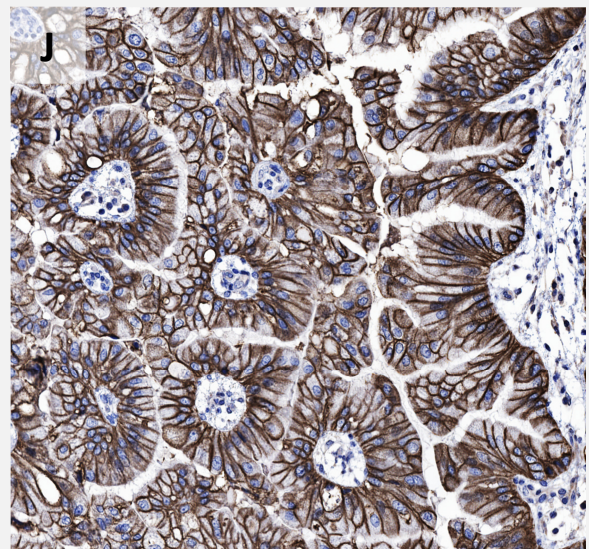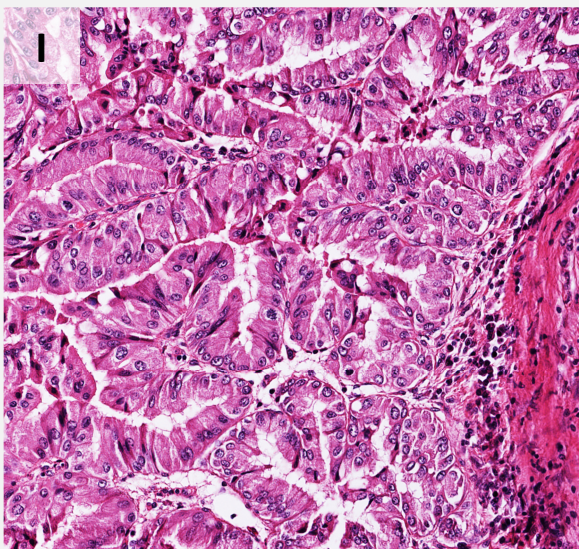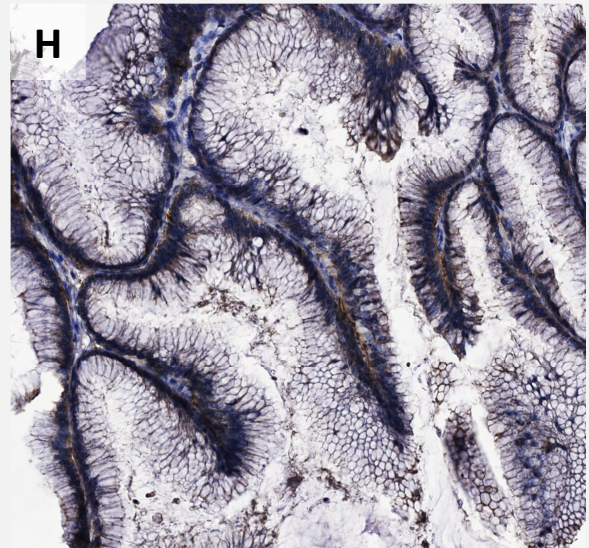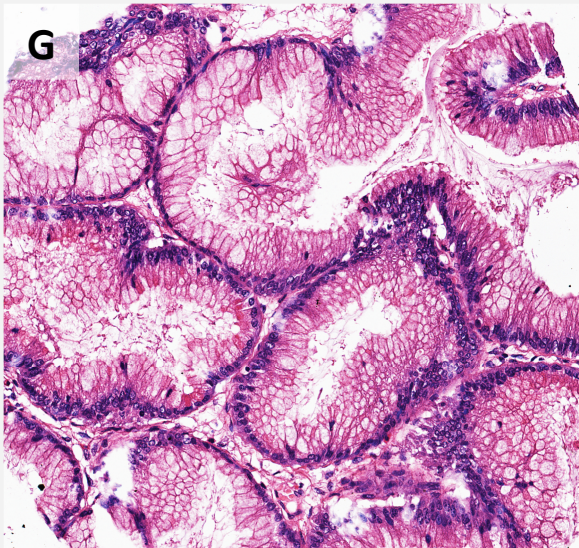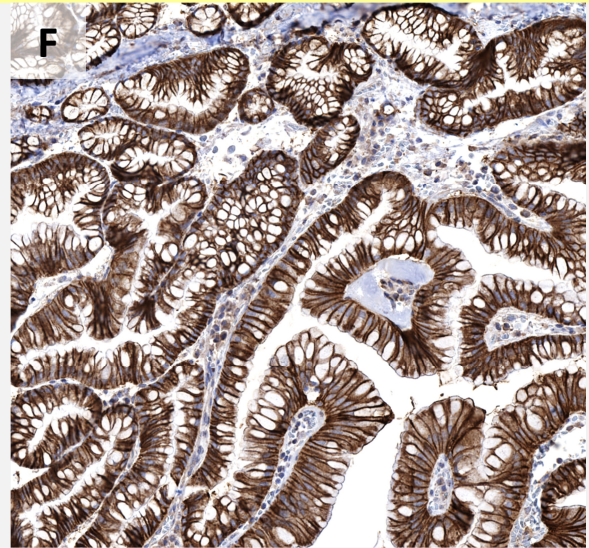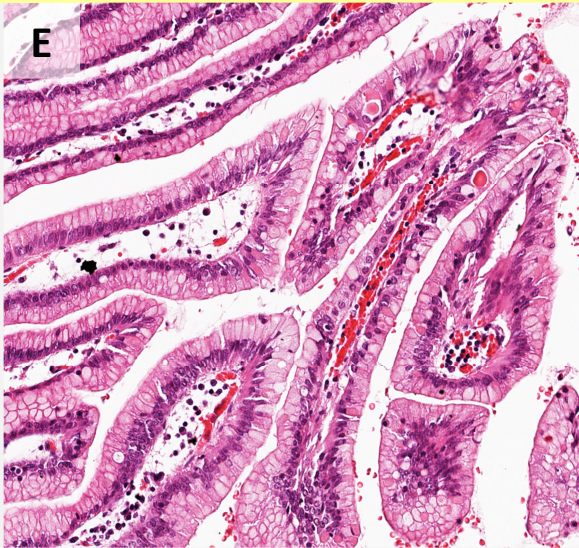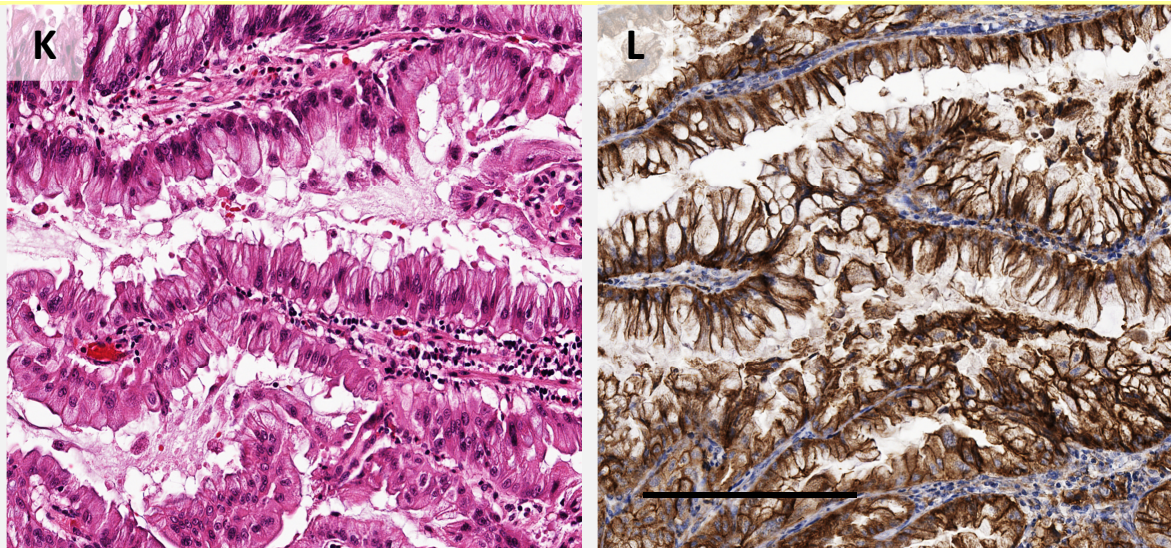
Figure 6 Expression of Claudin-18 in IPMN

Analogous to PanIN, positivity for claudin-18 expression (A) was correlated with low grade dysplasia in IPMN (p=0.006). Also, staining intensity (B) was stronger in low-grade lesions than in high grade IPMN (p=0.002). With regard to phenotypical features, expression patterns, i.e. both positivity (C, p<0.001) and intensity (D, p<0.001), differed notably between IPMN subtypes. Gastric type IPMN (E, F), mostly associated with low grade dysplasia, showed robust claudin-18 expression (F) in contrast to intestinal type IPMN (G, H). Claudin-18 expression was also observed in the majority of pancreatobiliary (I, J) and oncocytic (K, L) type IPMN, despite a high grade of dysplasia that is characteristic for those lesions. Bar = 200 µm

Interestingly, staining results differed substantially in intestinal type IPMN when a monoclonal antibody was used. Cytoplasmic staining was increased and some cases showed nuclear positivity regardless of grade of dysplasia, sometimes being the only relevant detectable staining (figure 7). Nuclear positivity was also observed in some cases of pancreatobiliary type IPMN, but always in association with membranous and cytoplasmic staining and affecting fewer cells.
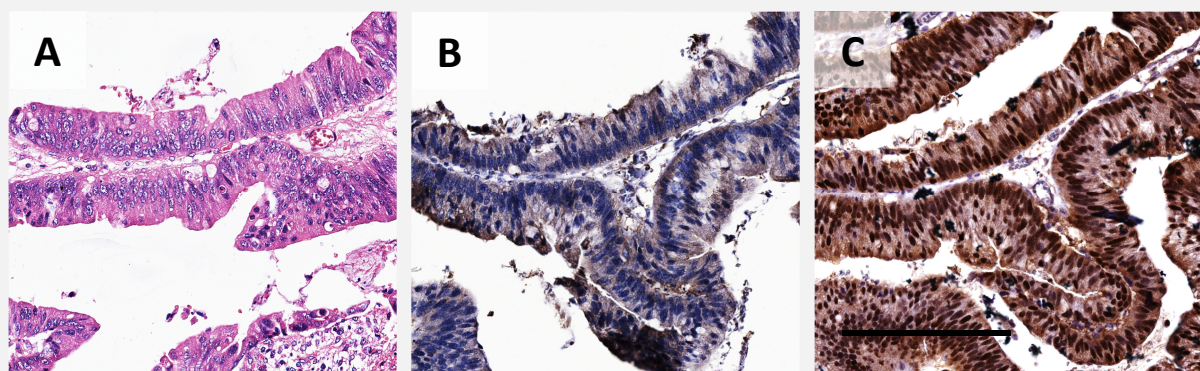
Figure 7 Nuclear Staining of Claudin-18 in Intestinal Type IPMN

Illustration of intestinal type IPMN with HE stain (A) as well as IHC results (B,C). Immunoreactivity of nuclear localization was not observed in intestinal type IPMN when a polyclonal primary antibody was used for staining (B) in contrast to sections that were stained using a monoclonal antibody (C). Here, nuclear positivity was not uncommon. Bar = 200 µm

2.3 Claudin-18 Expression in Mucinous Cystic Neoplasm

The expression patterns of claudin-18 were assessed in a set of 44 samples of MCN. Staining patterns were usually rather homogeneous in low-grade as well as in high-grade MCN. Similar to PanIN and IPMN, immunopositivity for claudin-18 was detected in 40 cases (90.9%) irrespective of frequency and intensity, with only 4 cases (9.1%) showing no labeling. Thirty cases (68.2%) exhibited relevant levels of claudin-18 expression, therefore being scored as positive. Twenty-three low-grade lesions showed substantial levels of claudin-18 leading to a positivity score of 76.7%, which is notably higher than in high-grade MCN, where only seven (50.0%) samples were labeled as positive (p=0.077). Finally, immunoreactivity was more intense in low-grade lesions with a fraction of 23 cases (76.7%) showing moderate or strong staining (p=0.096). This observation was particularly impressive in areas of transition from low-grade to high-grade dysplasia. Staining results are listed in table 5; diagrams and representative tissue sections are shown in figure 8.

Table 5 Claudin-18 Expression in MCN

	Positivity [%]	Intensity [%]			
		3+	2+	1+	0
all (*n*=44)	30 [68,2]	21 [47,7]	9 [20,5]	10 [22,7]	4 [9,1]
low grade (*n*=30)	23 [76,7]	14 [46,7]	9 [30,0]	5 [16,7]	2 [6,7]
high grade (*n*=14)	7 [50,0]	7 [50,0]	0 [0,0]	5 [35,7]	2 [14,3]
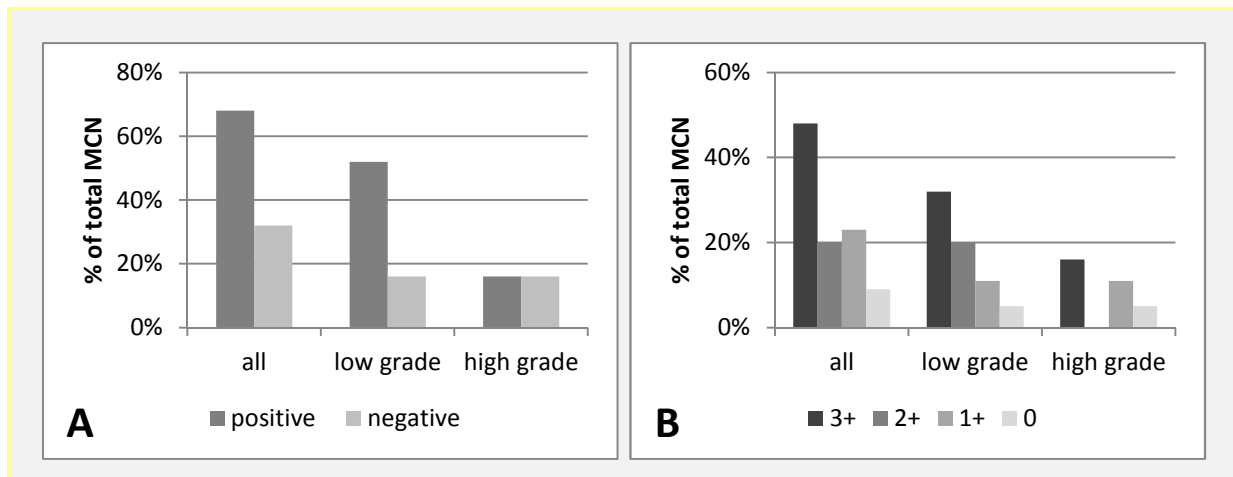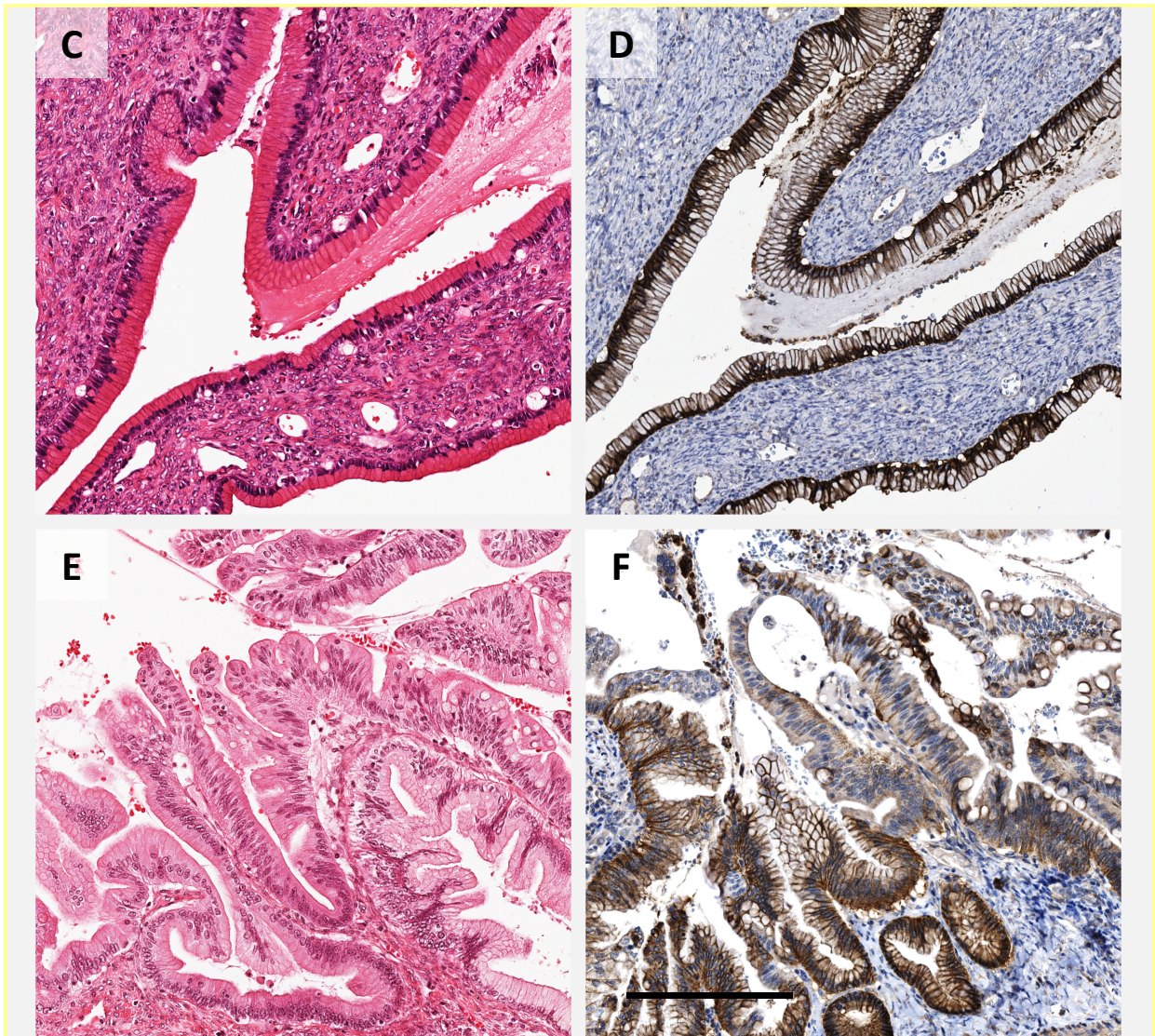
Figure 8 Claudin-18 Expression in MCN

Mirroring the results of other PDAC precursor lesions, IHC for claudin-18 showed correlation of positivity with low-grade dysplasia (A) in MCN (p=0.077). Also, staining intensity was notably stronger in low-grade lesions than in high-grade MCN (B, p=0.096). Whereas a strong homogeneous staining pattern was detectable in low-grade MCN (C (HE), D (IHC), tumor progression was associated with changes in claudin-18 expression with membranous immunopositivity and overall staining intensity decreasing in high grade sections (E (HE), F (IHC). Bar = 200 µm

Claudin-18 expression was mainly observed in a membranous pattern in both low-grade and high-grade MCN. Cytoplasmic staining, in association with membranous staining, was predominantly seen in high-grade MCN. On closer investigation, claudin-18 expression was associated with certain cytoarchitectural features in low-grade MCN, which are illustrated in figure 9. Whereas lesions with high columnar epithelial cells containing abundant apical mucin often labeled with a strong intensity, other MCN, lined by lower columnar or even cuboidal epithelial cells lacking extensive supranuclear mucin, presented staining patterns of a lower intensity and membranous positivity was sometimes altogether absent. Additionally, similar observations concerning the subcellular localization of immunoreactivity, which was more prominent on the basolateral membrane, were made in low-grade

MCN as in low-grade PanIN. Especially strong membranous staining was detected in goblet cells, which are a feature of intestinal differentiation and are positive for MUC2.

Seven cases of MCN (15.9%) were found to be associated with an invasive carcinoma. Of those, claudin-18 expression was maintained in only one invasive component in a membranous pattern, where cells were arranged in cohesive clusters. Apart from that, invasive carcinomas in association with MCN displayed highly undifferentiated neoplastic cells growing in loose, non-cohesive bundles, whereas two presented multinuclear cells, pointing at undifferentiated carcinoma with osteclastic-like giant cells. (Hruban, Pitman et al. 2007). There, immunoreactivity for claudin-18 could not be observed.
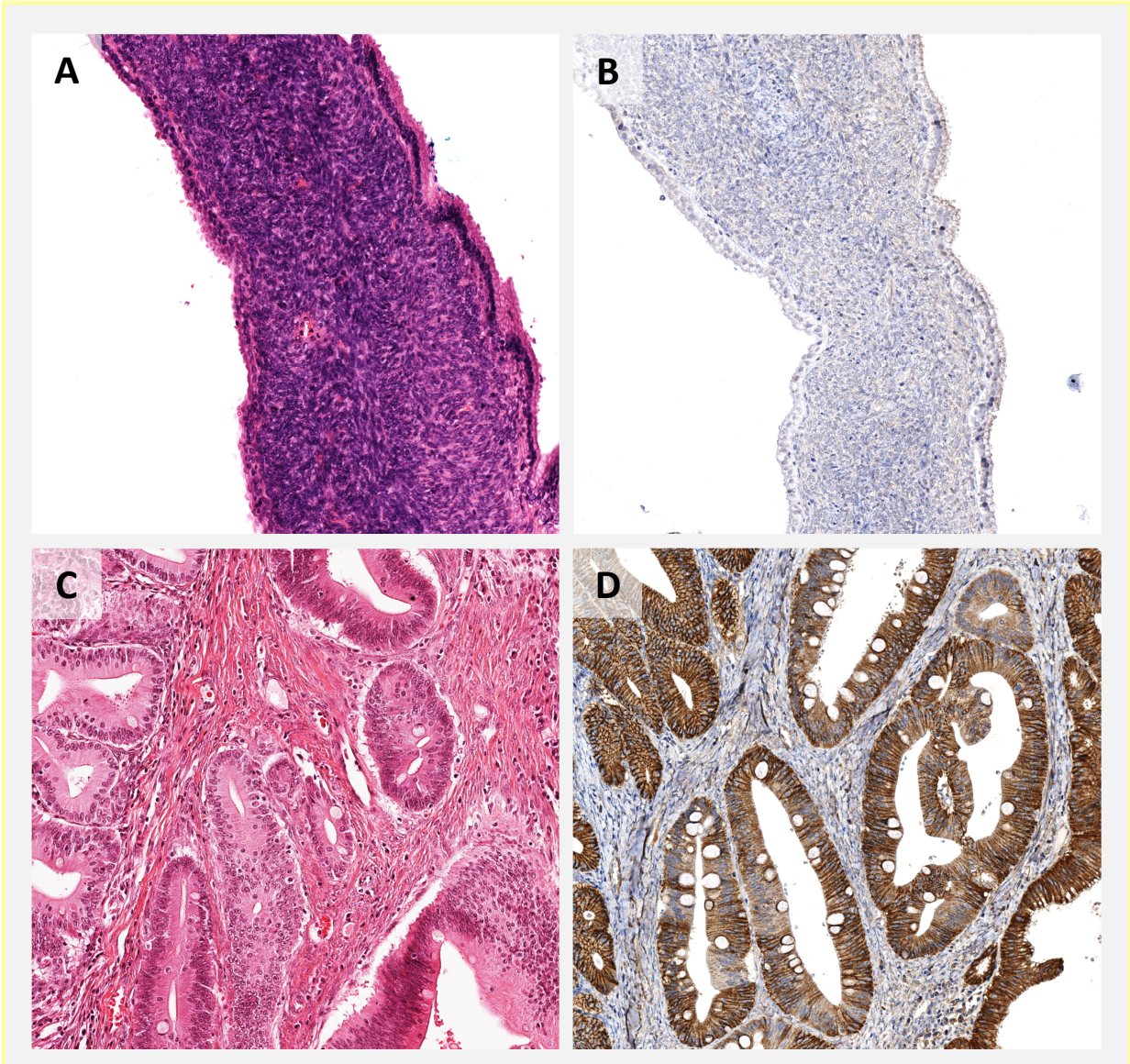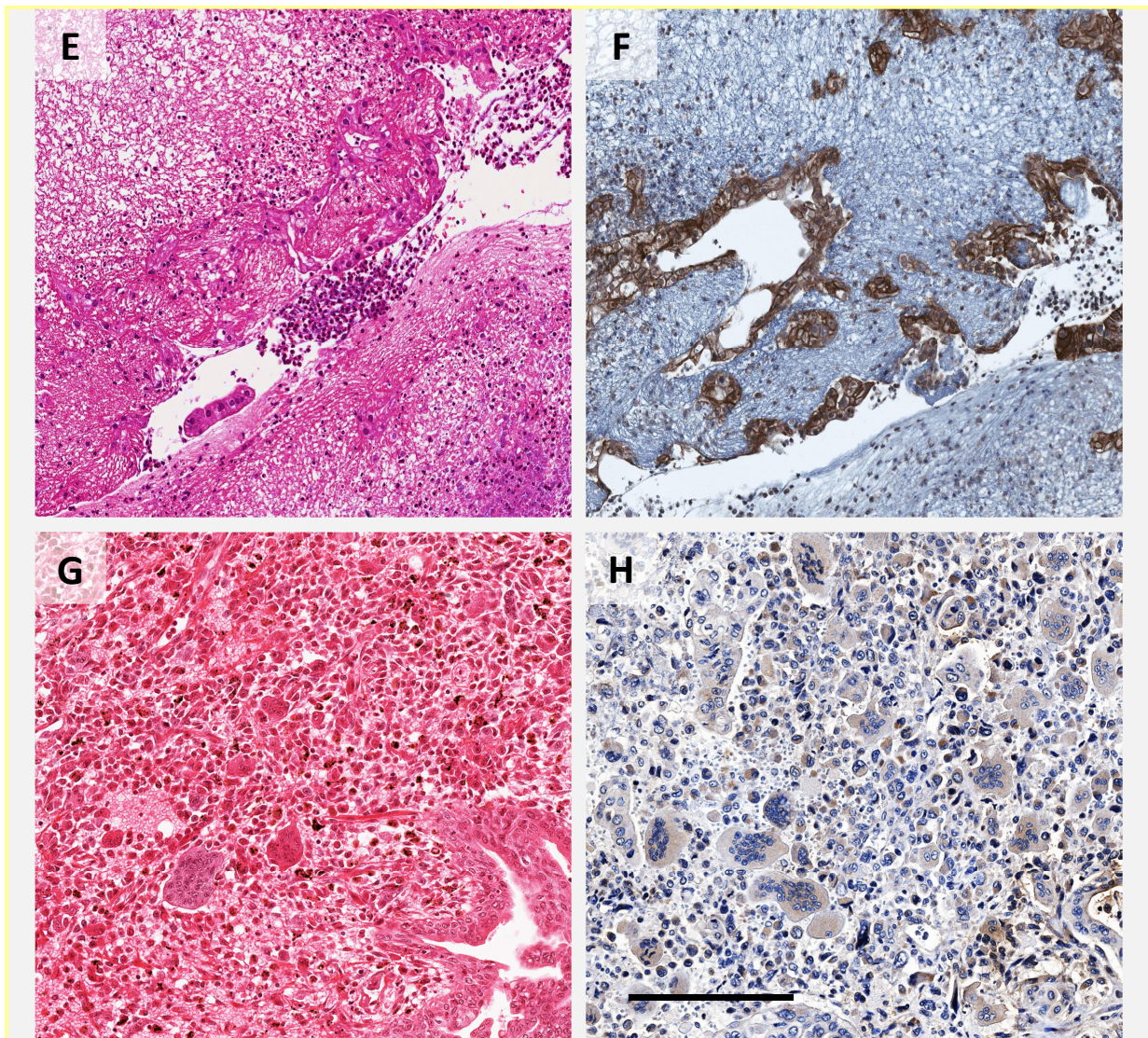
Figure 9 Peculiarities of Claudin-18 expression in MCN

Despite being low-grade lesions, some MCN were negative for claudin-18. Most of those cases displayed an epithelial lining consisting of low prismatic or cuboidal cells without apical accumulation of mucin (A, B). In contrast, immunopositivity for claudin-18 was observed in MCN showing at least partial intestinal differentiation with goblet cells (C, D). In MCN-associated invasive cancer, claudin-18 was expressed in cases displaying a cohesive growth pattern (E, F). On the other hand, a marked proportion of invasive carcinoma in association with MCN consisted of undifferentiated adenocarcinomas consisting of loose non-cohesive cells, such as in undifferentiated carcinoma with osteoclast-like giant cells (G, H). Here, no immunopositivity for claudin-18 could be detected. Bar = 200 μm

2.4   Claudin-18 Expression in Intraductal Tubulopapillary Neoplasm

In this study, 6 cases of ITPN were assessed for their expression profile of claudin-18 by immunohistochemistry.

In contrast to the findings in other pre-malignancies, ITPN did not display a membranous staining pattern regardless of which antibody was used. Four of 6 ITPN showed cytoplasmic immunoreactivity of various degrees. Cytoplasmic positivity was notably weaker when a polyclonal antibody was used.

Finally, frequent nuclear immunolabeling was observed in 4 cases, sometimes only weakly, in other sections rather pronounced (figure 10).
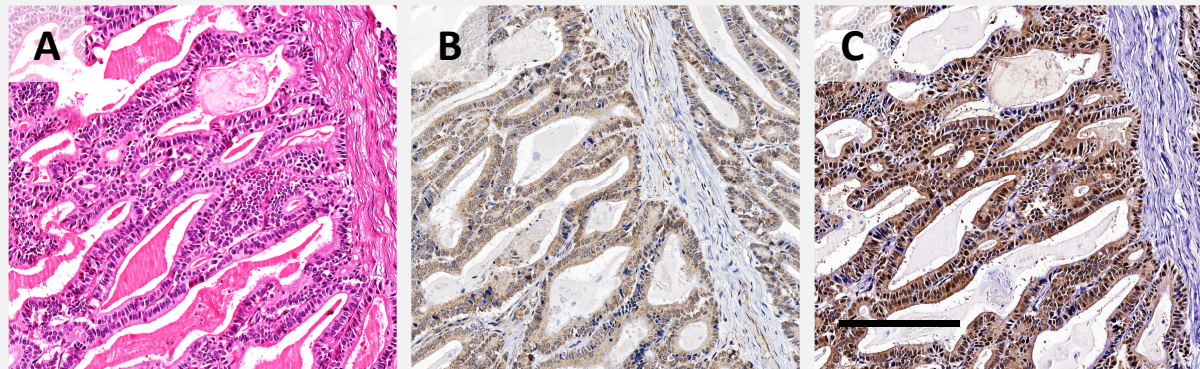
Figure 10 Claudin-18 Expression in ITPN

ITPN is a new entity of ductal pancreatic neoplasms that is characterized by tubules of back-to-back glands lined by epithelial cells displaying features of high-grade dysplasia (A). In contrast to other pancreatic preinvasive lesions, claudin-18 was not expressed in a membranous pattern in ITPN (B,C). In contrast to sections stained with the use of a polyclonal antibody (B), which revealed cytoplasmic positivity only, nuclear immunopositivity could be observed in 4 of 6 cases on using a monoclonal primary antibody (C). Bar = 200 μm

3. Claudin-18 Expression in Pancreatic Ductal Adenocarcinoma

Representative areas of 142 cases of PDAC from patients that underwent resection were assembled in tissue microarrays for analysis. To reduce the interference of tumor heterogeneity, each case was represented by three sections from different tumor regions. All cases were stained with the polyclonal primary antibody; furthermore, 82 cases were also stained with the monoclonal primary antibody.

In PDAC, staining patterns were notably more heterogeneous than they were in non-invasive neoplasms with varying intensities found in one single lesion. Moreover, cytoplasmic positivity was a common finding, in some sections without membranous staining. As in the case of premalignant lesions, immunoreactivity for claudin-18 was observed in more than 92.3% of investigated cases with only 11 cases (7.7%) scored 0. Significant immunolabeling was observed in only a fraction of the collective (33.1%). Those sections were rated as positive and displayed a clear membranous expression pattern, sometimes in association with cytoplasmic immunoreactivity. With respect to tumor grading, well differentiated carcinoma labeled more frequently and more intensely for claudin-18 than tumors of higher grading (p=0.019). Poorly differentiated PDAC displayed the lowest positivity rate (24.7%) and intensity levels (17.8%) with strong or moderate labeling (p=0.007). Immunohistochemical results for PDAC are listed in table 6 and illustrated in figure 11.

Table 6 Claudin-18 Expression in PDAC

	Positivity [%]	Intensity [%]			
		3+	2+	1+	0
all (*n*=142)	47 [33,1]	11 [7,7]	26 [18,3]	94 [66,2]	11 [7,7]
G1 (*n*=9)	6 [66,7]	1 [11,1]	5 [55,6]	2 [22,2]	1 [11,1]
G2 (*n*=60)	23 [38,3]	8 [13,3]	10 [16,7]	41 [68,3]	2 [3,3]
G3 (*n*=73)	18 [24,7]	2 [2,7]	11 [15,1]	52 [71,2]	8 [11,0]
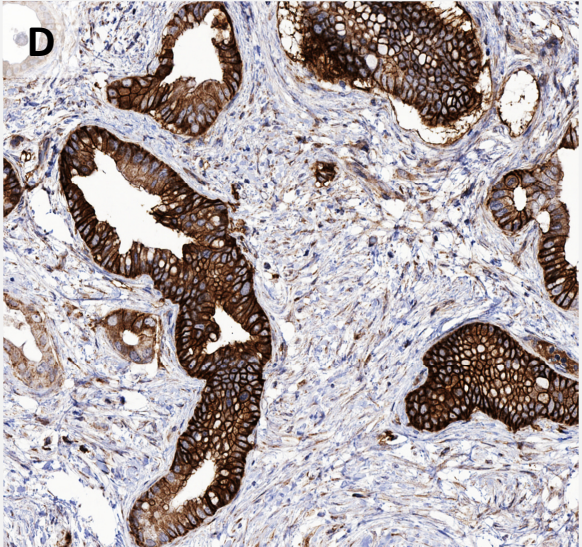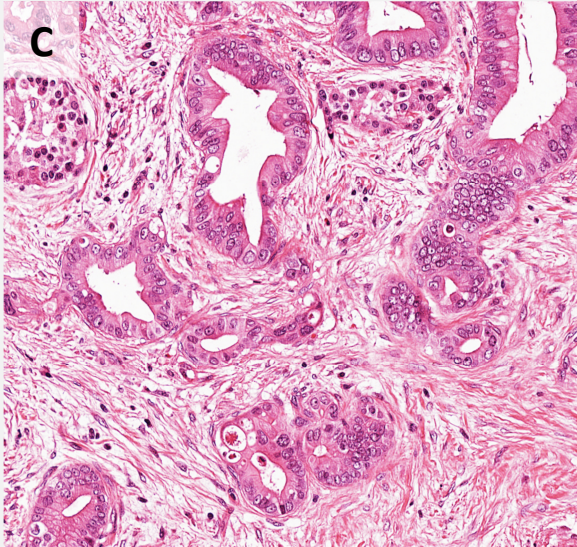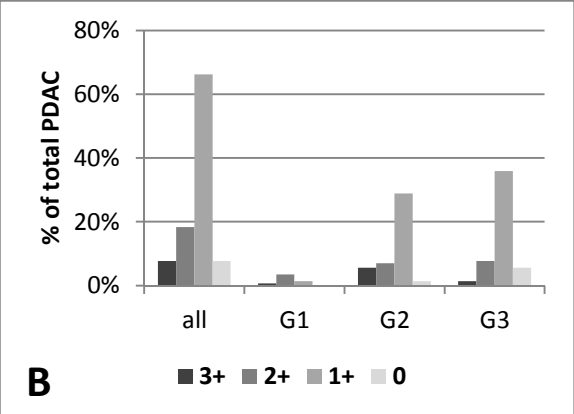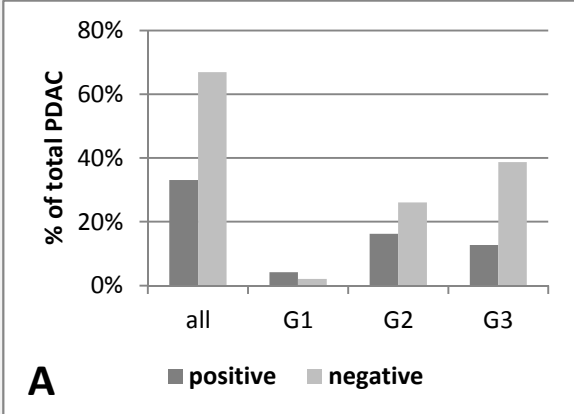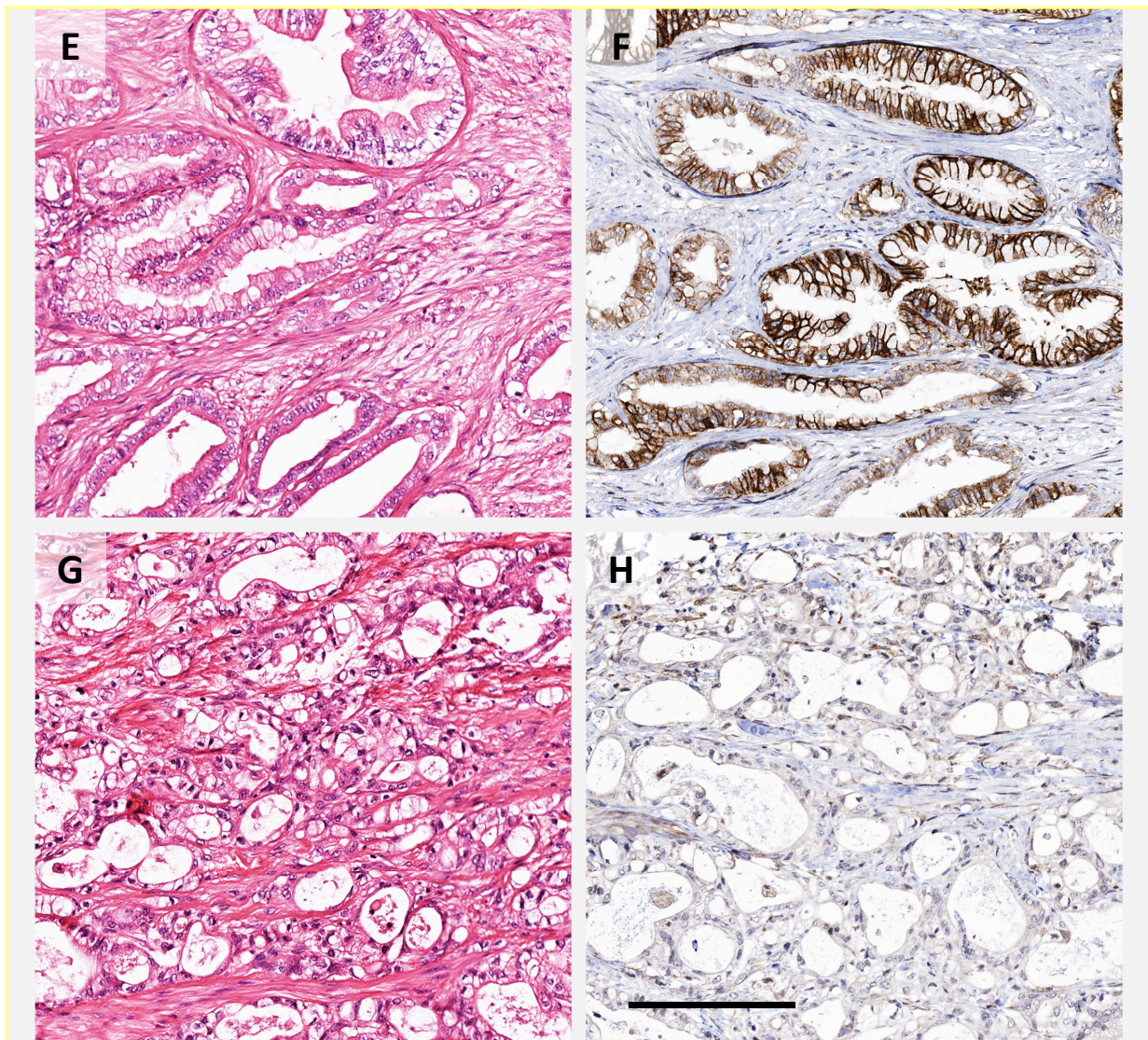
Figure 11 Claudin-18 Expression in PDAC

The analysis of claudin-18 expression in PDAC showed that both positivity (A) and intensity (B) of staining is correlated with the grade of differentiation. Overall, 33.1% of cases were rated as positive, but the proportion was notably higher in well differentiated carcinomas (> 66.7%, C, D) than in moderately (38.3%, E, F) or poorly (24.7%, G, H) differentiated PDAC (p=0.019). Also, staining intensity decreased with loss of differentiation (p=0.007) with the highest proportion of unlabeled cases found among poorly differentiated carcinomas (H). Bar = 100 μm

When a monoclonal primary antibody was used, nuclear positivity was observed in about 18.3% of moderately and poorly differentiated PDAC, in some cases with the nucleus being the location of most intense immunoreactivity. Nuclear staining was usually found in cases with no (0) or weak (1+) membranous staining (figure 12). Otherwise, labeling results with the two antibodies were similar with a slight tendency for more non-specific cytoplasmic staining with the monoclonal antibody.
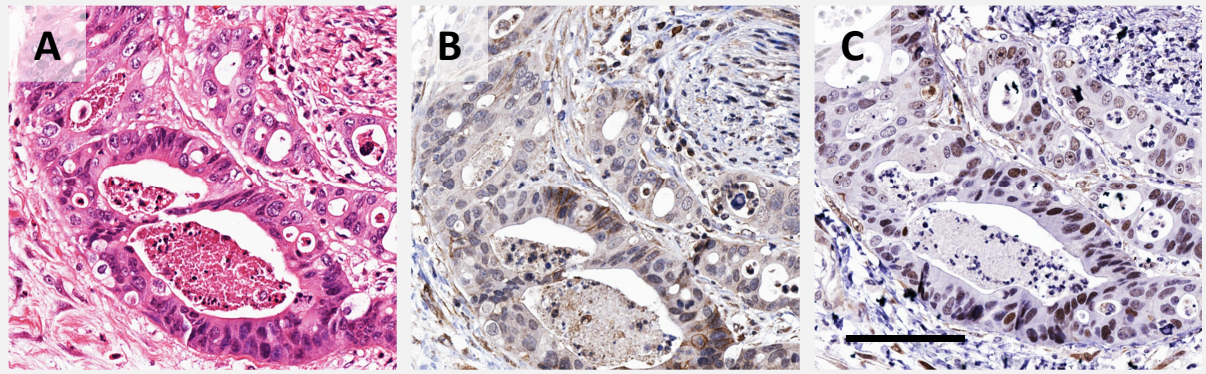
Figure 12 Nuclear staining in PDAC

HE of PDAC (A) and IHC results (B,C) with two different antibodies. Here again, no nuclear staining could be detected with the pAB, whereas immunopositivity of nuclei was observed in some cases of PDAC using a mAB (C), sometimes being the only noteworthy labeling as in this case. Bar = 100 µm

When comparing the expression of claudin-18 in PanIN lesions and PDAC, immunoreactivity was both more frequent and stronger in low-grade PanIN than in PDAC (p<0.001). Interestingly, immunolabeling for claudin-18 of any intensity was detected in a higher percentage in PDAC than in high-grade PanIN. Moreover, both positivity rate and intensity were slightly higher in PDAC than in high-grade PanIN (figure 13).
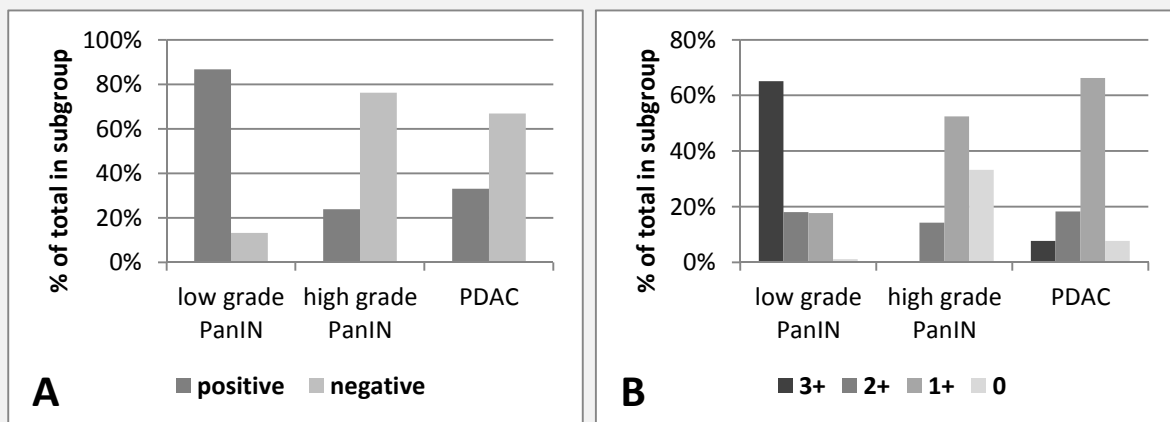
**Figure 13** Expression of Claudin-18 in PanIN and PDAC

Comparison of staining results of claudin-18 IHC between PDAC and PanIN showed that the fraction of positive cases and lesions, respectively was higher in low-grade PanIN and PDAC than in high-grade PanIN (A, p<0.001). Also, the fraction of cases that predominantly displayed weak (1+) or no (0) labeling is higher high-grade PanIN than in PDAC (B, p<0.001).

Finally, claudin-18 expression in PDAC was correlated with some clinicopathological parameters. First, positivity rates concerning claudin-18 in PDAC were compared in subgroups relevant for staging of PDAC, i.e. locoregional extension (T-stage) and lymph node infiltration/metastasis (N-stage). Relevant information with respect to N-stage and T-stage were obtainable for 125 cases (88.0%). Subsequently, positivity for claudin-18 was correlated with survival data to determine differences in overall patient survival between positive and negative cases by Kaplan-Meier analysis. Results

regarding correlation with staging parameters are listed in table 7, complemented by graphical illustrations in figure 14. Cases with advanced regional growth (T3 and T4) tended to be more frequently positive for claudin-18 than cases showing rather limited local expansion (T1 and T2) with 38 (32.5%) and 1 (12.5%) positive cases, respectively (p=0.238). No marked difference in immunoreactivity for claudin-18 was detectable between cases with or without lymph node metastases with 12 (32.4%) and 26 (29.5%) positive cases, respectively (p=0.749). Despite differences in immunoreactivity between grades of differentiation, claudin-18 expression did not have a significant impact on overall patient survival (p=0.712) in the investigated collective of PDAC (figure 14).

Table 7 Correlation of Claudin-18 Positivity with Staging Parameters

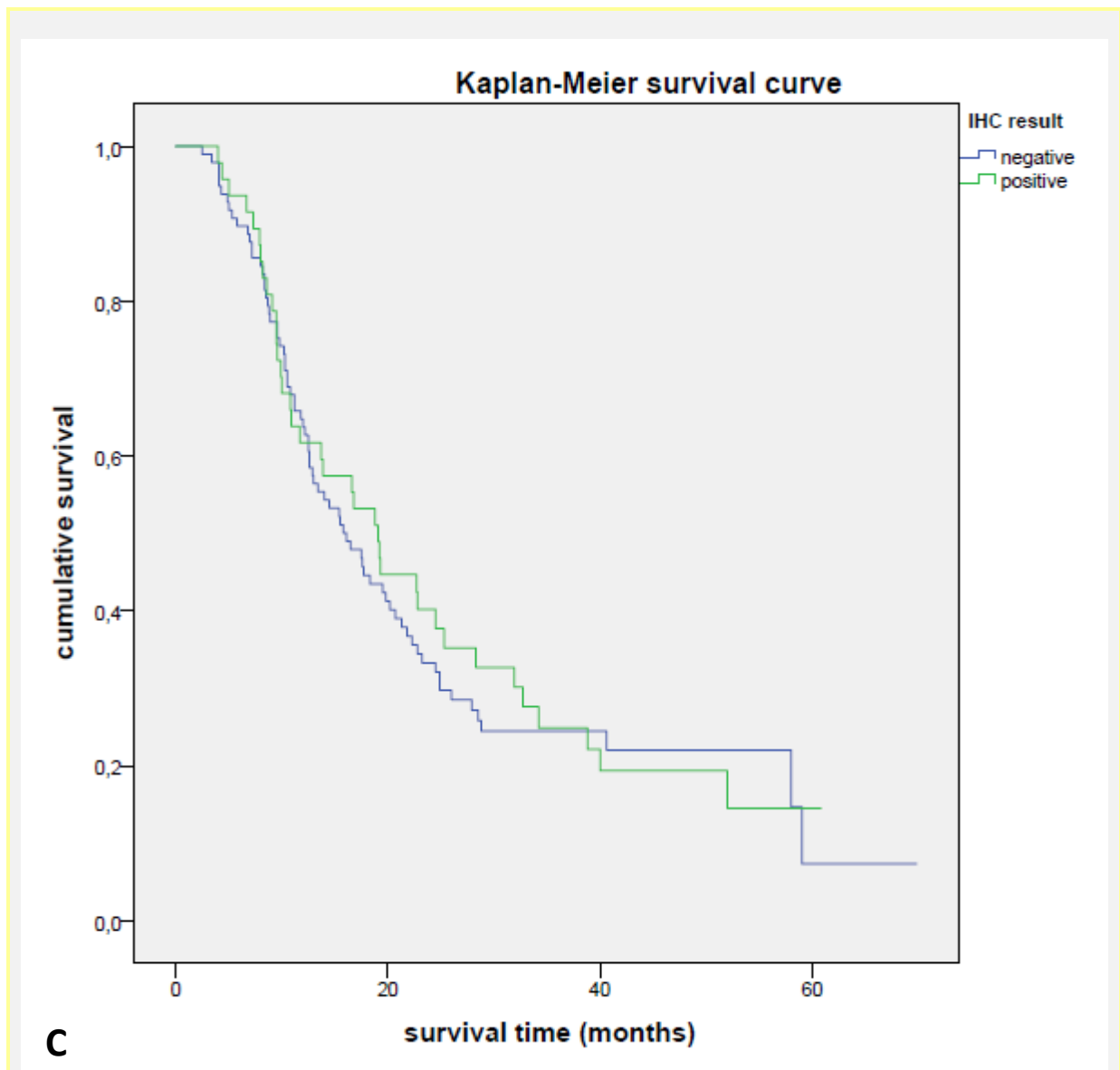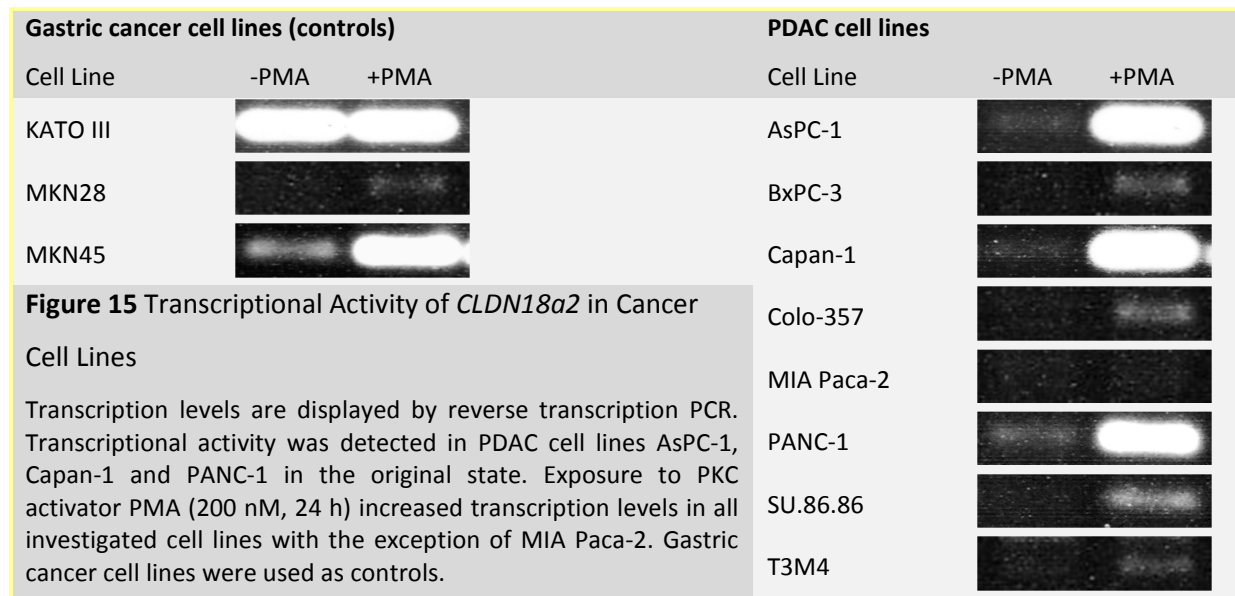|	N-stage		T-stage	
	N0 (*n*=37)	N1 (*n*=88)	T1/T2 (*n*=8)	T3/T4 (*n*=117)
Positivity [%]	12 [32,4]	26 [29,5]	1 [12,5]	38 [32,5]
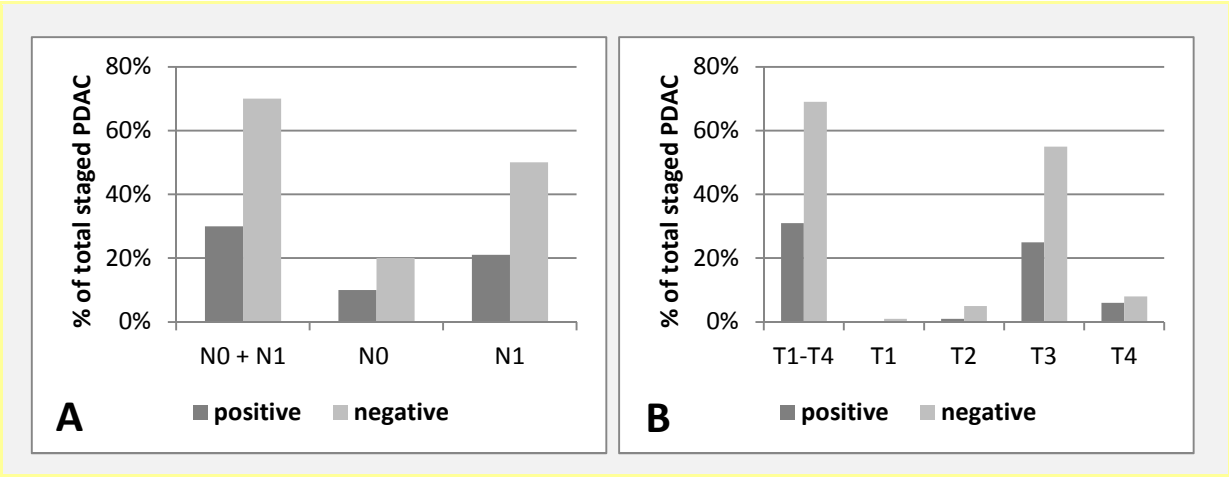
Figure 14 Correlation of Claudin-18 Expression with Clinicopathological Data in PDAC

With ~30% of positive cases in both N0 and N1 group, no correlation of claudin-18 positivity and lymph node infiltration could be shown (A, p=0.749). On the other hand, positivity for claudin-18 is associated with advanced locoregional growth (T3 and T4) at the time of resection (B, p=0.238). Finally, claudin-18 positivity did not significantly affect overall patient survival (C, p=0.712).
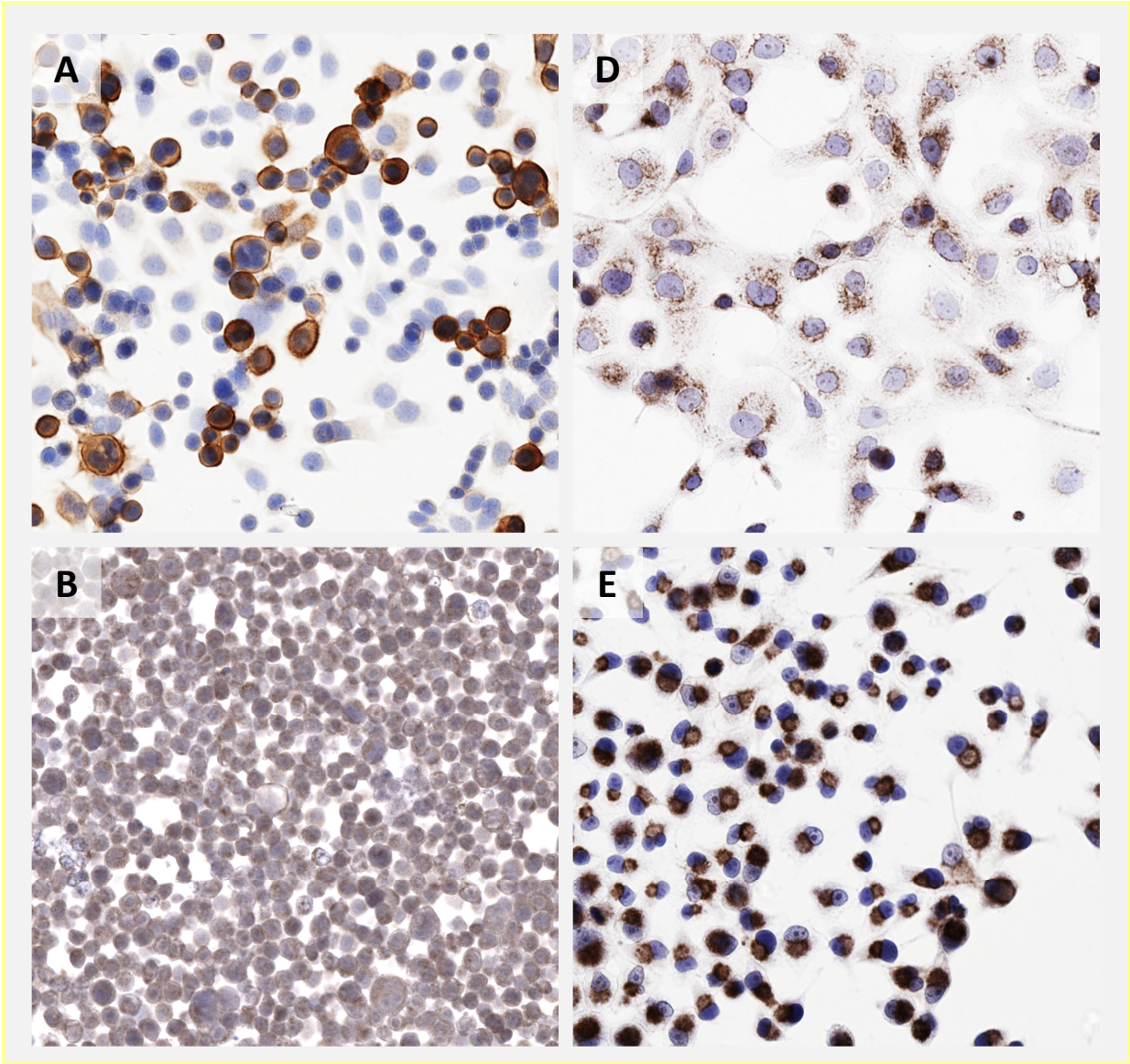
4. Claudin-18 in Pancreatic Cancer Cell Lines

To assess functional aspects of claudin-18 expression in PDAC, claudin-18 expression at the mRNA and protein level was evaluated in 8 PDAC cell lines of various grading and genetic background. All experiments were conducted with and without exposing cells to the PKC activator PMA. Claudin-18 cDNA could be detected on a low level in unstimulated cultures of pancreatic cancer cell lines AsPC-1, Capan-1 and PANC-1as well as in 2 control cell lines (gastric cancer cell lines KATO III and MKN45). Interestingly, assessment of transcriptional activity in cells exposed to PMA revealed

stronger bands in relation to unstimulated cells irrespective of lineage or grading (figure 15), confirming the involvement of PKC signaling in the regulation of claudin-18 expression in cancer cells. The only exceptions were gastric cancer cell line KATO III, which already showed a remarkably strong band in the unstimulated fraction, hampering comparative analysis and the PDAC cell line MIA Paca-2 with no stimulation effect detectable by PCR.

Figure 15 Transcriptional Activity of *CLDN18a2* in Cancer Cell Lines

Transcription levels are displayed by reverse transcription PCR. Transcriptional activity was detected in PDAC cell lines AsPC-1, Capan-1 and PANC-1 in the original state. Exposure to PKC activator PMA (200 nM, 24 h) increased transcription levels in all investigated cell lines with the exception of MIA Paca-2. Gastric cancer cell lines were used as controls.

Western Blotting of total cell and tissue lysates revealed unspecific antibody reactions with a multitude of signals, often notably stronger than the claudin-18 associated signal detectable in tissue lysates of mouse stomach and lung. In contrast, none of the investigated cell lines displayed a signal at approximately the right level (~27 kDA), even after PMS-stimulation (not shown). Moreover, no difference of immunoblotting results was observed between the two primary antibodies.

Immunocytochemical staining was used to investigate expression patterns of claudin-18 in cancer cell lines using fluorescence and enzyme-dependent detection systems. With the exception of KATO III, all investigated cells displayed various degrees of diffuse, i.e. cytoplasmic labeling, but no membranous staining. KATO III was the only cell line that exhibited a robust membranous staining pattern in a fraction of investigated cells. This observation was more pronounced in enzyme-dependent labeling techniques than in immunofluorescence. Immunostaining of PMA-stimulated cells revealed scattered single cells, which displayed strong membranous immunoreactivity among otherwise unlabeled cells only in the gastric cancer cell line MKN45 (figure 16). Using the monoclonal primary antibody, a focal nuclear immunoreactivity was observed in most cell lines (figure 17).
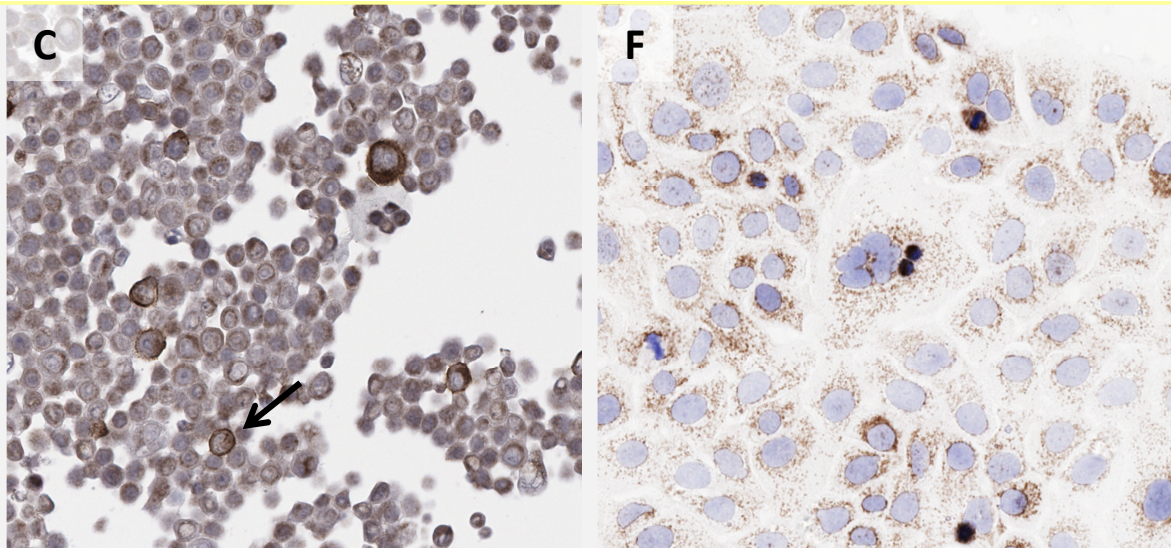
Figure 16 Immunocytostaining of Gastric and Pancreatic Cancer Cells

Immunocytolabeling of gastric (A,B,C) and pancreatic (D,E,F) cancer cell lines revealed membranous immunoreactivity only in gastric cancer cell line KATO III (A), whereas PDAC cell lines only displayed cytoplasmic positivity to various degrees. PMA stimulation increased claudin-18 expression in the gastric cancer cell line MKN45 only, with few scattered immunopositive cells displaying a membranous staining pattern (C, arrow).
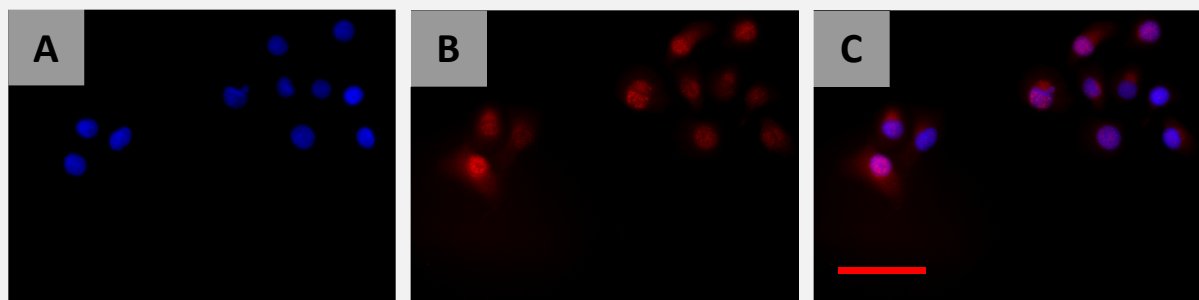

Figure 17 Immunofluorescence Staining of PDAC Cell Line PANC-1

Exemplary result of IF staining using a mAb. (A) shows DAPI nuclear counterstaining. In addition to faint cytoplasmic positivity, PDAC cell line PANC-1 displayed focal nuclear immunoreactivity when a monoclonal anti-claudin-18 primary antibody was used for staining (B). Note that cells did not show a membranous staining pattern (B, C). Bar = 200 µm

IV. DISCUSSION

Claudins are essential tight junction molecules and are expressed in a tissue-specific manner. This expression pattern is subject to change in the course of neoplastic transformation (Singh, Sharma et al. 2010). In recent years, the functional role of various claudins in diverse cancer entities has been the issue of a multitude of studies. Claudin-18, which is normally expressed in the lung and stomach of vertebrates, has been reported to be ectopically activated in pancreatic neoplasms, in particular in ductal adenocarcinoma (Sahin, Koslowski et al. 2008) as well as in various pre-invasive lesions like PanIN (Tanaka, Shibahara et al. 2011). Our understanding of pancreatic carcinogenesis is growing constantly, nonetheless, there were no major breakthroughs in the search for methods of early detection or efficient therapeutic strategies up to this point, and consequently, PDAC is still associated with a particularly poor prognosis.

The main aim of the presented study was to shed light on the role of claudin-18 expression in the course of pancreatic carcinogenesis. Our results show that claudin-18, due to its extensive expression in precursor lesions, might serve as a reliable biomarker for early detection. In addition, its specific expression in neoplastic cells suggests a potential role as a target structure for personalized therapy of PDAC.

Confirming previous investigations, we showed that the most common PDAC precursors like PanIN, IPMN and MCN express claudin-18. Expression levels are significantly higher in low-grade lesions, as well as in lesions with certain phenotypical markers, such as gastric type IPMN (Tanaka, Shibahara et al. 2011). ITPN did not show membranous immunoreactivity for claudin-18, supporting the concept of a new tumor entity with a different molecular pathogenesis compared to other intraductal neoplasms, such as IPMN. In PDAC, we found a proportion of about one third of our cases to be positive for claudin-18. This fraction is lower than in some other publications describing positivity rates of 60-70% (Sahin, Koslowski et al. 2008, Tanaka, Shibahara et al. 2011, Woll, Schlitter et al. 2014). Reasons for this discrepancy may be differences in the composition of samples (microarray vs whole tissue investigation), differences in the study population (Caucasian vs Japanese) and, most importantly, different scoring systems.

The presented data on claudin-18 expression in precancerous lesions and PDAC samples clearly demonstrates that the stomach-specific tight junction molecule is ectopically up-regulated in pancreatic carcinogenesis, since no immunoreactivity could be detected in normal pancreatic ductal structures and parenchyma. Our observations suggest that the activation of claudin-18 expression is an early event in the process of pancreatic carcinogenesis with the strongest expression patterns in low-grade lesions and well-differentiated cases of PDAC. Especially in low grade PanIN, IPMN and MCN, claudin-18 appears to be expressed in its native physiological pattern with high membranous immunoreactivity of epithelial cells. These findings are in line with previous studies and observations

describing claudin-18 as an early stage marker in pancreatic neoplasms (Tanaka, Shibahara et al. 2011). Up-regulation of claudin expression has been shown to have both tumor promoting and inhibiting effects in a tissue specific manner (Kwon 2013). Intuitively, expression activation of junctional molecules suggests an increase of stabilizing elements as a response to molecular changes that in turn affect morphological and biological changes of neoplastic cells. Similarly, claudin-18 might contribute to the formation of stable neoplastic tubular structures, as those observed in low-grade ductal precursors, such as PanIN or IPMN or of well-differentiated PDAC. Moreover, aberrant claudin expression is suspected to affect functional properties of tight junction complexes causing changes in paracellular transport and breakdown of cell polarity and thereby contributing to neoplastic transformation (Singh, Sharma et al. 2010). This transformation might further set up new requirements about the composition of tissue environment, warranting paracellular passage of different solutes than in a healthy state. Additionally, polarity breakdown could affect the distribution of cell surface proteins such as membrane-bound receptors mediating cell growth and proliferation. Both aspects could possibly contribute to the susceptibility of neoplastic cells to oncogenic stimuli (Singh, Sharma et al. 2010).

A feature of PDAC is its extensive formation of desmoplastic stroma (Bosman, Carneiro et al. 2010). Investigation on pancreatic stromal reaction has revealed a close interaction between tumor cells and so called pancreatic stellate cells, which may affect tumor properties such as invasiveness and metastasis (Erkan, Reiser-Erkan et al. 2012). Therefore, it is even thinkable that aberrant claudin expression in neoplastic cells supports stromal formation by changing the equilibrium in the surrounding of neoplastic glands and thereby affecting tumor behavior.

Another result of this study is the correlation of claudin-18 expression with degree of dysplasia in premalignant lesions as well as in invasive adenocarcinoma, being less frequent and less intense in high-grade lesions and poorly differentiated cancer. High-grade lesions are associated with a higher chance to progress to invasive carcinoma and poorly differentiated carcinomas are known for their aggressiveness concerning proliferation, invasion and metastasis. Our findings show that claudin-18 expression is inversely associated with tumor aggressiveness and proliferative potential. In this context, down-regulation of claudin-18 expression would facilitate invasive growth and metastasis by reducing cell-cell interaction and increasing cell motility. Claudin-18 has previously been described to be down-regulated at the invasive front in gastric cancer and RNAi of claudin-18 in gastric cancer cell lines was showed to increase proliferation and invasion (Oshima, Shan et al. 2013), thus supporting our findings. Further experiments like invasion and proliferation assays of PDAC cells expressing claudin-18 would contribute to the understanding of claudin-18 function in PDAC and its impact on such cancer related properties.

Additionally, loss of differentiation in tumor cells is conducted by mechanisms involved in EMT. Consequently, loss of claudin-18 as an epithelial marker might as well be a sign of EMT in PDAC cells. This interpretation is supported by observations in premalignant lesions like PanIN and IPMN,

which showed lower positivity and intensity scores for high grade lesions accompanied by phenotypical changes of epithelial cells and, quite possibly, a higher turnover of epithelial markers in the process of loss of differentiation and EMT, respectively.

Down-regulation of other claudins have already been demonstrated to be associated with high levels of EMT and stem cell markers as in claudin-low breast cancer (Prat, Parker et al. 2010) or in ovarian cancer, where inhibition of claudin-3 and claudin-4 promoted EMT by influencing E-cadherin expression and PI3K signaling (Lin, Shang et al. 2013). On the other hand, claudins have also been shown to enhance EMT, e.g. claudin-1 which induces transcription factors like Slug (SNAI2) in human liver cells (Suh, Yoon et al. 2013).

EMT-related TF are involved in the regulation of claudin expression. The same is true for cellular signaling pathways that involve protein kinase C. We could confirm earlier findings that claudin-18a2 expression can be upregulated by enhancement of PKC-signaling by exposure of cancer cells to PKC activator PMA (Ito, Kojima et al. 2011), although effects on protein level were only observed in one control cell line (MKN45). We assume that the regulation of claudin expression both in healthy tissue and in cancer is complex and involves a variety of mechanisms including transcriptional regulation by cell signaling, TF and epigenetic processes like DNA methylation which also has been reported to play a role for claudin-18a2 expression (Sahin, Koslowski et al. 2008). Recent studies have revealed the contribution of post-transcriptional elements in the regulation of claudin expression by demonstrating that the expression of claudin-1 can be inhibited by miRNA in ovarian cancer stem cells (Qin, Ren et al. 2013). Similar mechanisms could explain the discrepancy between claudin-18 transcription and actual expression on protein level that was detected in pancreatic and gastric cancer cell lines in our series of tests.

Extensive scientific efforts in recent years have focused on the clinicopathological implications of claudin expression in malignant tumors. Interestingly, both activation and down-regulation of claudin expression has emerged as independent prognostic factors with effects on patient survival and disease recurrence. For instance, low levels of claudin-1 expression were associated with poor survival and disease recurrence in stage II colon cancer (Resnick, Konkin et al. 2005) and similar effects have been reported for claudin-4 in PDAC (Tsutsumi, Sato et al. 2012). Conversely, positivity for claudin-7 was found to be linked to shorter recurrence-free survival in breast cancer (Bernardi, Logullo et al. 2012). Earlier studies on the prognostic relevance of claudin-18 expression in PDAC have come to controversial conclusions (Karanjawala, Illei et al. 2008, Soini, Takasawa et al. 2012). Despite a significant correlation between claudin-18 and tumor grading, which represents a relevant prognostic factor in PDAC (Hartwig, Hackert et al. 2011), no differences in overall patient survival with respect to claudin-18 expression was found in this study.

Being membrane associated proteins with two extracellular domains, claudins have been considered as potential targets for therapeutic strategies in cancer treatment. Thus far, a variety of methods have

been suggested to target claudins for antitumor effects. Some claudins are receptors for Clostridium perfringens enterotoxin (CPE), such as claudin-3 and claudin-4 that are expressed in a variety of cancer entities. Coupling of CPE with tumor necrosis factor has caused tumor cell death in ovarian cancer cells that showed up-regulation of claudin-3 and claudin-4 (Yuan, Lin et al. 2009). Another strategy pursued the effects of RNAi on tumor cells with tumor-related properties like invasiveness and proliferation associated with claudin expression. Transfection of siRNA into claudin-3 positive tumor cells caused significant reduction of tumor growth and metastasis in mouse and human ovarian cancer xenografts (Huang, Bao et al. 2009). Moreover, Klamp et al. demonstrated that vaccination with chimeric antigens combining both virus-like particles and a peptide sequence specific for claudin-18a2, induces production of auto-antibodies which causes tumor cell death (Klamp, Schumacher et al. 2011). Finally, the conception of monoclonal antibodies (mAbs) that specifically recognize claudins as antigens can be used to mediate antibody-dependent cellular cytotoxicity (ADCC) as well as complement-dependent cytotoxicity (CDC) (Kwon 2013). Moreover, the binding of mAbs might interfere with functional properties of claudins as tight junction components in cancer cells (Sahin, Koslowski et al. 2008). In former studies, it was demonstrated that specific mAbs directed against stomach specific claudin-18a2, which bind to claudin-18 positive gastric cancer cells can be generated. With the lungs being highly sensitive to toxic effects of therapeutic agents, it is of utmost importance to avoid cross-reactivity of anti-claudin-18 mAbs to acquire eligibility in the field of individualized tumor therapy (Sahin, Koslowski et al. 2008). With cross-reactivity ruled out, gastric mucosal epithelium is the only tissue relevant for toxic side effects. Sahin et al. noticed that claudin-18 expression is restricted to differentiated glandular cells and cannot be detected in mucosal stem cells (Sahin, Koslowski et al. 2008), which indicates the maintenance of regenerative potential of gastric epithelium in case of toxic effects in the course of claudin-18 targeted cancer therapy. Ganymed Pharmaceuticals has developed IMAB362, later promoted as claudiximab, a mAb that binds exclusively to stomach-specific claudin-18a2 and mediates cytotoxic effects (ADCC and CDC) as well as direct antiproliferative and proapoptotic effects, thereby killing cancer cells and inhibiting tumor growth in gastric cancer. IMAB362 is currently being tested in a clinical Phase IIb trial for therapy of advanced stage gastric and lower esophageal cancer (NCT01630083). Against this background, Woll et al. investigated a large set of pancreatic primary cancers including PDAC and acinar cell carcinoma for their expression patterns of claudin-18a2 to determine whether PDAC is potentially suitable to be treated with IMAB362. They found out that, in contrast to acinar cell carcinoma and neuroendocrine neoplasms, PDAC shows frequent expression of claudin-18 with 60% classified as positive. Intriguingly, claudin-18 expression was detected in metastases of PDAC with similar frequency and intensity as in corresponding primary tumors, suggesting PDAC, even at a metastatic stage, to be approachable by therapeutic trials using a monoclonal antibody such as IMAB362 (Woll, Schlitter et al. 2014). Despite different primary antibodies used for immunolabeling and different scoring systems applied, our findings are in line with these conclusions suggesting that claudin-18 is indeed a potential

target for antibody-mediated treatment of PDAC. We deemed a proportion of ~32% of primary PDAC as positive for claudin-18, but there is no evidence that efficacy of treatment generally correlates with staining intensity and the fraction of positive cells (Woll, Schlitter et al. 2014).

Limitations of the Study

For both diagnostic and therapeutic purposes, specific anti-claudin-18.2 antibodies are essential. In addition to a polyclonal primary anti-claudin-18 antibody that has been widely used in previous studies, a monoclonal primary antibody was used for staining in this study. Both primary antibodies recognize carboxy-terminal sequences of the target molecule claudin-18, therefore being unspecific for the gastric isoform claudin-18a2 which differs from the lung-specific claudin-18a1 by some residues of the first ECL. In addition to membranous expression patterns that are detected by each primary antibody to the same degree, both also evoked cytoplasmic staining of cells. Alas, background staining could not be eliminated by optimization of staining protocols. This finding made it difficult to discern actual cytoplasmic positivity from collateral background stain. Most intriguingly, staining with a monoclonal primary antibody revealed nuclear positivity in tissues as well as cell lines in a seemingly specific manner, particularly in intestinal IPMN and some cases of PDAC suggesting internalization of a membrane associated protein and translocation to the nucleus. At the same time, cross reactivity with another, a nuclear component might be possible. Cross-reactivity is even more likely, given that IEM has shown that claudin-18 is only detectable in membrane bound TJ complexes (Niimi, Nagashima et al. 2001). Then again, these investigations were conducted on murine stomach and lung tissue and not on cancer. To ascertain the nuclear localization of claudin-18, immunoblotting of nuclear extracts needs to be performed. Oddly, Western Blot analysis failed to reveal claudin-18 expression in investigated samples despite positivity in immunocytochemistry (KATO III), at the same time displaying numerous bands that suggest cross-reactivity with other cellular components. These patterns indicate that available antibodies are unfit to detect claudin-18 in human culture cells by immunoblotting and simultaneously, are cross-reacting with other proteins. Establishing protocols for Western Blot analysis of claudin-18 is vital for further investigations which are aimed at functional properties of claudin-18 expressing tumor cells like invasion and proliferation.

V. CONCLUSION

Claudin-18 could be confirmed as a reliable biomarker of low-grade pancreatic neoplasms as well differentiated PDAC with predominantly membranous expression patterns. As such, the tight junction molecule could be diagnostically and therapeutically exploited which is imperative since major advancements in the management of pancreatic cancer are scant. Still, our knowledge is limited, especially concerning functional properties of claudin-18 up-regulation in pancreatic neoplasms. For instance, the meaning of the observed nuclear reactivity in some entities can only be speculated on. Also, the clinicopathological significance of claudin-18 expression in pancreatic neoplasms is yet to be revealed, so that we strongly suggest further scientific endeavors in this regard.

References

Aichler, M., C. Seiler, M. Tost, J. Siveke, P. K. Mazur, P. Da Silva-Buttkus, D. K. Bartsch, P. Langer, S. Chiblak, A. Durr, H. Hofler, G. Kloppel, K. Muller-Decker, M. Brielmeier and I. Esposito (2012). "Origin of pancreatic ductal adenocarcinoma from atypical flat lesions: a comparative study in transgenic mice and human tissues." J Pathol **226**(5): 723-734.

Andea, A., F. Sarkar and V. N. Adsay (2003). "Clinicopathological correlates of pancreatic intraepithelial neoplasia: a comparative analysis of 82 cases with and 152 cases without pancreatic ductal adenocarcinoma." Mod Pathol **16**(10): 996-1006.

Angelow, S., R. Ahlstrom and A. S. Yu (2008). "Biology of claudins." Am J Physiol Renal Physiol **295**(4): F867-876.

Basturk, O., V. Adsay, G. Askan, D. Dhall, G. Zamboni, M. Shimizu, K. Cymes, F. Carneiro, S. Balci, C. Sigel, M. D. Reid, I. Esposito, H. Baldaia, P. Allen, G. Kloppel and D. S. Klimstra (2017). "Intraductal Tubulopapillary Neoplasm of the Pancreas: A Clinicopathologic and Immunohistochemical Analysis of 33 Cases." Am J Surg Pathol **41**(3): 313-325.

Basturk, O., S. M. Hong, L. D. Wood, N. V. Adsay, J. Albores-Saavedra, A. V. Biankin, L. A. Brosens, N. Fukushima, M. Goggins, R. H. Hruban, Y. Kato, D. S. Klimstra, G. Kloppel, A. Krasinskas, D. S. Longnecker, H. Matthaei, G. J. Offerhaus, M. Shimizu, K. Takaori, B. Terris, S. Yachida, I. Esposito and T. Furukawa (2015). "A Revised Classification System and Recommendations From the Baltimore Consensus Meeting for Neoplastic Precursor Lesions in the Pancreas." Am J Surg Pathol **39**(12): 1730-1741.

Bernard, P., J. Y. Scoazec, M. Joubert, X. Kahn, J. Le Borgne, F. Berger and C. Partensky (2002). "Intraductal papillary-mucinous tumors of the pancreas: predictive criteria of malignancy according to pathological examination of 53 cases." Arch Surg **137**(11): 1274-1278.

Bernardi, M. A., A. F. Logullo, F. S. Pasini, S. Nonogaki, C. Blumke, F. A. Soares and M. M. Brentani (2012). "Prognostic significance of CD24 and claudin-7 immunoexpression in ductal invasive breast cancer." Oncol Rep **27**(1): 28-38.

Berrington de Gonzalez, A., S. Sweetland and E. Spencer (2003). "A meta-analysis of obesity and the risk of pancreatic cancer." Br J Cancer **89**(3): 519-523.

Bosetti, C., E. Lucenteforte, D. T. Silverman, G. Petersen, P. M. Bracci, B. T. Ji, E. Negri, D. Li, H. A. Risch, S. H. Olson, S. Gallinger, A. B. Miller, H. B. Bueno-de-Mesquita, R. Talamini, J. Polesel, P. Ghadirian, P. A. Baghurst, W. Zatonski, E. Fontham, W. R. Bamlet, E. A. Holly, P. Bertuccio, Y. T. Gao, M. Hassan, H. Yu, R. C. Kurtz, M. Cotterchio, J. Su, P. Maisonneuve, E. J. Duell, P. Boffetta and C. La Vecchia (2012). "Cigarette smoking and pancreatic cancer: an analysis from the International Pancreatic Cancer Case-Control Consortium (Panc4)." Ann Oncol **23**(7): 1880-1888.

Bosman, F. T., F. Carneiro, I. A. f. R. o. Cancer and R. H. Hruban (2010). WHO Classification of Tumours of the Digestive System, International Agency for Research on Cancer.

Breitbart, W., B. Rosenfeld, K. Tobias, H. Pessin, G. Y. Ku, J. Yuan and J. Wolchok (2014). "Depression, cytokines, and pancreatic cancer." Psychooncology **23**(3): 339-345.

Brugge, W. R. (2015). "Diagnosis and management of cystic lesions of the pancreas." J Gastrointest Oncol **6**(4): 375-388.

Castillo, C. F. d. and N. V. Adsay (2010). "Intraductal Papillary Mucinous Neoplasms of the Pancreas." Gastroenterology **139**(3): 708-713.e702.

Conroy, T., F. Desseigne, M. Ychou, O. Bouche, R. Guimbaud, Y. Becouarn, A. Adenis, J. L. Raoul, S. Gourgou-Bourgade, C. de la Fouchardiere, J. Bennouna, J. B. Bachet, F. Khemissa-Akouz, D. Pere-Verge, C. Delbaldo, E. Assenat, B. Chauffert, P. Michel, C. Montoto-Grillot and M. Ducreux (2011). "FOLFIRINOX versus gemcitabine for metastatic pancreatic cancer." N Engl J Med **364**(19): 1817-1825.

Crippa, S., C. Fernandez-Del Castillo, R. Salvia, D. Finkelstein, C. Bassi, I. Dominguez, A. Muzikansky, S. P. Thayer, M. Falconi, M. Mino-Kenudson, P. Capelli, G. Y. Lauwers, S. Partelli, P. Pederzoli and A. L. Warshaw (2010). "Mucin-producing neoplasms of the pancreas: an analysis of distinguishing clinical and epidemiologic characteristics." Clin Gastroenterol Hepatol **8**(2): 213-219.

Crippa, S., R. Salvia, A. L. Warshaw, I. Dominguez, C. Bassi, M. Falconi, S. P. Thayer, G. Zamboni, G. Y. Lauwers, M. Mino-Kenudson, P. Capelli, P. Pederzoli and C. F. Castillo (2008). "Mucinous cystic neoplasm of the pancreas is not an aggressive entity: lessons from 163 resected patients." Ann Surg **247**(4): 571-579.

de Wilde, R. F., R. H. Hruban, A. Maitra and G. J. A. Offerhaus (2012). "Reporting precursors to invasive pancreatic cancer: pancreatic intraepithelial neoplasia, intraductal neoplasms and mucinous cystic neoplasm." Diagnostic Histopathology **18**(1): 17-30.

Distler, M., D. Aust, J. Weitz, C. Pilarsky and R. Grutzmann (2014). "Precursor lesions for sporadic pancreatic cancer: PanIN, IPMN, and MCN." Biomed Res Int **2014**: 474905.

Erkan, M., G. Adler, M. V. Apte, M. G. Bachem, M. Buchholz, S. Detlefsen, I. Esposito, H. Friess, T. M. Gress, H. J. Habisch, R. F. Hwang, R. Jaster, J. Kleeff, G. Kloppel, C. Kordes, C. D. Logsdon, A. Masamune, C. W. Michalski, J. Oh, P. A. Phillips, M. Pinzani, C. Reiser-Erkan, H. Tsukamoto and J. Wilson (2012). "StellaTUM: current consensus and discussion on pancreatic stellate cell research." Gut **61**(2): 172-178.

Erkan, M., C. Reiser-Erkan, C. W. Michalski, B. Kong, I. Esposito, H. Friess and J. Kleeff (2012). "The impact of the activated stroma on pancreatic ductal adenocarcinoma biology and therapy resistance." Curr Mol Med **12**(3): 288-303.

Esposito, I., B. Konukiewitz, A. M. Schlitter and G. Kloppel (2012). "[New insights into the origin of pancreatic cancer. Role of atypical flat lesions in pancreatic carcinogenesis]." Pathologe **33 Suppl 2**: 189-193.

Esposito, I., A. Segler, K. Steiger and G. Kloppel (2015). "Pathology, genetics and precursors of human and experimental pancreatic neoplasms: An update." Pancreatology **15**(6): 598-610.

Everhart, J. and D. Wright (1995). "Diabetes mellitus as a risk factor for pancreatic cancer: A meta-analysis." JAMA **273**(20): 1605-1609.

Furukawa, T., G. Kloppel, N. Volkan Adsay, J. Albores-Saavedra, N. Fukushima, A. Horii, R. H. Hruban, Y. Kato, D. S. Klimstra, D. S. Longnecker, J. Luttges, G. J. Offerhaus, M. Shimizu, M. Sunamura, A. Suriawinata, K. Takaori and S. Yonezawa (2005). "Classification of types of intraductal papillary-mucinous neoplasm of the pancreas: a consensus study." Virchows Arch **447**(5): 794-799.

Furukawa, T., Y. Kuboki, E. Tanji, S. Yoshida, T. Hatori, M. Yamamoto, N. Shibata, K. Shimizu, N. Kamatani and K. Shiratori (2011). "Whole-exome sequencing uncovers frequent GNAS mutations in intraductal papillary mucinous neoplasms of the pancreas." Sci Rep **1**: 161.

Furuse, M., K. Fujita, T. Hiiragi, K. Fujimoto and S. Tsukita (1998). "Claudin-1 and -2: Novel Integral Membrane Proteins Localizing at Tight Junctions with No Sequence Similarity to Occludin." The Journal of Cell Biology **141**(7): 1539-1550.

68

Goel, G., H. P. Makkar, G. Francis and K. Becker (2007). "Phorbol esters: structure, biological activity, and toxicity in animals." Int J Toxicol **26**(4): 279-288.

Hartwig, W., T. Hackert, U. Hinz, A. Gluth, F. Bergmann, O. Strobel, M. W. Buchler and J. Werner (2011). "Pancreatic cancer surgery in the new millennium: better prediction of outcome." Ann Surg **254**(2): 311-319.

Hewitt, K. J., R. Agarwal and P. J. Morin (2006). "The claudin gene family: expression in normal and neoplastic tissues." BMC Cancer **6**: 186.

Hezel, A. F., A. C. Kimmelman, B. Z. Stanger, N. Bardeesy and R. A. Depinho (2006). "Genetics and biology of pancreatic ductal adenocarcinoma." Genes Dev **20**(10): 1218-1249.

Hidalgo, M. (2010). "Pancreatic cancer." N Engl J Med **362**(17): 1605-1617.

Hruban, R. H., N. V. Adsay, J. Albores-Saavedra, C. Compton, E. S. Garrett, S. N. Goodman, S. E. Kern, D. S. Klimstra, G. Kloppel, D. S. Longnecker, J. Luttges and G. J. Offerhaus (2001). "Pancreatic intraepithelial neoplasia: a new nomenclature and classification system for pancreatic duct lesions." Am J Surg Pathol **25**(5): 579-586.

Hruban, R. H., M. B. Pitman, D. S. Klimstra, A. R. o. Pathology and A. F. I. o. Pathology (2007). Tumors of the Pancreas, American Registry of Pathology in collaboration with the Armed Forces Institute of Pathology.

Hruban, R. H., K. Takaori, D. S. Klimstra, N. V. Adsay, J. Albores-Saavedra, A. V. Biankin, S. A. Biankin, C. Compton, N. Fukushima, T. Furukawa, M. Goggins, Y. Kato, G. Kloppel, D. S. Longnecker, J. Luttges, A. Maitra, G. J. Offerhaus, M. Shimizu and S. Yonezawa (2004). "An illustrated consensus on the classification of pancreatic intraepithelial neoplasia and intraductal papillary mucinous neoplasms." Am J Surg Pathol **28**(8): 977-987.

Huang, Y. H., Y. Bao, W. Peng, M. Goldberg, K. Love, D. A. Bumcrot, G. Cole, R. Langer, D. G. Anderson and J. A. Sawicki (2009). "Claudin-3 gene silencing with siRNA suppresses ovarian tumor growth and metastasis." Proc Natl Acad Sci U S A **106**(9): 3426-3430.

Iacobuzio-Donahue, C. A., D. S. Klimstra, N. V. Adsay, R. E. Wilentz, P. Argani, T. A. Sohn, C. J. Yeo, J. L. Cameron, S. E. Kern and R. H. Hruban (2000). "Dpc-4 protein is expressed in virtually all human intraductal papillary mucinous neoplasms of the pancreas: comparison with conventional ductal adenocarcinomas." Am J Pathol **157**(3): 755-761.

Ilic, M. and I. Ilic (2016). "Epidemiology of pancreatic cancer." World J Gastroenterol **22**(44): 9694-9705.

Ito, T., T. Kojima, H. Yamaguchi, D. Kyuno, Y. Kimura, M. Imamura, A. Takasawa, M. Murata, S. Tanaka, K. Hirata and N. Sawada (2011). "Transcriptional regulation of claudin-18 via specific protein kinase C signaling pathways and modification of DNA methylation in human pancreatic cancer cells." J Cell Biochem **112**(7): 1761-1772.

Itoh, M., M. Furuse, K. Morita, K. Kubota, M. Saitou and S. Tsukita (1999). "Direct binding of three tight junction-associated MAGUKs, ZO-1, ZO-2, and ZO-3, with the COOH termini of claudins." J Cell Biol **147**(6): 1351-1363.

Jemal, A., E. P. Simard, C. Dorell, A. M. Noone, L. E. Markowitz, B. Kohler, C. Eheman, M. Saraiya, P. Bandi, D. Saslow, K. A. Cronin, M. Watson, M. Schiffman, S. J. Henley, M. J. Schymura, R. N. Anderson, D. Yankey and B. K. Edwards (2013). "Annual Report to the Nation on the Status of Cancer, 1975-2009, featuring the burden and trends in human papillomavirus(HPV)-associated cancers and HPV vaccination coverage levels." J Natl Cancer Inst **105**(3): 175-201.

Jemal, A., E. M. Ward, C. J. Johnson, K. A. Cronin, J. Ma, B. Ryerson, A. Mariotto, A. J. Lake, R. Wilson, R. L. Sherman, R. N. Anderson, S. J. Henley, B. A. Kohler, L. Penberthy, E. J. Feuer and H. K. Weir (2017). "Annual Report to the Nation on the Status of Cancer, 1975-2014, Featuring Survival." J Natl Cancer Inst **109**(9).

Jones, S., X. Zhang, D. W. Parsons, J. C. Lin, R. J. Leary, P. Angenendt, P. Mankoo, H. Carter, H. Kamiyama, A. Jimeno, S. M. Hong, B. Fu, M. T. Lin, E. S. Calhoun, M. Kamiyama, K. Walter, T. Nikolskaya, Y. Nikolsky, J. Hartigan, D. R. Smith, M. Hidalgo, S. D. Leach, A. P. Klein, E. M. Jaffee, M. Goggins, A. Maitra, C. Iacobuzio-Donahue, J. R. Eshleman, S. E. Kern, R. H. Hruban, R. Karchin, N. Papadopoulos, G. Parmigiani, B. Vogelstein, V. E. Velculescu and K. W. Kinzler (2008). "Core signaling pathways in human pancreatic cancers revealed by global genomic analyses." Science **321**(5897): 1801-1806.

Karanjawala, Z. E., P. B. Illei, R. Ashfaq, J. R. Infante, K. Murphy, A. Pandey, R. Schulick, J. Winter, R. Sharma, A. Maitra, M. Goggins and R. H. Hruban (2008). "New markers of pancreatic cancer identified through differential gene expression analyses: claudin 18 and annexin A8." Am J Surg Pathol **32**(2): 188-196.

Keane, M. G., L. Horsfall, G. Rait and S. P. Pereira (2014). "A case-control study comparing the incidence of early symptoms in pancreatic and biliary tract cancer." BMJ Open **4**(11): e005720.

Kim, S. G., T. T. Wu, J. H. Lee, Y. K. Yun, J. P. Issa, S. R. Hamilton and A. Rashid (2003). "Comparison of epigenetic and genetic alterations in mucinous cystic neoplasm and serous microcystic adenoma of pancreas." Mod Pathol **16**(11): 1086-1094.

Klamp, T., J. Schumacher, G. Huber, C. Kuhne, U. Meissner, A. Selmi, T. Hiller, S. Kreiter, J. Markl, O. Tureci and U. Sahin (2011). "Highly specific auto-antibodies against claudin-18 isoform 2 induced by a chimeric HBcAg virus-like particle vaccine kill tumor cells and inhibit the growth of lung metastases." Cancer Res **71**(2): 516-527.

Klein, A. P., K. A. Brune, G. M. Petersen, M. Goggins, A. C. Tersmette, G. J. Offerhaus, C. Griffin, J. L. Cameron, C. J. Yeo, S. Kern and R. H. Hruban (2004). "Prospective risk of pancreatic cancer in familial pancreatic cancer kindreds." Cancer Res **64**(7): 2634-2638.

Klimstra DS, A. N., Dhall D, Shimizu M, Cymes K, Basturk O et al. (2007). "Intraductal tubular carcinoma of the pancreas: clinicopathologic and immunohistochemical analysis of 18 cases." Mod Pathol **20: 285A**.

Kloppel, G. and M. Kosmahl (2001). "Cystic lesions and neoplasms of the pancreas. The features are becoming clearer." Pancreatology **1**(6): 648-655.

Ko, A. H. (2015). "Progress in the treatment of metastatic pancreatic cancer and the search for next opportunities." J Clin Oncol **33**(16): 1779-1786.

Koito, K., T. Namieno, T. Ichimura, N. Yama, M. Hareyama, K. Morita and M. Nishi (1998). "Mucin-producing pancreatic tumors: comparison of MR cholangiopancreatography with endoscopic retrograde cholangiopancreatography." Radiology **208**(1): 231-237.

Kosmahl, M., U. Pauser, K. Peters, B. Sipos, J. Lüttges, B. Kremer and G. Klöppel (2004). "Cystic neoplasms of the pancreas and tumor-like lesions with cystic features: a review of 418 cases and a classification proposal." Virchows Archiv **445**(2): 168-178.

Kwon, M. J. (2013). "Emerging roles of claudins in human cancer." Int J Mol Sci **14**(9): 18148-18180.

Lee, J. H., K. S. Kim, T. J. Kim, S. P. Hong, S. Y. Song, J. B. Chung and S. W. Park (2011). "Immunohistochemical analysis of claudin expression in pancreatic cystic tumors." <u>Oncol Rep</u> **25**(4): 971-978.

Lin, X., X. Shang, G. Manorek and S. B. Howell (2013). "Regulation of the Epithelial-Mesenchymal Transition by Claudin-3 and Claudin-4." <u>PLoS One</u> **8**(6): e67496.

Lu, P. Y., L. Shu, S. S. Shen, X. J. Chen and X. Y. Zhang (2017). "Dietary Patterns and Pancreatic Cancer Risk: A Meta-Analysis." <u>Nutrients</u> **9**(1).

Luttges, J., B. Feyerabend, T. Buchelt, M. Pacena and G. Kloppel (2002). "The mucin profile of noninvasive and invasive mucinous cystic neoplasms of the pancreas." <u>Am J Surg Pathol</u> **26**(4): 466-471.

Mahadevan, D. and D. D. Von Hoff (2007). "Tumor-stroma interactions in pancreatic ductal adenocarcinoma." <u>Mol Cancer Ther</u> **6**(4): 1186-1197.

Matthaei, H., R. D. Schulick, R. H. Hruban and A. Maitra (2011). "Cystic precursors to invasive pancreatic cancer." <u>Nat Rev Gastroenterol Hepatol</u> **8**(3): 141-150.

Merikallio, H., P. Paakko, T. Harju and Y. Soini (2011). "Claudins 10 and 18 are predominantly expressed in lung adenocarcinomas and in tumors of nonsmokers." <u>Int J Clin Exp Pathol</u> **4**(7): 667-673.

Michaud, D. S., E. Giovannucci, W. C. Willett, G. A. Colditz, M. J. Stampfer and C. S. Fuchs (2001). "Physical activity, obesity, height, and the risk of pancreatic cancer." <u>Jama</u> **286**(8): 921-929.

Nakao, A., A. Harada, T. Nonami, T. Kaneko, S. Inoue and H. Takagi (1995). "Clinical significance of portal invasion by pancreatic head carcinoma." <u>Surgery</u> **117**(1): 50-55.

Nakata, K., K. Ohuchida, S. Aishima, Y. Sadakari, T. Kayashima, Y. Miyasaka, E. Nagai, K. Mizumoto, M. Tanaka, M. Tsuneyoshi and Y. Oda (2011). "Invasive carcinoma derived from intestinal-type intraductal papillary mucinous neoplasm is associated with minimal invasion, colloid carcinoma, and less invasive behavior, leading to a better prognosis." <u>Pancreas</u> **40**(4): 581-587.

Niimi, T., K. Nagashima, J. M. Ward, P. Minoo, D. B. Zimonjic, N. C. Popescu and S. Kimura (2001). "claudin-18, a novel downstream target gene for the T/EBP/NKX2.1 homeodomain transcription factor, encodes lung- and stomach-specific isoforms through alternative splicing." <u>Mol Cell Biol</u> **21**(21): 7380-7390.

Oettle, H., S. Post, P. Neuhaus and et al. (2007). "Adjuvant chemotherapy with gemcitabine vs observation in patients undergoing curative-intent resection of pancreatic cancer: A randomized controlled trial." <u>JAMA</u> **297**(3): 267-277.

Oshima, T., J. Shan, T. Okugawa, X. Chen, K. Hori, T. Tomita, H. Fukui, J. Watari and H. Miwa (2013). "Down-regulation of claudin-18 is associated with the proliferative and invasive potential of gastric cancer at the invasive front." <u>PLoS One</u> **8**(9): e74757.

Ottenhof, N. A., R. F. de Wilde, A. Maitra, R. H. Hruban and G. J. Offerhaus (2011). "Molecular characteristics of pancreatic ductal adenocarcinoma." <u>Patholog Res Int</u> **2011**: 620601.

Patel, S. A., R. Adams, M. Goldstein and C. A. Moskaluk (2002). "Genetic analysis of invasive carcinoma arising in intraductal oncocytic papillary neoplasm of the pancreas." <u>Am J Surg Pathol</u> **26**(8): 1071-1077.

Piontek, J., L. Winkler, H. Wolburg, S. L. Muller, N. Zuleger, C. Piehl, B. Wiesner, G. Krause and I. E. Blasig (2008). "Formation of tight junction: determinants of homophilic interaction between classic claudins." Faseb j **22**(1): 146-158.

Prat, A., J. S. Parker, O. Karginova, C. Fan, C. Livasy, J. I. Herschkowitz, X. He and C. M. Perou (2010). "Phenotypic and molecular characterization of the claudin-low intrinsic subtype of breast cancer." Breast Cancer Res **12**(5): R68.

Procacci, C., G. Carbognin, S. Accordini, C. Biasiutti, A. Guarise, F. Lombardo, C. Ghirardi, R. Graziani, N. Pagnotta and R. De Marco (2001). "CT features of malignant mucinous cystic tumors of the pancreas." Eur Radiol **11**(9): 1626-1630.

Qin, W., Q. Ren, T. Liu, Y. Huang and J. Wang (2013). "MicroRNA-155 is a novel suppressor of ovarian cancer-initiating cells that targets CLDN1." FEBS Lett **587**(9): 1434-1439.

Raimondi, S., A. B. Lowenfels, A. M. Morselli-Labate, P. Maisonneuve and R. Pezzilli (2010). "Pancreatic cancer in chronic pancreatitis; aetiology, incidence, and early detection." Best Pract Res Clin Gastroenterol **24**(3): 349-358.

Resnick, M. B., T. Konkin, J. Routhier, E. Sabo and V. E. Pricolo (2005). "Claudin-1 is a strong prognostic indicator in stage II colonic cancer: a tissue microarray study." Mod Pathol **18**(4): 511-518.

Sahin, U., M. Koslowski, K. Dhaene, D. Usener, G. Brandenburg, G. Seitz, C. Huber and O. Tureci (2008). "Claudin-18 splice variant 2 is a pan-cancer target suitable for therapeutic antibody development." Clin Cancer Res **14**(23): 7624-7634.

Sato, N., T. Ueki, N. Fukushima, C. A. Iacobuzio-Donahue, C. J. Yeo, J. L. Cameron, R. H. Hruban and M. Goggins (2002). "Aberrant methylation of CpG islands in intraductal papillary mucinous neoplasms of the pancreas." Gastroenterology **123**(1): 365-372.

Schnelldorfer, T., M. G. Sarr, D. M. Nagorney, L. Zhang, T. C. Smyrk, R. Qin, S. T. Chari and M. B. Farnell (2008). "Experience with 208 resections for intraductal papillary mucinous neoplasm of the pancreas." Arch Surg **143**(7): 639-646; discussion 646.

Schonleben, F., W. Qiu, N. T. Ciau, D. J. Ho, X. Li, J. D. Allendorf, H. E. Remotti and G. H. Su (2006). "PIK3CA mutations in intraductal papillary mucinous neoplasm/carcinoma of the pancreas." Clin Cancer Res **12**(12): 3851-3855.

Schonleben, F., W. Qiu, H. E. Remotti, W. Hohenberger and G. H. Su (2008). "PIK3CA, KRAS, and BRAF mutations in intraductal papillary mucinous neoplasm/carcinoma (IPMN/C) of the pancreas." Langenbecks Arch Surg **393**(3): 289-296.

Sener, S. F., A. Fremgen, H. R. Menck and D. P. Winchester (1999). "Pancreatic cancer: a report of treatment and survival trends for 100,313 patients diagnosed from 1985-1995, using the National Cancer Database." J Am Coll Surg **189**(1): 1-7.

Shaib, Y., J. Davila, C. Naumann and H. El-Serag (2007). "The impact of curative intent surgery on the survival of pancreatic cancer patients: a U.S. Population-based study." Am J Gastroenterol **102**(7): 1377-1382.

Shi, C., R. H. Hruban and A. P. Klein (2009). "Familial pancreatic cancer." Arch Pathol Lab Med **133**(3): 365-374.

Singh, A. B., A. Sharma and P. Dhawan (2010). "Claudin family of proteins and cancer: an overview." J Oncol **2010**: 541957.

Singh, P., S. Toom and Y. Huang (2017). "Anti-claudin 18.2 antibody as new targeted therapy for advanced gastric cancer." J Hematol Oncol **10**(1): 105.

Sobin, L. H., M. K. Gospodarowicz, C. Wittekind and C. International Union against (2009). TNM classification of malignant tumours. Chichester, West Sussex, UK; Hoboken, NJ, Wiley-Blackwell.

Sohn, T. A., C. J. Yeo, J. L. Cameron, L. Koniaris, S. Kaushal, R. A. Abrams, P. K. Sauter, J. Coleman, R. H. Hruban and K. D. Lillemoe (2000). "Resected adenocarcinoma of the pancreas-616 patients: results, outcomes, and prognostic indicators." J Gastrointest Surg **4**(6): 567-579.

Soini, Y., A. Takasawa, M. Eskelinen, P. Juvonen, V. Karja, T. Hasegawa, M. Murata, S. Tanaka, T. Kojima and N. Sawada (2012). "Expression of claudins 7 and 18 in pancreatic ductal adenocarcinoma: association with features of differentiation." J Clin Pathol **65**(5): 431-436.

Sperti, C., C. Pasquali and S. Pedrazzoli (1997). "Ductal adenocarcinoma of the body and tail of the pancreas." J Am Coll Surg **185**(3): 255-259.

Suh, Y., C. H. Yoon, R. K. Kim, E. J. Lim, Y. S. Oh, S. G. Hwang, S. An, G. Yoon, M. C. Gye, J. M. Yi, M. J. Kim and S. J. Lee (2013). "Claudin-1 induces epithelial-mesenchymal transition through activation of the c-Abl-ERK signaling pathway in human liver cells." Oncogene **32**(41): 4873-4882.

Tanaka, M., J. Shibahara, N. Fukushima, A. Shinozaki, M. Umeda, S. Ishikawa, N. Kokudo and M. Fukayama (2011). "Claudin-18 is an early-stage marker of pancreatic carcinogenesis." J Histochem Cytochem **59**(10): 942-952.

Tsutsumi, K., N. Sato, R. Tanabe, K. Mizumoto, K. Morimatsu, T. Kayashima, H. Fujita, K. Ohuchida, T. Ohtsuka, S. Takahata, M. Nakamura and M. Tanaka (2012). "Claudin-4 expression predicts survival in pancreatic ductal adenocarcinoma." Ann Surg Oncol **19 Suppl 3**: S491-499.

Wada, K. (2002). "p16 and p53 gene alterations and accumulations in the malignant evolution of intraductal papillary-mucinous tumors of the pancreas." J Hepatobiliary Pancreat Surg **9**(1): 76-85.

Woll, S., A. M. Schlitter, K. Dhaene, M. Roller, I. Esposito, U. Sahin and O. Tureci (2014). "Claudin 18.2 is a target for IMAB362 antibody in pancreatic neoplasms." Int J Cancer **134**(3): 731-739.

Wu, J., Y. Jiao, M. Dal Molin, A. Maitra, R. F. de Wilde, L. D. Wood, J. R. Eshleman, M. G. Goggins, C. L. Wolfgang, M. I. Canto, R. D. Schulick, B. H. Edil, M. A. Choti, V. Adsay, D. S. Klimstra, G. J. Offerhaus, A. P. Klein, L. Kopelovich, H. Carter, R. Karchin, P. J. Allen, C. M. Schmidt, Y. Naito, L. A. Diaz, Jr., K. W. Kinzler, N. Papadopoulos, R. H. Hruban and B. Vogelstein (2011). "Whole-exome sequencing of neoplastic cysts of the pancreas reveals recurrent mutations in components of ubiquitin-dependent pathways." Proc Natl Acad Sci U S A **108**(52): 21188-21193.

Wu, V. M., J. Schulte, A. Hirschi, U. Tepass and G. J. Beitel (2004). "Sinuous is a Drosophila claudin required for septate junction organization and epithelial tube size control." J Cell Biol **164**(2): 313-323.

Yamaguchi, H., Y. Kuboki, T. Hatori, M. Yamamoto, K. Shimizu, K. Shiratori, N. Shibata, M. Shimizu and T. Furukawa (2013). "The discrete nature and distinguishing molecular features of pancreatic intraductal tubulopapillary neoplasms and intraductal papillary mucinous neoplasms of the gastric type, pyloric gland variant." The Journal of Pathology **231**(3): 335-341.

Yamaguchi, H., M. Shimizu, S. Ban, I. Koyama, T. Hatori, I. Fujita, M. Yamamoto, S. Kawamura, M. Kobayashi, K. Ishida, T. Morikawa, F. Motoi, M. Unno, A. Kanno, K. Satoh, T. Shimosegawa, H. Orikasa, T. Watanabe, K. Nishimura, Y. Ebihara, N. Koike and T. Furukawa (2009). "Intraductal tubulopapillary neoplasms of the pancreas distinct from pancreatic intraepithelial neoplasia and intraductal papillary mucinous neoplasms." Am J Surg Pathol **33**(8): 1164-1172.

Yamao, K., K. Ohashi, T. Nakamura, T. Suzuki, Y. Watanabe, Y. Shimizu, Y. Nakamura and I. Ozden (2001). "Evaluation of various imaging methods in the differential diagnosis of intraductal papillary-mucinous tumor (IPMT) of the pancreas." <u>Hepatogastroenterology</u> **48**(40): 962-966.

Yano, K., T. Imaeda and T. Niimi (2008). "Transcriptional activation of the human claudin-18 gene promoter through two AP-1 motifs in PMA-stimulated MKN45 gastric cancer cells." <u>Am J Physiol Gastrointest Liver Physiol</u> **294**(1): G336-343.

Yonezawa, S., M. Higashi, N. Yamada and M. Goto (2008). "Precursor lesions of pancreatic cancer." <u>Gut Liver</u> **2**(3): 137-154.

Yuan, X., X. Lin, G. Manorek, I. Kanatani, L. H. Cheung, M. G. Rosenblum and S. B. Howell (2009). "Recombinant CPE fused to tumor necrosis factor targets human ovarian cancer cells expressing the claudin-3 and claudin-4 receptors." <u>Mol Cancer Ther</u> **8**(7): 1906-1915.

Acknowledgments

Declaration

I, Ralph-Tobias Daraban, hereby declare that I prepared the present dissertation independently, using only the references and resources stated. This work has not been submitted to any examination board yet. The content of this work, in whole or in part, has not yet been published in any scientific journals.

Erklärung

Hiermit erkläre ich, Ralph-Tobias Daraban, dass ich die vorliegende Dissertation selbständig verfasst und ausschließlich die angegebenen Quellen und Hilfsmittel verwendet habe. Die Arbeit wurde noch keiner Prüfungskommission vorgelegt. Der Inhalt dieser Arbeit wurde bislang weder als Ganzes noch in Teilen in wissenschaftlichen Fachzeitschriften veröffentlicht.

Ralph-Tobias Daraban

München, 8. März 2019